MASONRY

Materials, Testing, and Applications

JOSEPH H. BRISCH
ROBERT L. NELSON
HARRY L. FRANCIS
EDITORS

ASTM STP 1356

STP 1356

Masonry: Materials, Testing, and Applications

J. H. Brisch, R. L. Nelson, and H. L. Francis, Editors

ASTM Stock #: STP1356

ASTM
100 Barr Harbor Drive
West Conshohocken, PA 19428-2959

Library of Congress Cataloging-in-Publication Data

Symposium on Masonry: Materials, Testing, and Applications (1998: Nashville, Tenn.).
Masonry: materials, testing, and applications/J. H. Brisch, R. L. Nelson, and H. J. Francis, editors.
(STP; 1356)
p. cm.
"ASTM stock #: STP 1356."
ISBN 0-8031-2600-X
1. Masonry-Materials 2. Masonry-Testing 3. Masonry
I. Brisch, J. H., (Joseph H.), 1947-. II. Nelson, R. L., (Robert L.), 1936-.
III. Francis, H. J., (Harry J.), 1933-.
TA425.M37 1999
693'.1—dc21 99-36980
CIP

Peer Review Policy

Each paper published in this volume was evaluated by two peer reviewers and at least one editor. The authors addressed all of the reviewers' comments to the satisfaction of both the technical editor(s) and the ASTM Committee on Publications.

To make technical information available as quickly as possible, the peer-reviewed papers in this publication were prepared "camera-ready" as submitted by the authors.

The quality of the papers in this publication reflects not only the obvious efforts of the authors and the technical editor(s), but also the work of the peer reviewers. In keeping with long-standing publication practices, ASTM maintains the anonymity of the peer reviewers. The ASTM Committee on Publications acknowledges with appreciation their dedication and contribution of time and effort on behalf of ASTM.

Printed in Toronto, Ontario, Canada
August 1999

Foreword

This publication, *Masonry: Materials, Testing, and Applications,* contains papers presented at the Symposium on Masonry: Materials, Testing, and Applications presented 8 December, 1998 in Nashville, TN. The symposium was sponsored by Committees C-7 on Lime, C-1 on Cement, C-12 on Mortars and Grouts for Unit Masonry, and C-15 on Manufactured Masonry Units.

The symposium was chaired by Joseph H. Brisch, with Rockwell Lime Company, Manitowoc, WI; Robert L. Nelson, of Robert L. Nelson & Associates, Schaumburg, IL; and Harry L. Francis, of Elliston, VA. Each of these men served as editor of this resulting publication.

Contents

Overview

Masonry is one of mankind's oldest arts. The construction of shelters, buildings, castles, and fortresses has been the life work of untold numbers of artists, architects, masons, plasterers, and laborers. Today we marvel at the ancient structures still standing after hundreds and thousands of years. Works such as the Great Wall of China, The Roman Coliseum, the cathedrals of Europe, and masonry bridges still in use after hundreds of years of wear and tear, encourage us to better understand the art, the mechanics, and the chemistries involved in building and maintaining these structures.

In this seminar, and the resulting publication *Masonry: Materials, Testing and Applications, ASTM STP 1356*, the authors attempt to convey their experiences towards a better understanding of the principles and mechanics involved in designing and building masonry structures. The papers presented do just that.

Beginning with Session I, Materials, the presenters review findings on new additives and materials that are being effectively used to beneficially modify traditional mortars; explain the properties and benefits of Autoclave Aerated Concrete—a relatively new material now available in the United States; an economic overview of the use of brick in building; and the use of X-Ray Fluorescence in the analysis and comparison of limestones and Dolomite.

In Session II, Testing (A), the presenters review methods of evaluating new unbonded capping systems for concrete masonry units as well as quantifying out-of-plane shear strength valves for masonry walls. In Session III, Testing (B), the presenters evaluate the use of ruggedness testing to develop an interlaboratory testing protocol for various types of cement mortars, and discuss the development of an unbonded capping system for clay masonry prisms. In Session IV, Testing (C), the presenters explore the properties of brick and masonry veneer structures in the papers "The Importance of Testing to Evaluate the Effect Masonry Walls Have on High-Rise Building Stiffness" and "In-Situ Evaluation of Pre-Compressed Brick Veneer Using the Flatjack Technique." In Session V, Applications, the presenters summarized the real world application of the proceeding materials and testing presentations by examining actual projects in renovation of existing masonry loft buildings for residential use, and a new measurement system for detecting the degree of grout fill in cement masonry units.

The presentation sessions were followed by a review of the Alan H. Yorkdale Memorial Award, including a review of past recipients by the Yorkdale Committee, and presentation of the 1998 Alan H. Yorkdale Memorial Award by R. H. Brown, chairman of the Award Committee, to Jason Thompson for his presentation of *Tension Lapped Splices in Reinforced Concrete Masonry.*

The Joint Committees of C-1 on Cement; C-7 on Lime; C-12 on Mortars and Grouts for Unit Masonry; C-15 on Manufactured Masonry Units, and the symposium co-chairmen welcome you to review the presentations and profit from the information presented by the participants. The effective and economical use of masonry has a wonderful historical background, and a promising future in the building of structures and protection of the world's citizens. To be effective, we must learn and pass on to our future generations the art of evaluating and utilizing these materials.

Joint Symposium committee members are as follows: Donald M. Taubert and Tim Conway (C-1); Joseph H. Brisch and Harry L. Francis (C-7); Bruce S. Kaskel (C-12); Dianne B. Throop and John H. Matthys (C-15).

Joseph H. Brisch

Rockwell Lime Company
Manitowoc, WI
Symposium cochairman and coeditor

Harry L. Francis

Elliston, VA
Symposium cochairman and coeditor

Robert L. Nelson

Robert L. Nelson & Associates
Schaumburg, IL
Symposium cochairman and coeditor

Sung Gun Chu[1], Thomas J. Podlas[2], and Teng Shau Young[3]

New Polymer Additives for Mortar Cement

REFERENCE: Chu, S. G., Podlas, T. J., and Young, T. S., **"New Polymer Additives for Mortar Cement,"** *Masonry: Materials, Testing, and Applications, ASTM STP 1356*, J. H. Brisch, R. L. Nelson, and H. L. Francis, Eds., American Society for Testing and Materials, West Conshohocken, PA, 1999.

ABSTRACT: Mortar cement is a hydraulic cement similar to masonry cement in use and function, introduced to enhance one or more of the latter's properties, such as workability, durability, and water retention. In addition, mortar cement must have lower air content, and it has minimum flexural bond strength requirements. In response to fulfilling these needs, a new family of water soluble polymers has been developed. The new polymer additives are designed to optimize air void distribution and rheology of wet mortar, allowing improved workability with low air content. Furthermore, these polymers impart high water retention to the mortar, and allow the production of mortar with enhanced board life and flexural bond strength.

KEYWORDS: mortar cement, mortar rheology, flexural bond strength, workability, water retention, board life, air content, adhesive failure, cohesive failure

In 1996, flexural bond strength (FBS) requirements were included in the ASTM Standard Specification for Mortar Cement (C 1329). Flexural bond strength is important for the structural integrity of masonry walls subjected to lateral loads. In areas of high seismic activity and wind shear, flexural bond strength is important to masonry construction *[1]*. At issue is the need to meet C 1329 low air and high flexural bond strength specifications without any loss of workability or other desirable mortar properties. Table 1 reviews the requirements of select mortar products.

[1]Senior Research Scientist, Hercules Incorporated, Aqualon Division, Research Center, 500 Hercules Road, Wilmington, Delaware, 19808.
[2]Research Scientist, Hercules Incorporated, Aqualon Division, Research Center, 500 Hercules Road, Wilmington, Delaware, 19808.
[3]Program Manager, Hercules Incorporated, Aqualon Division, Research Center, 500 Hercules Road, Wilmington, Delaware, 19808

TABLE 1--*ASTM C 1329 Specification of Mortar Cement*

	Mortar Cement Type N	Mortar Cement Type S	Mortar Cement Type M
Flexural bond strength 28 days, min, kPa	483	690	793
Air content of mortar Min, volume % Max, volume %	 8 16	 8 14	 8 14
Compressive strength 7 days, kPa 28 days, kPa	 3,448 6,205	 8,964 14,480	 12,411 19,995
Time of setting, Gillmore method: Initial set, min, not less than Final set, min, not more than	 120 1440	 90 1440	 90 1440
Water retention value, min % of original flow	70	70	70

Masonry mortars based on portland cement/lime blends which do meet flexural bond strength specifications, as well as masonry cements, are available. However, the cement industry is constantly striving to improve mortar properties and masons acceptance of existing products, especially at lower air content *[2]*. Alternatives to replace lime have been sought.

In response to meeting these requirements, water-soluble, cellulose ether-based polymeric additives have been recently developed. Nexton® M20W and Nexton® M21W, introduced by Hercules Incorporated, hereinafter referred to as WSPA and WSPB respectively, has been designed to improve mortar workability over portland cement/lime mortars and masonry cements and enhance other properties so that ASTM C 1329 requirements are met. Hercules laboratory scale evaluations of WSPA and WSPB have demonstrated their efficacy. This work has been done in conjunction with large-scale evaluations under the supervision of V. S. Dubovoy at Construction Technology Laboratories, Inc. (CTL), Skokie, Illinois. Fundamental aspects of the effects of WSPA and WSPB on flexural bond strength, workability, board life, as well as air morphology, water retention, and compressive strength of mortars are presented herein.

Experimental Method

Materials

Water-soluble polymer (WSP): WSPA and WSPB
Air entraining agents (if necessary): ASTM C 260
Portland cement Type I: ASTM C 150
Sands: Graded Silica (Ottawa Sand): ASTM C 144
 20/30 Silica (Ottawa Sand): ASTM C 144
Masonry cement Type S: ASTM C 91
Hydrated lime: ASTM C 207
Mortar cement Type S: ASTM C 1329
Concrete bricks: UBC Standard No. 24-30

Mortar Formulation Details

Cement (Masonry Type S or Portland Type I)	23.8%
Graded silica sand	38.1%
20/30 silica sand	38.1%
WSPA or WSPB	0.02%-0.08%*
Deionized water	as needed for desired flow

*Throughout this publication WSPA and WSPB contents are based on the cement content of the mortars. All ingredients are given as % by weight.

Dry ingredients were mixed with water in a laboratory Hobart mixer, according to ASTM Standard Test Method for Preconstruction and Construction Evaluation of Mortars for Plain and Reinforced Unit Masonry (C 780). Water content was based on desired flow. Air content of mortar was measured at an initial flow of 110 $\pm$5%. Evaluations of workability, water retention, and board life were determined on mortar with an initial flow of 125 $\pm$ 5 %. Mortar workability was subjectively rated based on plasticity, tendency to tear, spreadability, flowability, and trowelability. Initial and 60-minute penetrations were measured to determine the board life of mortar samples.

Flexural Bond Strength Measurement

Flexural bond strength was measured at the Hercules Research Center and CTL. Research Center FBS data were obtained from 5 couplet samples for each formulation. The couplet preparation procedure is described in *[3]*. Cure time was 28 days. FBS was measured according to ASTM Standard Method for Measurement of Masonry Flexural Bond Strength (C 1072). The flexural bond wrench, Soil Test Model ELE CT-400, was upgraded with a computer automated test control and data acquisition system. The flexural bond strength index data reported in Tables 3, 5, 10, and Figure 1 are normalized with respect to the control sample without polymer additive. The FBS data in Tables 2, 6, and Figure 2 are the absolute values in psi.

Air Void Morphology and Failure Mode of Flex Samples

Failure mode photographs of mortar cement (Figure 1) were of couplets following FBS testing.

Air void images (Figure 2) were obtained from thin slices of cured mortar from between unbroken couplets. Mortar samples were impregnated with liquid epoxy under vacuum prior to slicing, and surface polished to distinguish air voids, cement, and sand. The size and distribution of air voids were recorded by computer imaging.

Results

Construction Technology Laboratories Work

Blends of cement clinker and WSPA were prepared with a pilot ball mill at CTL. Mortar formulations and performance data are summarized in Tables 2 and 4. Flexural bond strength was obtained from 30 joints using 6 prisms according to ASTM C 1329. Workability characteristics related to the rate of stiffening of mortars containing WSPA, as shown in Table 4, were determined with CTL's workability apparatus *[4]*. The slope of the workability curve represents a rate of workability loss, thus is directly related to board life, the lower the slope, the longer the board life. Centerline average (CLA) describes cohesiveness or butteriness of mortar under trowel. A higher workability product (WP) value, determined from the area under the workability curve, indicates poorer workability over the board life.

TABLE 2A–*Mortar Formulation (S Type) Prepared at CTL.*
(Based on ASTM C 91 Mortar Cement)

	Weight, kg
Cement	7.10
Graded Ottawa Sand	11.34
20/30 Ottawa Sand	11.34
WSPA	0.0036 (0.05wt%)
Mix Water	3.40
Total	33.1836

TABLE 2B--*Mortar Properties Measured at CTL.*
(Based on ASTM C 91 Mortar Cement)

Properties	Mortar with 0.05 wt % WSPA
Cone penetration, mm	Initial : 51 After 45 mins: 28
Air content, %	12.9
Water retention, %	80
Compressive strength, kPa, after 28 days	33,579
Flexural bond strength, kPa	903

WSPA and WSPB function to contribute improved water retention, good low air workability, and flexural bond strength enhancement. They can be added with the feed at a cement plant finish mill, or as admixtures in a blending operation. Table 3 shows the beneficial changes of mortar properties, obtained by the addition of 0.02 to 0.08 wt% WSPA to mortar formulated with an Eastern U.S. cement. With increasing polymer concentration, air content, water retention, and board life were increased. With this particular mortar, FBS was increased with up to 0.05 %, but decreased with 0.08 % WSPA. It has been demonstrated that approximately 0.05% WSPA is often sufficient to produce a mortar cement with optimum workability and board life, together with high FBS. The exact amount must be determined experimentally for a specific mortar formulation.

The improved mortar properties imparted by WSPA and WSPB, relative to commercial Type S mortar cement and Portland cement/lime blends, are shown in Tables 4 and 5. The effects of WSPB, developed to increase the air content of mortar, are shown in Table 4.

TABLE 3--*Effect of WSPA Concentration on Mortar Properties.*

Mortar with WSPA	Air content (%)	Water retention (%)	Board life (minutes)	Workability[1]	FBS index[2]
Without WSPA[3]	5.6	50	23	1	100
0.02 wt%	7.7	78	45	2	120
0.04 wt%	9.3	84	55	3	120
0.05 wt%	10.5	89	58	4	183
0.08 wt%	11.8	95	53	3	133

1. Workabilty of mortar graded as: 1=Poor, 4=Excellent.
2. FBS index of the control sample (without WSPA) is normalized to 100.
3. Control sample contains 0.004 % air entraining agent.

TABLE 4--*Effect of WSPB on ASTM C 91 Air Content and Workability*

Mortar samples	ASTM C 91 Air content (%)	Workability
Lime mortar (Type S portland/lime)	8.2	2
Blank cement without WSP	8.9	2
0.05 wt% WSPA	9.5	3.5
0.05 wt% WSPB	14.6	4

TABLE 5--*Effect of WSPB on FBS and Compressive Strength.*

Mortar samples	Air content (%)	FBS Index[1]	Compressive strength (kPa)
S Type mortar cement	11.4	100	26,739
Blank cement with 0.055 wt% WSPB	12.2	140	25,222
Type M mortar cement specification	8-14	-	19,995

1. FBS index of the S type mortar sample (without WSPB) is normalized to 100.

The higher FBS of mortars with WSPA and WSPB is believed due, in part, to high water retention properties and improved mortar paste rheology. The WSP-containing mortar can easily penetrate into porous brick surfaces. Consequently, masonry mortars containing WSPA (or WSPB, not shown in Figure 1) show strong adhesion, and a cohesive failure mode, in contrast to adhesive failure mode of the commercial masonry and portland cement/lime mortars. (Figure 1).

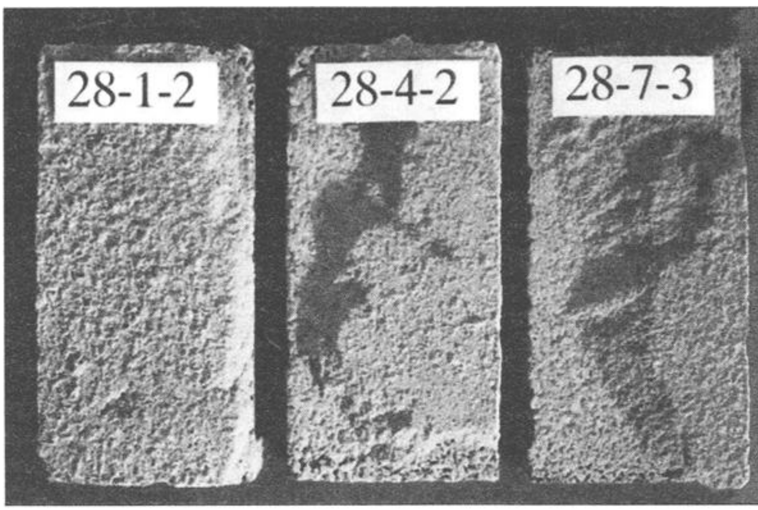

Without polymer	With 0.05% WSPA	With 0.08% WSPA
FBS Index: 100	FBS Index: 180	FBS Index: 133
Adhesive failure	Cohesive failure	Cohesive failure

FIGURE 1--*Effect of WSPA on FBS and Bond Failure Mode.*

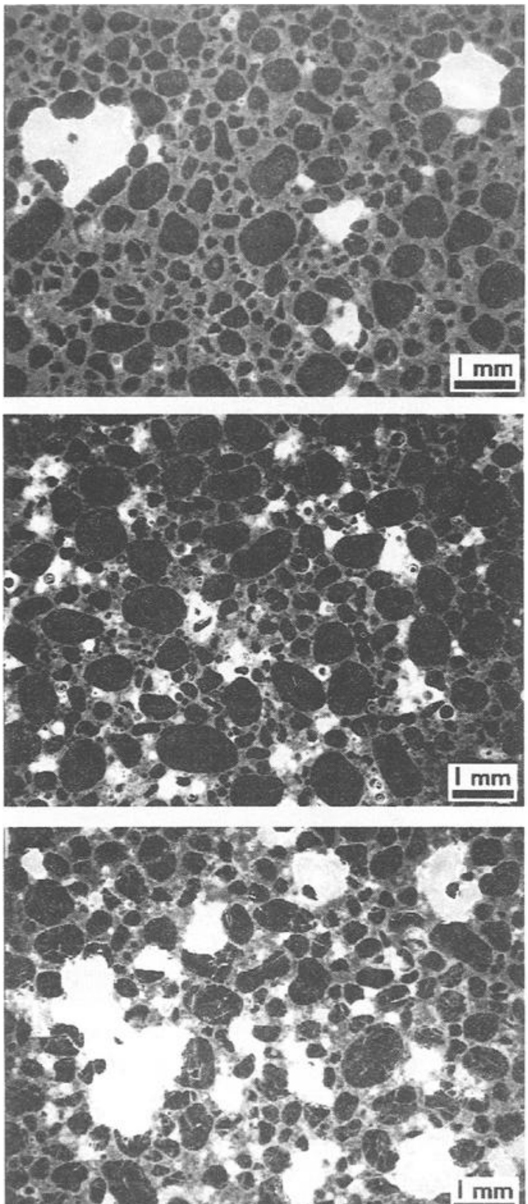

Mortar
without additive
5.6% air, large voids
FBS 683 kPa

Mortar
with 0.08 wt% WSPA
11.2 % air, small voids
FBS 938 kPa

Mortar with 0.0032 wt%
air entraining agent
13.7 % air, large voids
FBS 455 kPa

FIGURE 2--*Effect of Additives on Air Void Distribution of Various Mortars.*

Air voids are the lightest images. Darkest images are sand.

Air void characteristics in mortar with WSPA are shown in Figure 2 and described in Table 6. Couplets were prepared using cement from a Central U.S. location and were cured for 28 days. Mortar with WSPA showed a more homogeneous distribution of fine air bubbles compared to the control mortar and another with a conventional air entraining agent. The more homogeneous distribution and smaller size of the air bubbles result in increased FBS, compared to what is obtained when large heterogeneous air voids are present. WSPA also functions to efficiently entrap and stabilize small air bubbles in the wet stage, which enhances the workability and other important properties of mortar cements and other construction products containing Portland cement, gypsum, lime, and limestone.

TABLE 6--*Air Void Analysis and FBS of Mortar Samples.*[1]

Mortar samples	Air content by weight %	Air void size and shape	FBS (kPa)
Without additive	5.6	1.0-2.0 mm large, irregular	683
0.08 wt% WSPA	11.2	0.3-0.5 mm small, homogeneous	938
0.0008 wt % air entraining agent	8.6	0.8-1.0 mm* large, irregular	724
0.0032 wt % air entraining agent	13.7	0.8-1.5 mm large, irregular	455

[1]Refer to Table 2A for formulation.
*Not shown in Figure 2.

Mortars containing 0.02 to 0.08 wt% WSPA displayed lower paste viscosity and plasticity at needed flows. They were easier to mix than controls. This is believed to result from high water retention capacity and dispersing power of the polymer which was confirmed by CTL's data (Table 7). The mortar with 0.05% WSPA gave a better workability rating (A-), lower workability product value, lower centerline average (CLA), and slope in the plot of stylus pressure and time. The better workability and longer board life of a mortar with WSPB were also confirmed in an industry yard test (see Table 8).

TABLE 7--*Mortar Workability Data Measured at CTL.*

	Mortar without Additive	Mortar with 0.05 wt% WSPA	Conventional Mortars*
Workability rating** (Center Line Average)	C 2.05	A- 1.10	C- 1.38-2.43
Workability product	549	238	1060-1410
Board life (Slope)	0.608	0.343	0.848-1.122
Troweling ability	Average	Very Good	Average to Poor

* Reference 3

** A=Excellent, B=Good, C=Average, D=Poor.

As seen in Table 8, mortar with 0.05 wt% WSPB has a higher masons' workability rating (4 vs. 2) and longer board life (94 vs. 70 minutes) compared to S Type commercial mortar. It also outperforms the M Type masonry mortar and the blank without an additive.

TABLE 8--*Effect of WSPB on Mortar Workability. Evaluated in Professional Mason Field Tests.*

Cement base for mortar[1]	Air content (%)	Board life (minutes)	Water retention (%)	Masons grading
M Type masonry	16.2	37	-	1.5
S Type mortar	12.3	70	82	2
Blank cement	10.2	32	-	0.5
Blank cement with 0.05 wt% WSPB	11.0	94	83.5	4

[1]The first, third, and fourth mortars were based on the same clinker/stone ratio of raw materials.

The compatibility of WSPA with commercial masonry cements is illustrated in Table 9. The board life of 4 commercial masonry cements, available throughout the U.S., was extended more than 30% to 70% with addition of 0.04 wt% WSPA.

TABLE 9--*Effect of WSPA on Mortar Board Life.**

Cement base for mortar	Without WSPA, (%) retention after 60 minutes	With 0.04 wt% WSPA, (%) retention after 60 minutes
Upper Midwest, Type N	50	81
Upper Midwest, Type S	49	83
Central, Type M	45	72
Midwest, Type N	72	93

*Board life measured by cone penetration retention after 60 minutes (initial=61-64 mm) at room temperature.

The effect of sand/cement ratios on FBS, with addition of 0.05 wt% WSPA was studied. In Table 10, the performances of the control mortar and of three formulations containing the polymer are shown. Water content was adjusted to give a flow of 125±5%. With increasing sand/cement ratio from 3.2 to 3.6, no significant deterioration of mortar workability was noted. The mortars with the higher sand concentration require more water to maintain desired flow, but they still gave the needed low air content, water retention, and workability. A total of 20 couplets was prepared for FBS measurements. The control gave a much lower FBS value. Furthermore, FBS values of WSP-containing mortars with higher sand loadings (sand/cement ratio = 3.6) were not significantly different from those of the mortars with the lower sand/cement ratio, showing that WSPA may impart higher sand carrying capacity.

TABLE 10--*Mortar Properties with Varied Sand/Cement Ratio.*

Mortar sand/cement (S/C) ratios	Air content (%)	Flow retention (%)	Board life (minutes)	Workability[1]	FBS index[2]
S/C = 3.2 Control	11.9	-	-	1	100
S/C = 3.2 0.05 wt% WSPA	10.5	89	52	4	180
S/C = 3.4 0.05 wt% WSPA	10.7	85	55	3	173
S/C = 3.6 0.05 wt% WSPA	10.8	86	57	3	200

1. Workabilty of mortar graded as: 1= Poor, 4=Excellent
2. FBS index of the control sample (without WSPA) is normalized to 100.

WSPA and WSPB are compatible with conventional cement admixtures, such as air entraining agents and set retarders. Air content and set times of mortar can be further optimized, if necessary, with conventional admixtures. Cements with WSPA and WSPB have been observed to remain stable after simulated silo storage conditions (7 days aging at 180°F). Table 11 shows the data with WSPA.

TABLE 11--*High Temperature Stability of Mortar Cement Containing WSPA.*

Aging time at 180°F	Viscosity retention (%)
1 day	100
2 days	100
4 days	100
7 days	90

Conclusion

WSPA and WSPB water-soluble polymers have been shown to be efficient functional additives for masonry and mortar cements. Masonry mortars containing these new polymers have exhibited improved physical properties and workability at low air with respect to existing mortar products. These polymer additives lead to enhanced water retention, which improves wet mortar rheology and gives longer board life and high flexural bond strength.

References

[1] Hedstrom, E. G., Tarhini Kassim, M., Thomas, R. D., Dubovoy, V. S., Klingner, R. E., and Cook, R. A., "Flexural Bond Strength of Concrete Masonry Prisms Using Portland Cement and Hydrated Lime Mortars", *TMS Journal*,, February 1991, pp. 8-22.

[2] Hime, W. and Martinek, R. A., "Masonry Cements Peas in a Pod, or Apples and Turnips?", *Proceeding of Seventh North America Masonry Conference*, June 1996, p. 785.

[3] Tresouthick, S. W., Dubovoy, V. S., and Gajda, J. W., "Mortar Workability Apparatus: A New Approach", *Cement Concrete, and Aggregates*, CCAGDP, Volume 15, No. 1, 1993, pp. 89-92.

John H. Matthys,[1] and Robert L. Nelson[2]

Structural Properties of Autoclaved Aerated Concrete Masonry

REFERENCE: Matthys, J. H. and Nelson, R. L. "**Structural Properties of Autoclaved Aerated Concrete Masonry,**" *Masonry: Materials, Testing, and Applications, ASTM STP 1356,* J. H. Brisch, R. L. Nelson, and H. L. Francis, Eds., American Society for Testing and Materials, 1999.

ABSTRACT: Autoclaved aerated concrete masonry units are manufactured from portland cement, quartz sand, water, lime, gypsum and a gas forming agent. The units are steam cured under pressure in an autoclave transforming the material into a hard calcium silicate. The autoclaved aerated concrete masonry units are large-size solid rectangular prisms which are laid using thin-bed mortar layers into masonry assemblages. The system and product are not new - patented in 1924 by Swedish architect Johan Eriksson. Over a period of 60 years this product has been used in all areas of residential and industrial construction and in virtually all climates. However, the principal locations of application have been generally outside the U.S. Little information in the U.S. is available on the structural properties of this product. Due to the interest in use of this product in the construction industry and the construction of production plants in the U.S., the Construction Research Center at the University of Texas at Arlington and Robert L. Nelson & Associates conducted a series of tests to determine some of the basic structural properties of this product. This paper presents the findings of those investigations.

KEYWORDS: masonry units, masonry assemblages, autoclaved aerated concrete masonry, thin bed mortar

Autoclaved aerated concrete (AAC) is a building material that was developed in the early 1900's by a Swedish architect, Johan Axel Eriksson. The Swedish Government established thermal insulation standards for building material to alleviate the country's energy crisis that developed after World War I. AAC is a mixture of cement, sand, lime,

[1]Professor, Construction Research Center, University of Texas at Arlington, Arlington, TX 76019.

[2]President, Robert L. Nelson, & Associates, 1220 Remington Road, Schaumburg, IL 60173.

and aluminum powder which when steam cured produces a unique material - one that can be easily cut, drilled, and nailed like wood yet providing durability, strength, thermal insulation and fire resistance like concrete *[1]*. There are several major manufactures of AAC products throughout the world including the major players Ytong, Hebel, and Svanholm. Numerous plants exist in more than 20 countries. Their products are used worldwide in applications for residential and commercial buildings because of AAC's good thermal insulation, simple construction and universal applications. The myriad of construction components available include both unreinforced and reinforced slabs used for floor, roof, and wall construction. In 1994 Ytong developed a new "20kg generation" masonry block to increase construction productivity and minimize associated health problems for masons. All of the AAC construction products have been well received outside the continental United States. To address the need for evaluating the physical properties of AAC and provide guidance on non structural and structural application the European standard organization RILEM, established in the 1980's two committees: (1) The RILEM Technical Committee 78-MCA (Model Code for autoclaved aerated concrete based on RILEM Test Methods), and (2) RILEM Technical Committee 51-ALC (Test Methods for Autoclaved Lightweight Concrete) to prepare recommendations for test methods to characterize relevant properties of AAC. These two committees worked in cooperation for about 10 years with their efforts presented in a RILEM recommended practice *[2]*, and an international symposium on autoclaved aerated concrete *[3]*.

Ytong, along with other major manufactures of AAC products, is entering the U.S. design/building market. Several manufacturers have or are building major production facilities within the U.S. Before embracing this product the U.S. design community would probably insist that

1. appropriate standards to specify the material, to evaluate the physical properties and to provide appropriate test methods be developed through a national consensus organization such as ASTM.

This is currently in progress through ASTM committee C27 and C15.

2. appropriate physical testing to qualify as a recommended research report and eventual inclusion of provisions into national material design codes and specifications for AAC masonry material.

Ytong contracted with Robert L. Nelson & Associates to conduct a research investigation on some of the basic physical properties of AAC and on the performance of masonry assemblages built with Ytong block manufactured in Europe. At the time of this project no U.S.A. standards existed specifically to determine physical properties of AAC masonry material or masonry assemblage performance. The evaluations were to be made using current existing ASTM masonry test procedures to generate information that could be assessed. Such data might assist in the preliminary acceptance of this material by the U.S. professional design community.

Project Scope

Robert L. Nelson & Associates conducted the following masonry unit material evaluations and unit masonry prism evaluations using the indicated existing ASTM masonry standards.

1. AAC Unit Compressive Strength - ASTM C 140 "Test Methods of Sampling and Testing Concrete Masonry Units"
2. AAC Unit Shrinkage - ASTM C 426 "Test Method for Drying Shrinkage of Concrete Block."
3. AAC Prism Compressive Strength - ASTM C1388 "Test Methods for Compressive Strength of Laboratory Constructed Masonry Prisms."
4. AAC Bond Strength - ASTM C1390 "Test Method for Flexural Bond Strength of Masonry."

The Construction Research Center at the University of Texas at Arlington conducted the following AAC masonry assemblage tests using the indicated existing ASTM masonry standards.

1. Flexural Strength - ASTM E 72 "Standard Methods of Conducting Strength Tests of Panel for Building Construction."
2. Shear Strength - ASTM C1391 "Standard Test Method for Diagonal Tension (Shear) in Masonry Assemblages."

Two densities of AAC masonry units were evaluated: 25 pcf and 31 pcf. All units, material, and construction tools were shipped from Germany for these tests to the two sites in the U.S.

Construction and Testing

The AAC unit compressive strength was determined by evaluating ten nominal 4"x4"x4" cube specimens loaded perpendicular to the normal bed surface for each density type. Each specimen was capped with hydrocal. ASTM C 140 test procedure was followed.

The AAC unit absorption was determined, by evaluating 5 nominal 8"x8"x24" specimens for absorption in lb/cu.ft and % for each density type. ASTM C 140 procedures were followed.

The AAC unit drying shrinkage was determined by evaluating 3 specimens 8"x8"x24" of each density type according to ASTM C 426 procedures.

The AAC masonry prism compressive strength was determined using ten stack bonded prism 2 units high per density type built with nominal 8"x8"x24" units in stretcher position and tested according to ASTM C1388.

The AAC masonry bond strength was determined using five stack bonded prisms 3 units high built with nominal 8"x8"x24" units in the stretcher position and tested according to ASTM C1390 except that single point centerline loading was used.

Numerous tests over the years have been used to attempt to measure masonry assemblage shear capacity. Historically the most commonly used method was the ASTM E 72 racking test. Due to the size of the required specimen along with the indeterminate nature of the forces in the hold down tie rod for that test, various attempts have been made to generate a better shear test. To evaluate the shear capacity of the AAC masonry assemblages ASTM C1391 was selected. The ASTM C1391 standard test method covers determination of the shear strength of 4 ft x 4 ft masonry assemblages by loading them in compression along one diagonal, thus causing a diagonal tension failure with the specimen splitting apart parallel to the load direction. Three like specimens of each density unit were constructed in running bond on 8"x8"x24" units using full head and bedjoints of thin bed mortar. Specimens were stored in a temperature controlled laboratory. Each specimen was transported to a 400,000 lb. testing machine, and then seated in a centered and plumb position in a bed of hydrostone capping material in a lower loading shoe. After 4 hours curing the top loading shoe was centered and plumbed on the specimen. The hydrostone cap was allowed to cure two days prior to testing. Up to half of the maximum load was applied within five minutes, the remaining load was applied at a uniform rate so that the maximum load was reached within two minutes. The failure pattern was noted.

For evaluating flexural capacity of AAC masonry assemblages the test method needed to be recognized by the design community as representative of that encountered in service. ASTM E 72 was selected. Three specimens per unit density were constructed in running bond for determining flexural strength perpendicular to the wall bed joints. Specimens were 4 ft x 8 ft and tested in the vertical position. The walls were built on a steel channel resting on a cylindrical bar to simulate a "pinned" end condition. The wall was simply supported at top and bottom by a cylindrical pipe which is part of the reaction frame. A heavy duty air bag was placed between the wall test specimen and the reaction frame. Air was introduced at one end of the bag while being monitored by a liquid manometer at the other end to determine pressure on the wall at individual load increments. The failure pattern of each wall was noted.

Results

The unit compressive strengths for the 25 pcf and 31 pcf density units are given in Tables 1 and 2 respectively. The values were reasonably high ≈ 350 psi and extremely reproducible (cov ≈ 1.6%).

The unit absorptions for the 25 pcf and 31 pcf density units are given in Tables 1 and 2 respectively. Average absorption was approximately 12 pcf with coefficient of variation of about 1.3%.

The individual unit drying shrinkage values for the 25 pcf and 31 pcf density units are given in Table 3. The average percent shrinkage for the 25 pcf density unit was 0.06 while that for the 31 pcf density unit was 0.04%.

The unit prism compressive strengths for the 25 pcf and 31 pcf density units are given in Table 1 and 2 respectively. The averages were reasonably close to the average unit compressive strength values indicating minimal effect of mortar joint. The coefficients of variation were extremely small.

TABLE 1 - *Physical Properties Units & Prisms - 25 pcf Density.*

TEST NO.	MASONRY UNITS			MASONRY PRISMS	
	Compressive Strength psi	Absorption		Compressive Strength psi	Flexural Strength psi
		pcf	%		
1	328	12.0	43.2	322	115.3
2	321	11.7	42.2	321	115.0
3	319	11.8	42.5	315	114.5
4	332	12.0	43.2	320	114.3
5	328	12.0	43.1	317	115.0
6	325	--	--	315	--
7	320	--	--	319	--
8	317	--	--	322	--
9	329	--	--	323	--
10	331	--	--	316	--
Average	325	11.9	42.8	319	114.8
Standard Deviation	5.37	0.14	--	3.06	0.41
COV	1.7%	1.2%	--	1.0%	0.4%

MD:prism.tbl

TABLE 2 - *Physical Properties Units & Prisms - 31 pcf Density.*

TEST NO.	MASONRY UNITS			MASONRY PRISMS	
	Compressive Strength psi	Absorption		Compressive Strength psi	Flexural Strength psi
		pcf	%		
1	394	12.3	40.0	361	93.7
2	383	12.1	39.4	369	93.2
3	391	12.0	39.1	365	93.5
4	375	11.9	38.9	373	93.1
5	381	12.3	40.1	375	93.5
6	385	--	--	368	--
7	392	--	--	364	--
8	387	--	--	370	--
9	393	--	--	373	--
10	389	--	--	372	--
Average	387	12.1	39.4	368	93.4
Standard Deviation	6.06	0.18	--	4.52	0.25
COV	1.6%	1.5%	--	1.2%	0.3%

MD:prism2.tbl

Table 3 *Drying Shrinkage of AAC Units.*

Unit Density		25 pcf			31 pcf		
Unit Number		1	2	3	1	2	3
Received Weight - lb		16.9200	17.1300	17.3100	19.1500	18.6300	20.1500
48 h Sat. Weight - lb		23.0600	22.8100	22.9300	24.6600	24.7500	25.1100
Initial Reading - in.		0.0033	0.0101	0.0204	0.0162	0.0213	0.0310
5 day Dry	Wt. (lb)	16.5900	16.8300	16.8900	17.9900	16.1500	18.2100
	Read (in.)	-0.0022	0.0050	0.0151	0.0141	0.0193	0.0294
	% Shrink	0.0550	0.0510	0.0530	0.0210	0.0200	0.0160
48 h Dry Period 1	Wt. (lb)	15.7000	16.1500	16.2100	17.0100	17.3100	17.2300
	Read (in.)	-0.0029	0.0044	0.0145	0.0137	0.0187	0.0282
	% Shrink	0.0620	0.0570	0.0590	0.0250	0.0260	0.0280
48 h Dry Period 2	Wt. (lb)	14.8500	15.0300	14.9700	16.1300	17.6100	17.1000
	Read (in.)	-0.0029	0.0042	0.0144	0.0127	0.0170	0.0272
	% Shrink	0.0620	0.0590	0.0600	0.0350	0.0430	0.0380
% Average Shrinkage		0.0600%			0.039%		
Standard Deviation, S		0.00153			0.00404		
Coefficient Variation, COV		2.5%			10.4%		

MD:table3

Table 4 *Wall Shear Strength.*

Specimen Number	Unit Density pcf	Test Age Days	*w* in.	*h* in.	*t* in.	S_S psi	Average Shear psi	*S* Std. Deviation psi	COV %
1	25	53	47 1/4	47 1/4	7 13/16	34.5			
2	25	60	47 1/4	47 1/4	7 13/16	46.9			
3	25	53	47 1/4	47 1/4	7 13/16	40.6	40.7	6.2	15.2
1	31	70	47 3/8	47 3/8	7 13/16	40.1			
2	31	72	47 1/4	47 1/4	7 13/16	43.1			
3	31	78	47 1/4	47 1/4	7 13/16	46.5	43.2	3.2	7.4

Table 5 *Wall Flexure Strength.*

Specimen Number	Unit Density pcf	Test Age Days	H_2O in.	Failure +/-	Δ* in.	*fr* psi	Average *fr* psi	*S* psi	COV %
1	25	53	18"	-1	0.06	61.9			
2	25	60	14"	-1	0.06	48.7			
3	25	53	20"	0	0.04	72.2	60.9	11.8	19.4
1	31	70	16"	-2	--	50.9			
2	31	72	18"	+1	0.05	64.2			
3	31	78	19"	0	0.04	72	61.7	9.8	15.9

MD:tbl4

The unit prism flexural bond strengths for the 25 pcf and 31 pcf density units are given in Tables 1 and 2 respectively. Failure occurred by tension failure through the unit for all specimens. The amount of scatter in the data was extremely small. The unit prism flexural bond strength of the 25 pcf density units was 15 to 20% higher than that of the 31 pcf density units.

The results of conducting ASTM E 519 shear test on three like specimens of running bond masonry assemblages, built with 25 pcf and 31 pcf density units are given in Table 4. The average shear strength of 43.2 psi for the 31 pcf density specimens was only slightly larger than the average shear stress of 40.7 psi for the 25 pcf density assemblages. Coefficients of variation were quite good for masonry type construction. The failure patterns of the six specimens were basically ideal - a vertical crack from the top loading shoe down to the bottom loading shoe. The strength of the AAC unit material controlled the shear failure performance rather than the mortar joint materials as is commonly associated with clay and concrete block masonry.

In the national MSJC masonry code *[4]*, the allowable in plane shear for running bond masonry with conventional mortar is the smallest of (1) $1.5\sqrt{f'm}$. (2) 120 psi or (3) $v+0.45\ N_v/A_n$. Assuming f'm of 368 psi for the 31 pcf prism test data, the allowable shear stress would be 28.6 psi, based on $1.5\sqrt{f'm}$. By direct comparison the shear data indicates a factor of safety of approximately 1.5.

The results of conducting ASTM E 72 flexure test on three like specimens of running bond assemblages built with 25 pcf and 31 pcf density units are given in Table 5. The average flexural strengths are virtually identical for both densities. The failure pattern of five of the six specimens consisted of a horizontal crack through the unit material along the wall centerline, on one course above centerline (+1), or one course below centerline (-1). The first wall of the 31 pcf density unit showed a failure surface indicating half of the failure occurred in the joint material and half of the failure occurred in the unit. This wall was the first specimen built by the mason and its failure possibly could be associated with below average construction. In the MSJC masonry code the allowable tension normal to the bedjoint for conventional non-air-entrained type S mortar with clay or concrete block is 40 psi. By direct comparison these flexure data suggest a factor of safety of approximately 1.6.

Conclusions and Recommendations

1. The compressive strength of the units varied according to the density of the unit and were extremely reproducible.
2. The absorption characteristics were relatively constant.
3. The drying shrinkage behavior was as expected.
4. The unit prism compressive strength values mirrored the density of the units.
5. The unit prism flexural strength exhibited a 20% larger capacity for the less dense units.
6. The failure modes for shear were as anticipated and extremely reproducible. The capacity was controlled by the block material.

7. The failure modes for flexure were as anticipated and reproducible. The capacity was controlled by the block material.
8. More testing needs to be conducted to statistically validate the results.
9. Shear testing for specimens with application of axial load needs to be conducted.
10. Flexure testing for walls spanning horizontally (tension parallel to bedjoint) should be conducted for verification purposes.
11. Bond wrench testing on stack bonded prisms for comparison to full-scale wall tests is encouraged to eliminate full-scale wall tests and provide an easier test for quality control purposes.

References

[1] Barnett, R. "Autoclaved Aerated Concrete," Technical Presentation at The Masonry Expo. February 1998.

[2] Autoclaved Aerated Concrete - *Properties, Testing and Design*, S. Aroni, G.J. de Grout, M.J. Robinson, G. Suanholm, F.H. Wittman, Eds., E&FN Spon, 1993, 404 p.

[3] Advances in Autoclaved Aerated Concrete, Wittmann, F.H., Ed. Proceeding 3rd RILEM International Symposium on Autoclaved Aerated Concrete, ETH Zurich, Balkema, Rotterdam.

[4] Building Code Requirements for Masonry Structures (ACI 530-95/ASCE 5-95/TMS 402-95) 1995.

Clayford T. Grimm,[1] and Brent Gabby[2]

U.S. Brick Econometrics: 1930-1992

REFERENCE: Grimm, C. T. and Gabby, B., "**U.S. Brick Econometrics: 1930-1992,**" *Masonry: Materials, Testing, and Applications, ASTM STP 1356,* J. H. Brisch, R. L. Nelson, and H. L. Francis, Eds., American Society for Testing and Materials, 1999.

ABSTRACT: Nine graphs illustrate econometric patterns of change that have occurred in the U.S. brick industry for well over six decades. Production is related to population, building activity, construction cost, brick price, and the mason trade. Eight sources of statistical data are cited. No explanation is given for the social, economic, or political reasons for the patterns of change. A loss of market share with time is clearly evident.

KEYWORDS: brick, building, construction, consumption, cost, market, mason, population, price, production

Introduction

It is difficult to know where you are or where you might go, if you do not know where you have been. Knowledge of the past is an aid to the interpretation of the future. [*2*]. History, it is said, can make men wise [*3*], and statistics are indispensable to historical analysis [*4*].

There seem to be two main issues in the study of history: the patterns of change and the causes for those patterns. With a few obvious exceptions this paper addresses only the patterns of change in US unglazed brick production between 1930 and 1992 and the relationship of that production to population, building activity, building cost, brick price, and the number of available masonry production workers. As Herodotus said, "The absence of romance in my history will detract somewhat from its interest, but if it be judged useful by those inquirers who derive an exact knowledge of the past...,I shall be content"[*1*].

1. Consulting Architectural Engineer, 1904 Wooten Dr, Austin, TX 78757-7702
2. Architectural Conservator, Simpson, Gumpertz & Heger, Inc, 297 Broadway, Arlington, MA 02174.

US Unglazed Brick Production vs. Population

Figure 1 is a plot of US annual unglazed brick production for the years 1930-1992 [*4, 5*]. The figure includes a third-degree polynomial best-fit curve. The greatest number of brick produced during that period was 8.71 billion in 1973, after which there was a general decline. It is obvious that depressions and wars have an adverse affect.

Figure 2 is a plot of US annual unglazed brick production per capita for the years 1930-1992 [*4-6*]. The maximum was achieved in 1956 at 48.4 brick per person. Since that time there has been a rather steady decline. A third degree polynomial best-fit curve is shown on the graph.

Figure 3 is a plot of US annual unglazed brick production vs. population. As population increased above 200 million, brick production declined [*4-6*]. The figure includes a third degree polynomial best-fit curve for the data.

Data are available from which regional per capita brick production may be determined. However, because of the considerable inter-regional and international shipments, little historical data are available on regional brick consumption prior to 1986. Note (Table 1) that the 1970 consumption varied more than eight-fold between regions. [*7*].

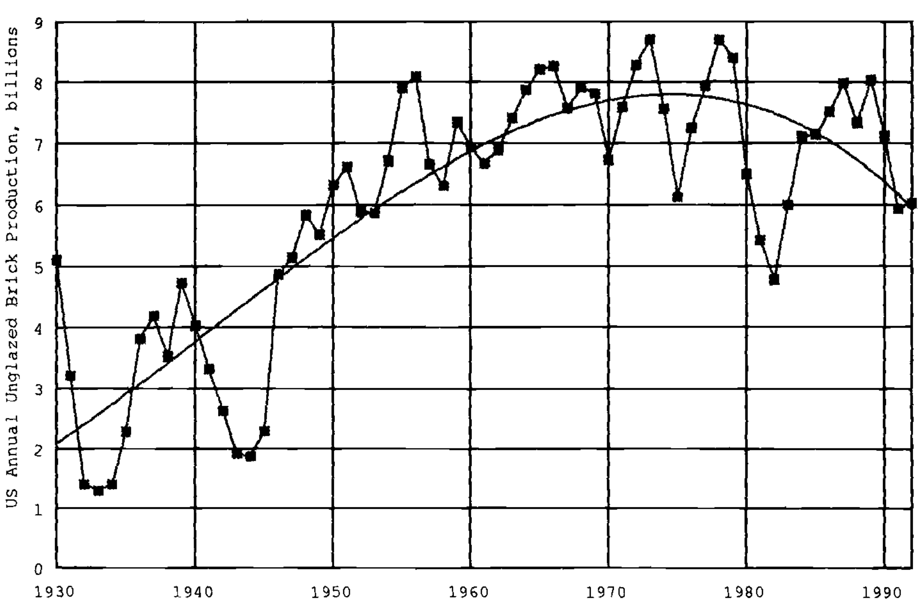

FIG.1 U.S. annual unglazed brick production vs. time.

TABLE 1.
1970 U.S. brick consumption per capita by census divisions.

Division	Estimated 1970 Brick Consumption per Capita[7]
New England	18.6
Middle Atlantic	23.0
East N. Central	34.4
West N. Central	21.4
South Atlantic	63.1
East South Central	52.7
West South Central	35.0
Mountain	21.9
Pacific	7.5
US Total	31.9

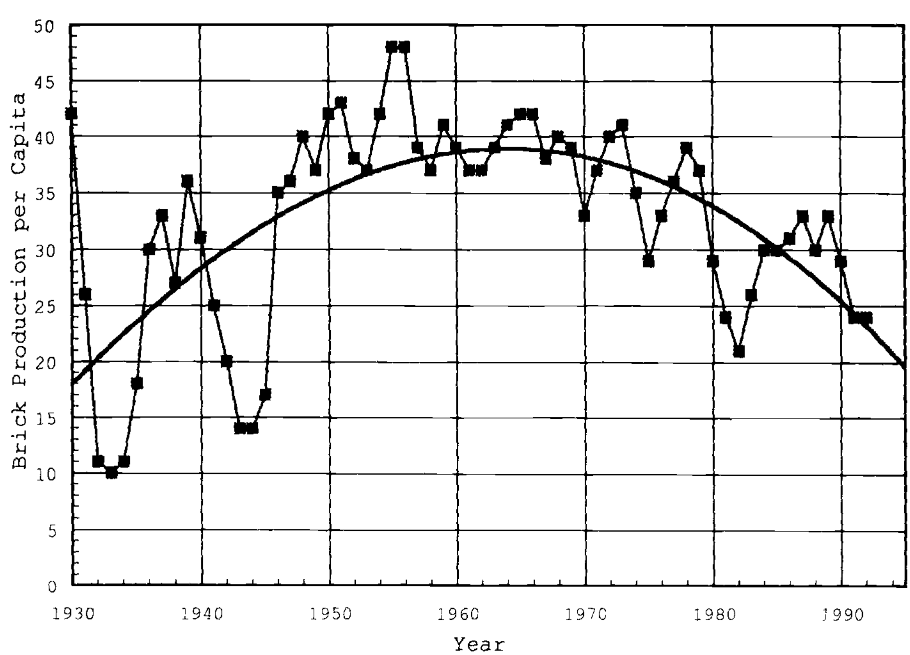

FIG.2--Unglazed brick production per capita vs. time

Brick Production per Square Foot of Building Construction

Figure 4 shows the time relationship of building construction floor area [*4, 8*]. The figure contains a third-degree polynomial best-fit curve. Maximum annual building construction floor area during this period was 4.101 million sq ft (0.381 million sq m) in 1978. After World War II annual building construction floor area increased steadily until 1970, when large fluctuations began to occur.

Figure 5 is a plot of US annual unglazed brick production per 1000 sq feet of building construction floor for the years 1930-1992 [*4, 5, 8*]. The figure includes a second- degree polynomial best- fit of that ratio over the same period. The maximum was achieved in 1930 when 10,012 unglazed brick were produced per sq ft of building construction. From 1930 to 1970 there was a rather steady decline, subsequent to which the ratio has been rather constant. This graph clearly shows that brick has lost market share over time. Again it is obvious that war is a deterrent to brick production.

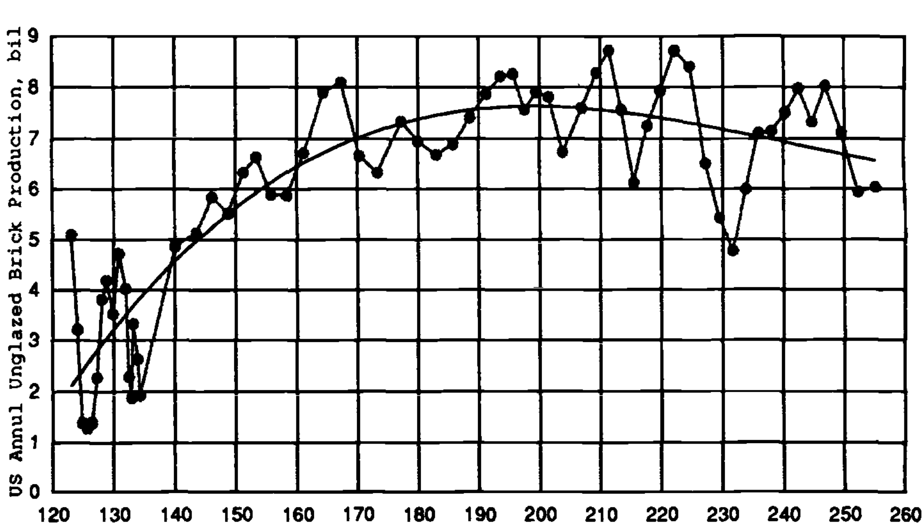

FIG. 3--U.S. annual unglazed brick production vs. population

US Unglazed Brick Price

Figure 6 is a plot of the wholesale price of US unglazed brick for the years 1930-1993 [4, 9]. During the 1970's the price of brick increased 187%, while the Engineering News-Record Building Construction Cost Index rose only 118% and the all-item consumer price index increased only 112% [10].

Figure 7 is a plot of wholesale brick price vs. annual building construction floor area [8, 9].

Figure 8 is a plot of the ratio a US unglazed brick price index (1930=100) to an ENR building construction cost index (1930=100) for the years 1930-1992. The figure includes a straight line best fit of those data [4, 9, 11]. From 1930 to 1969 brick was relatively more expensive than building generally. During most of the 70's brick was rather relatively less expensive than building generally, but in 1979 through 1982 brick prices were relatively high. After that brick prices were more in line with building costs.

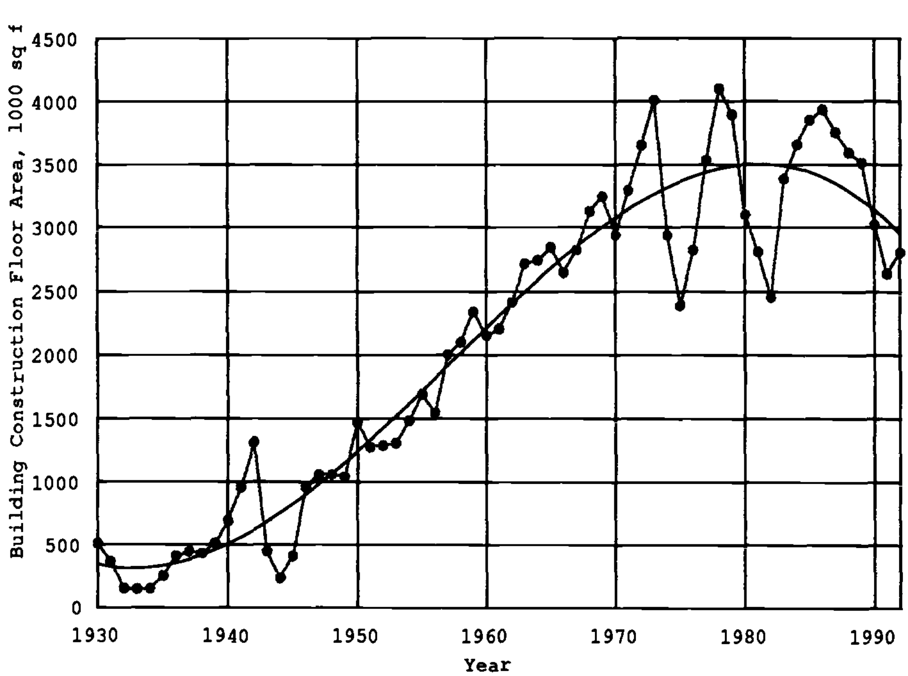

FIG. 4—Annual Building Construction Floor Area vs. Time

Brick Production Per Masonry Construction Worker

The ratio of US annual unglazed brick production to the number of masonry construction workers declined 15% in the quarter century 1967-1992 [*4, 5, 12*]. Figure 9 shows the variation over that period and a straight-line best fit of the data.

In a 1972 report to what is now the Brick Industry Association the Arthur D. Little, Inc. said, "We regret to say that the quality and extent of statistics available from the US brick industry are nothing short of disgraceful..."[*7*]. Some 14 years later the Brick Institute of America began issuing an annual *Brick Sales & Marketing Report*, which provides data on shipments from about two thirds of the nation's manufacturing plants. These reports include information on shipments by unit type, sales method, end use, and destination.

The Bureau of Census, *Current Industrial Reports*, "Clay Construction Products," Series MQ32D, provides quarterly data on brick production quantity, shipments quantity, and value of shipments by census region and for several states.

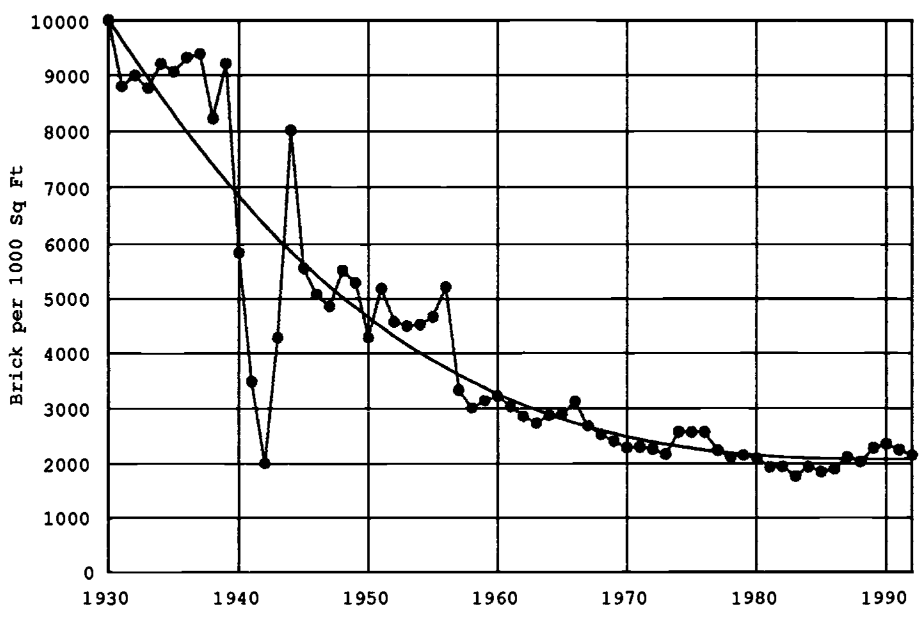

FIG. 5 —*ratio of US annual unglazed brick production to annual building construction floor area vs. time.*

Conclusions

The graphs herein illustrate national patterns of change, which have occurred in the brick industry for well over six decades. Production has been related to population, building activity, construction cost, and the mason trade.

These statistics are crude. They are useless as a marketing tool. No attempt has been made to address the social, economic, and political reasons for the patterns of change. Yet the data do illustrate gross market loss and should warn against further diminution.

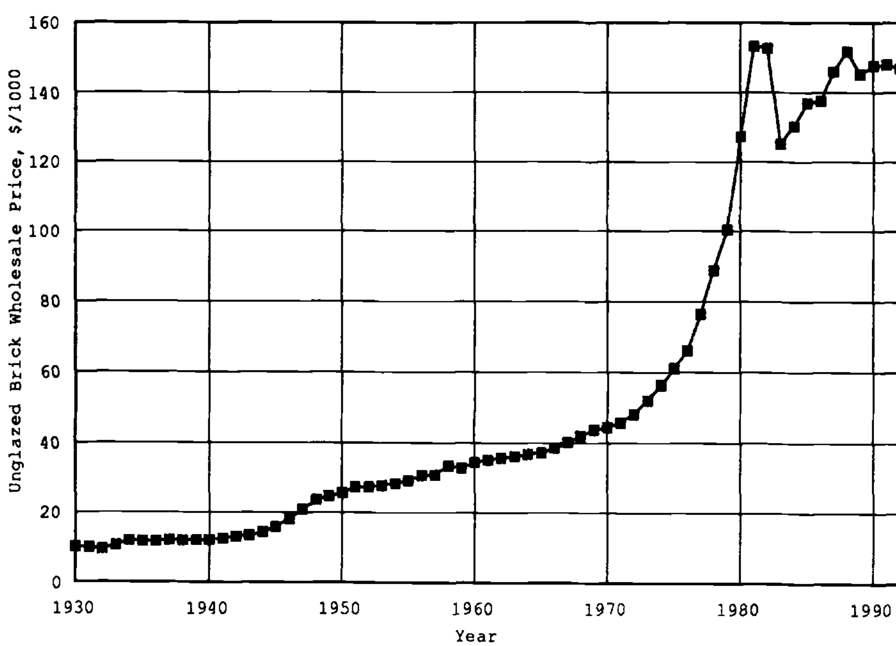

FIG.6--U.S. annual unglazed brick wholesale price vs.time

References

[1] Herodotus: "The History of Herodotus, c. 454 BC, Hutchins, Robert Maynard (Ed.): "History, " *Great Books of the Western World*, Encyclopaedia Britannica, Inc, Chicago, IL, 1952, p. 713.

[2] Thucydides: "History of the Peloponnesian War", c. 435 BC, Hutchins, Robert Maynard (Ed.): "History, " *Great Books of the Western World*, Encyclopedia Britannica, Inc, Chicago, IL, 1952, p. 718.

[3] Bacon, Francis, *Of Studies*, 15611626.

[4] Year: References 2 through 6 are excerpts from: US Bureau of the Census, *Historical Statistics of the United States, Colonial Times to 1957*, Washington, DC, 1960. For Sale by the Superintendent of Documents, US Government Printing Office, Washington, DC. [Data exclude Alaska and Hawaii.

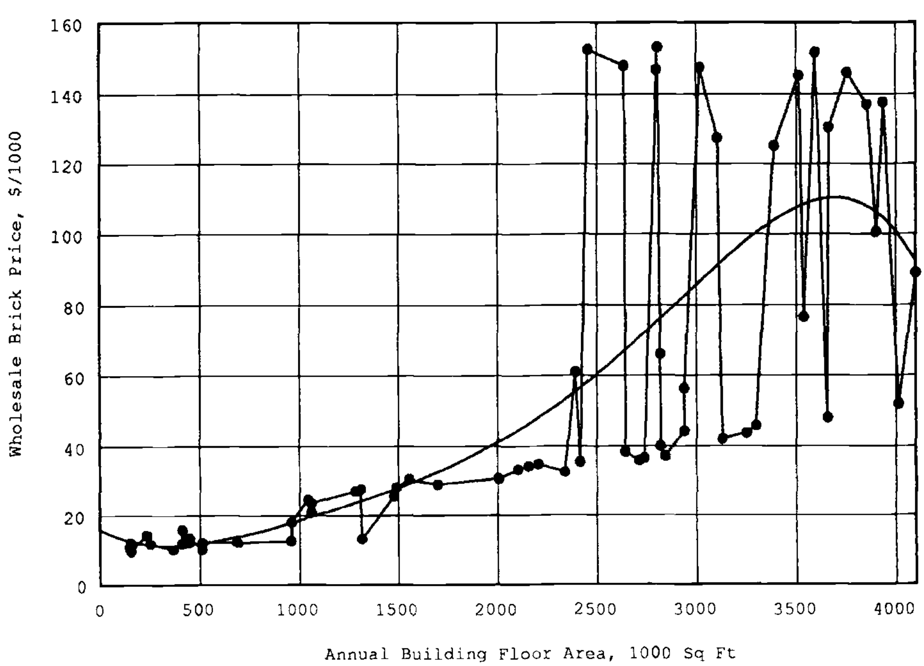

FIG. 7 --brick price vs. annual building construction floor area.

[5]Common and Face Brick Production, 1869-1957: Source: 1919-1939 (biennially), 1947, and 1954, *Census of Manufactures*, reports for various years; 1913-1956, *Bureau of the Census, Statistical Abstract of the United States*, various issues, 1925-1958; 1957, Bureau of the Census, *Facts for industry*, series M32D. Brick production statistics are not available for the years 1940, 1941, and 1942. Production for those years was estimated by interpolation on a straight line basis. Beginning with 1943, common and face brick are classified as "unglazed" brick.

[6] Estimated Population of the United States, 1790-1957: Source: 1900-1957, Bureau of the Census, *Current Population Reports*, Series P-25, Nos. 71, 114, 173, and unpublished Census Bureau records. Estimates for 1910-1957 are based on decennial censuses and statistics of births, deaths, immigration, emigration, and Armed Forces. These estimates are as of July 1 and, therefore, may differ from other estimates, which are as of the date of the census.

[7] *The Brick Industry: An Industry at the Crossroads*, Arthur D. Little, Inc., Cambridge, MA, March 1972, p. 17

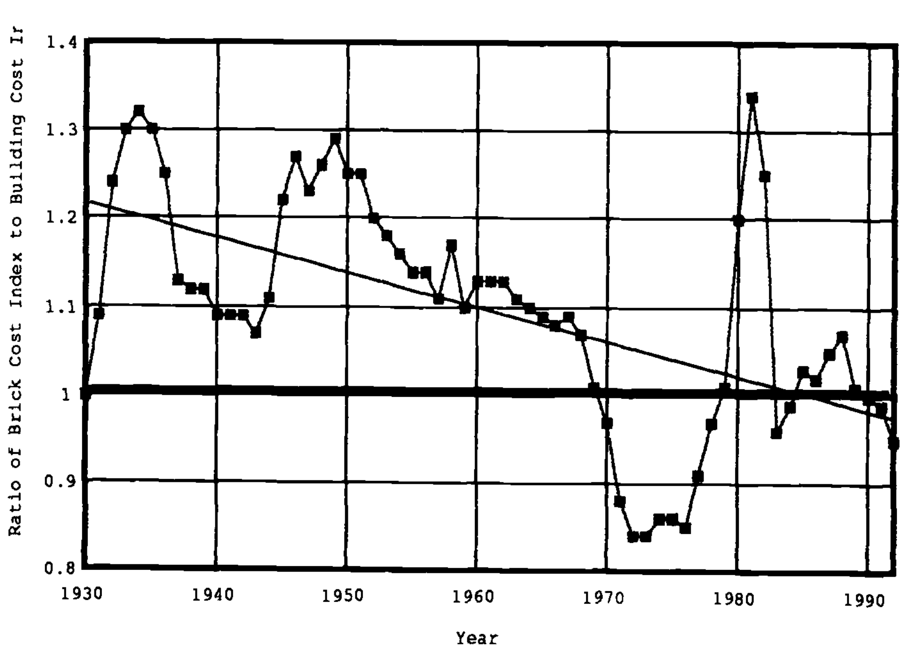

FIG.8—*ratio of US unglazed brick wholesale price index to ENR building cost index*

[8] Construction Contracts Awarded, 1925-1956: Source: F. W. Dodge Corporation, New York, NY. Construction contract statistics, for all categories except privately owned 1- and 2-family houses, compiled by the F. W. Dodge Corporation are based exclusively upon project news reports gathered daily by the Corporation's field staff operating in the 37 Eastern States. This field staff contacts owners, architects, engineers, contractors, financial institutions, real estate brokers, and others able to supply reliable information on construction projects. The figures include new construction, additions, and major alterations at the time the general contract is awarded or when work is about to start if there is no general contract. The figures exclude maintenance and repair work, farm building, shipbuilding, and a sizable proportion of force-account work done by firms and public agencies.

The method of compiling construction contract privately owned 1- and 2-family houses in the 37 Eastern States was changed effective January 1, 1957, and figures for 1947-1956 have been revised to approximate comparable coverage. This revision also affects total construction for the same years. Prior to 1947, the data were based exclusively upon project news reports gathered daily by the corporation's field staff operating in the 37 Eastern States, and have not been revised. For 1957, contract statistics of the 37 Eastern States for the privately owned 1- and 2-family house segments of residential building are based upon building permit information in standard metropolitan areas and a great number of other selected counties plus sampling in the less active areas. All building permit data are adjusted to approximate realistic construction costs.

The 11 Western States not covered are: Montana, Idaho, Wyoming, Colorado, New Mexico, Arizona, Utah, Nevada, Washington, Oregon, and California. The District of Columbia is included in the covered area. Beginning 1957, the source extended coverage for its contract statistics to all of the 48 States. Dodge also publishes those figures in greater detail in *Dodge Construction Statistics Services*, monthly.

[9] Brick Prices, 1849-1957: For 1930-1933, prices are for "Common. Red, Domestic, at New York"; 1933-1947, for "Common building, f.o.b. plant" (composite of approximately 50 firms); for 1947-1957, for "Building brick, f.o.b. plant or New York dock" (composite of approximately 25 firms). Changes in list of firms from time to time did not result in any significant differences in the annual average prices.

[10] US Bureau of the Census, *Statistical Abstracts of the United States*, Washington, DC, annual.

[11] Engineering News-Record Building Cost Index: "Materials and Labor Cost Trends in the US," *Engineering News-Record*, March 19, 1981 and "Market Trends" in the January issue for subsequent years.

[12] Number of Masons: Source - "Masonry, Stone Setting, and Other Stone Work - Special Trade Contractors (Industry 1741)," *Census of Construction Industries*, Superintendent of Documents, US Government Printing Office, Washington, DC 20402, 1967-1992.

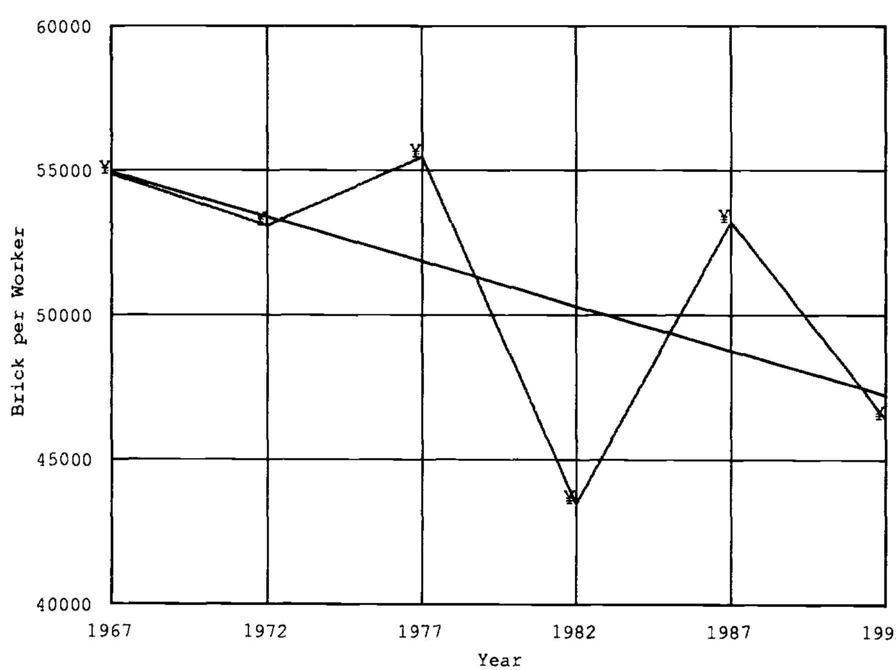

FIG. 9—U.S. annual unglazed brick production per masonry construction worker vs. time current data

Bradner D. Wheeler[1]

Analysis of Limestones and Dolomites by X-ray Fluorescence Spectroscopy

REFERENCE: Wheeler, B. N., "**Analysis of Limestones and Dolomites by X-ray Fluorescence Spectroscopy**," *Masonry: Materials, Testing, and Applications, ASTM STP 1356,* J. H. Brisch, R. L. Nelson, and H. L. Francis, Eds., American Society for Testing and Materials, West Conshohocken, PA, 1999.

ABSTRACT: Sources of calcium are generally widespread and quite extensive. These sources are limestone, dolomite, marl, chalk, and oyster shell. Cement plants account for nearly half of the demand, while two hundred lime plants in the United States and Puerto Rico consume about twenty five percent. Since the chemical composition of the limestone and other sources of calcium is critical in the cement and lime industry, particularly for the deleterious compounds such as sodium oxide, Na_2O, magnesium oxide, MgO, phosphorus pentoxide, P_2O_5, and potassium oxide, K_2O, accurate determinations are critical. Due to the tonnage per hour, these determinations must be made rapidly and accurately. X-ray fluorescence can thereby satisfy this need for accuracy and also precision. Production of lime is performed by calcining limestone or dolomite in which the industry is generally located and concentrated in the States of Michigan, Pennsylvania, and Michigan. The resulting product is quick-lime, CaO, and hydrated lime, $Ca(OH)_2$. Substantial amounts of quicklime is further processed into calcium carbide in order to produce acetylene gas. In this case, the determination of P_2O_5 is critical since minor quantities of phosphorus in acetylene gas can cause premature explosions. Other uses for lime are well known in the treatment of water, the paper and pulp industry, and in the steel industry for the production of slag to remove impurities. Dolomitic lime is heavily utilized in the manufacture of magnesite refractories by reacting dolomitic lime with brines from the Michigan Basin to produce magnesium oxide, MgO, and calcium chloride, $CaCl_2$. Sample preparation for these materials usually is performed by grinding and pelletizing or fusion with lithium-tetra-borate, $Li_2B_4O_7$.

KEY WORDS: Limestone, dolomite, sample preparation, mineralogy, matrix corrections, X-ray fluorescence, α coefficients

Calcium carbonate and calcium-magnesium carbonate in the form of limestone, dolomite, marl, chalk, and oyster shell are one of the most widely used non-metallic materials in the industrial world. The largest use of limestone or calcium carbonate is in the cement industry where it is the source of CaO in the raw feed and also in the concrete industry where it is used as the primary coarse aggregate. Following the cement and concrete industry, the next largest user would be the lime industry.

Geological materials present numerous problems as a result of the preponderance of low atomic numbered elements in a highly variable mineralogical and elemental

[1] Principal Scientist (Retired), Rigaku/USA, 199 Rosewood Drive, Danvers, MA 01923

matrix. X-ray fluorescence can provide the analyst with an accurate and precise method providing the analytical techniques are properly addressed and are consistent from sample to sample. The most serious problems to solve are absorption and enhancement effects, mineralogical differences among samples, and particle size effects which often influence the intensities of the analytical lines. Consequently, relative intensities of a standard and an unknown sample are often only approximate measurements and not directly proportional to the concentration since the matrix, in addition to the concentration of the assayed element as related to the measured characteristic radiation must be corrected for enhancement, absorption, and possible peak overlaps. These matrix effects are generally considered as absorption, enhancement, peak overlaps, mineralogical differences, and non-homongenity of the sample particles. Consideration of these problems, thereby providing a useful and workable procedure by X-ray fluorescence, has been approached by the use of internal standards[1], comparison to standards approximate in composition to the unknows[2], fusion and dilution with transparent materials such as lithium-tetra-borate[3,4,5], reduction of particle size through fine grinding[6,7,8,9], and a series of mathematical corrections[10,11,12,13,14]. The method utilized by the author employs the powder method, fine grinding and pelletizing, and empirical calculations for corrections due to absorption, enhancement, and peak overlaps.

Analysis of any material by X-ray fluorescence is best applied to materials where the compositional range is reasonably small. Calcium/magnesium carbonate rocks fall into this category even though the calcium/magnesium ratios plus the argillaceous fractions are quite variable. In order to successfully apply a X-ray fluorescence technique, the characteristics affecting the accuracy and reproducibility must be identified and corrected. These variables which can promote errors in the analysis are deviations in the particle size, mineralogy, and interelement effects due to varying chemical composition among samples.

Particle size and pelletizing pressure

Reproducible and accurate results by the powder method in the quantitative analysis of mineralogical samples requires proper sample preparation in order to minimize intensity fluctuations as a function of variations in the particle size distribution. Burnstein[15] has illustrated that the fluorescent intensity from a pure material will increase as the particle size is decreased. In limestones and dolomites the intensities from several elements may all increase, decrease, or one may decrease while others increase. Campbell and Thatcher[16], in measuring calcium in Wolframite where the calcium may be present as a carbonate, tungstate, or phosphate supported Burnstein's work. Differences in intensities were observed for equal concentrations of calcium in the three chemical states when the particle size is large as compared to the effective depth of penetration of the incident X-ray. Extensive grinding illustrated that the intensities from the various mineralogical forms approach a common value by reducing the absorption within the individual to a small value (100% minus 325 or

44μ). Figure 1 illustrates the relation of intensity with grinding time or a reduction in particle size Ca-Mg carbonate rocks. Reduction in particle size causes a reduction in the intensities for iron, sulfur, and potassium while the intensities of calcium and silica are increased. As the size of the individual particles are reduced, the intensities stabilize. Further reduction in particle size through continued grinding does not promote any additional improvement in the intensities. Referring to the example on figure 1, the minimum grinding time for a five gram sample would be five minutes. A lesser amount of time could cause significant intensity/concentration deviations among the standards and unknown samples. Now that a grinding time has been established, determining the proper pelletizing pressure must be determined. A similar study was performed as illustrated on figure 2. Examination of figure 2 reveals that in order to reproduce consistent sample pellet, a pelletizing pressure of fifteen tons per square inch is required.

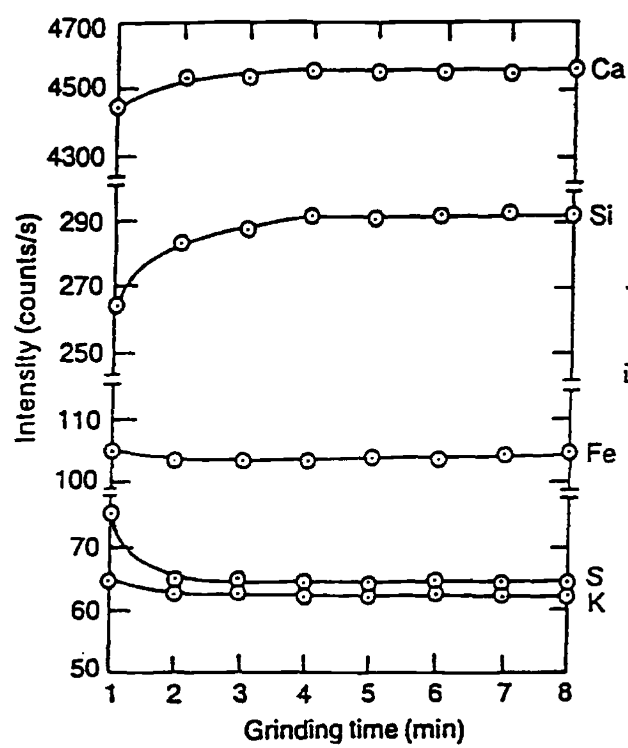

Figure 1. Grinding Time Verses Intensity.

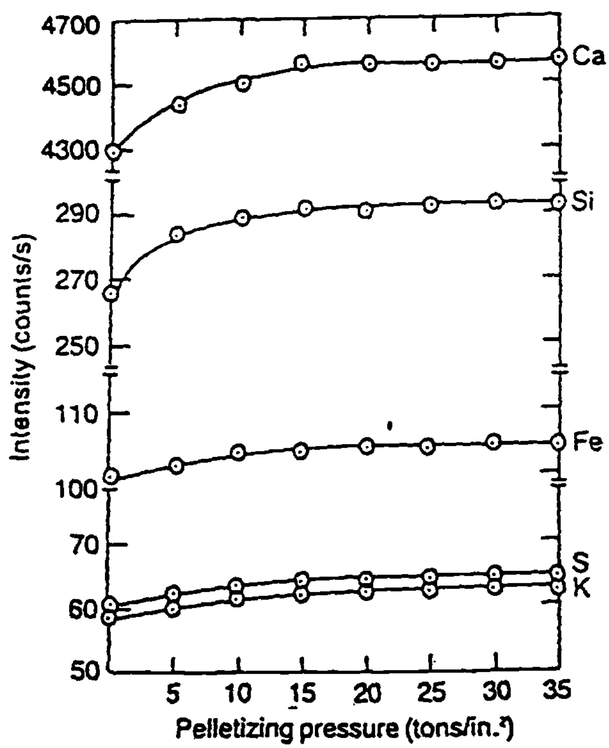

Figure 2. Pelletizing Pressure Versus Intensity.

Interelement effects

Quantitative analysis by X-ray fluorescence of any material requires that the measured intensity of a particular element is proportional to the percent composition. A matrix such as limestone or dolomite may reveal that the intensity of an element may not be directly proportional to the concentration due to the result of an additional characteristic radiation of one element excites another element, enhancement occurs. Absorption is observed when one element in the sample matrix has an absorption edge on the low energy side of the element of interest or has a mass absorption coefficient larger than the element of interest at the energy level of that element. Examples of these effects are illustrated on figure 3 (Mass Absorption Coefficient vs Energy in KEV). Since the Si Kα line occurs just on the high energy of the Al K-edge, secondary fluorescence will take place and conversely, silica is strongly absorbed by aluminum. A similar case is observed in the potassium-calcium system where calcium is strongly absorbed by potassium since the Ca Kα line lies just on the high energy side of the K K-edge as illustrated on figure 3. An additional complication is the fact that iron has a high mass absorption coefficient at the energy levels of the lower atomic numbered elements thereby acting a strong absorber.

Although absorption and enhancement effects can be severe, mathematical corrections can easily be applied. Numerous methods have been proposed[10,11,12,13,14], the author has proposed a method described LaChance[10] where a relationship is established that the relative intensity of a characteristic line in a binary system is directly proportional to the weight fraction of a given element (A) in the presence of (B). Utilization of this approach requires that element (A) and element (B) must sum to unity.

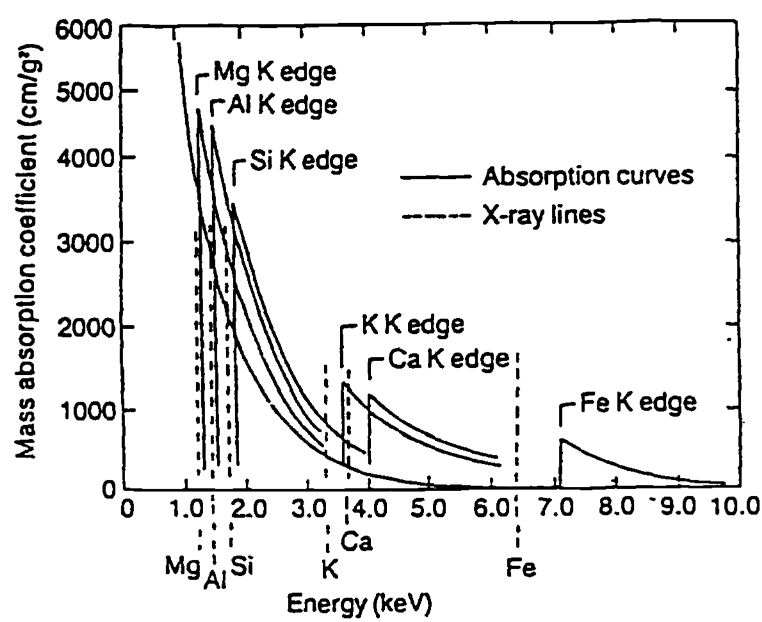

Figure 3. Elemental absorption Curve

The mathematical expression of this correction procedure would be as follows;

$$R_A = (C_a) / (1 + C_b\alpha AB) \quad (1)$$

$$R_B = (C_b) / (1 + C_a\alpha BA) \quad (2)$$

Defining αAB and αBA

$$\alpha AB = [((\mu_1 \csc\theta_1 + \mu_2 \csc\theta_2) * (B-1) / (\mu_1 \csc\theta_1 + \mu_2 \csc\theta_2) * B))] \quad (3)$$

$$\alpha BA = [((\mu_1 \csc\theta_1 + \mu_2 \csc\theta_2) * (A-1) / (\mu_1 \csc\theta_1 + \mu_2 \csc\theta_2) * A))] \quad (4)$$

where

$(\mu_1)A$ and $(\mu_1)B$ = the mass absorption coefficients of elements A and B at the effective wavelength for the excitation of radiation (A)

$(\mu_2)A$ and $(\mu_2)B$ = the mass absorption coefficients of elements A and B at the effective wavelength for the excitation of radiation (B)

θ_1 and θ_2 = the angle of incidence of the primary X-ray beam and the take off angle of the secondary radiation

C_a and C_b = the weight fractions of elements A and B

R_a and R_b = the relative intensities of elements A and B expressed as ratios of the net intensities of the elements A and B to the net intensities for pure elements A and B

Calibration of the standards involves an iterative process according to equations 3 and 4 which establishes the α coefficients which are then assigned to equations 1 and 2. The unknown sample data is then processed through multiple regression analysis utilizing equations 1 and 2.

Instrumentation

A Rigaku RIX-3100 X-ray spectrometer with a 4 KW generator was utilized for this analysis and was operated under the instrumental parameters as described on Table 1.

ELEMENT	Na_2O	MgO	Al_2O_3	SiO_2	P_2O_5	SO_3	K_2O	CaO	TiO_2	MnO	Fe_2O_3	SrO
ANODE	Rh											
ANODE VOLTAGE, KV	30		50									
ANODE CURRENT, MA	130		80									
SLIT	Coarse											
CRYSTAL	RX-40		PET		Ge				LiF			
DETECTOR			FP-C						SC			
FILTER	None											
PEAK 2θ ANGLE	17.65	14.15	144.65	109.04	141.10	110.80	70.00	61.95	86.18	62.96	57.49	25.13
COUNTING TIME, S	40		20									
PHA - LOWER	50		100									
PHA - UPPER	450		300									
ATMOSPHERE	Vacuum											

Table 1: Instrumental operating conditions for limestone and dolomite

Sample preparation

As previously discussed, particle size and distribution can have an effect on the intensities of most elements with the most severe being at the low Z portion of the periodic table. An illustration of this fact, figure 1, displays the effect of grinding time related to changes in intensity as a function of a reduction in particle size. Eight (8) separate samples of a single standard consisting of 5.0 grams of sample and 0.10 grams of Na-stearate as a grinding aid were placed in a tungsten carbide rotary swing mill and ground for one to eight minutes. The resulting powder was then pelletized at 15 tons per square inch with boric acid (H_3BO_3) as a backing material. Each pellet was measured with the resulting intensities plotted as a function of grinding time and displayed on figure 1. The grinding curve indicated a minimum grinding time of five minutes. As a result, each sample was ground for the minimum grinding time plus one minute for a total of six minutes.

After determination of the proper grinding time, eight samples of one standard were ground and the pettetized from five to 35 ton per square inch and measured. The measured intensities were then plotted as a function of pelletizing pressure as displayed on figure 2. Based on this data, no further deviations in intensity were observed after a pelletizing pressure of fifteen ton per square inch. As a result, all samples were ground for six minutes and pelletized at fifteen ton per square inch.

Results and conclusions

The sample utilized in this study were seven standards supplied the National Bureau of Standards[18], Ash Grove Cement Company[19], Hercules Cement Company[20], and well characterized unknown samples from Medusa Cement Company[21]. The standards were derived from diverse geographical and geological areas. In addition the mineralogical structure varied from calcite (rhomboidal – R-3c), vaterite (hexagonal – $P6_3mmc$), aragonite (orthorhombic – Pnm), aragonite (orthorhombic – Pmca) as listed in appendix A.

The results of analysis are contained on tables 2a,2b, and 2c while the individual calibration curves in appendix B. A typical spectra of limestone is contained in appendix C. Calcium oxide and magnesium oxide, the main components in Ca/Mg carbonate rocks, exhibited absolute errors of approximately two to four percent relative utilizing a simple least squares regression analysis. Utilizing the theoretical alpha routine as outlined by LaChance[11] with multiple least squared regression analysis, the errors were reduced to 0.07and 0.05 percent respectively. It should be noted that the CaO in the unknowns was initially determined by a $KMnO_4$ titration with no attempt to differentiate between CaO and SrO. In the $KmnO_4$ titrimetric determination of CaO, both the CaO and SrO are both precipitated as calcium-strontium oxalate and when titrated with $KmnO_4$, the oxalate ion is actually being determined. As a result, the determined value by this method will be CaO plus SrO. In a limestone or dolomite, the SrO could be from 0.05 to 0.30 percent. Therefore, since X-ray fluorescence determines CaO and SrO separately, the CaO and SrO determination by X-ray fluorescence must be combined in order to agree with the $KmnO_4$ titrimetric calculation.

Conclusions

The results of analysis illustrate that X-ray fluorescence is a viable technique for the analysis of limestone and dolomite. It further illustrates that with proper sample preparation, mineralogical differences become insignificant. Data reduction through the use of theoretical alphas automatically solves the problems associated with the absorption and enhancement effects.

Sample ID	Na_2O		MgO		Al_2O_3		SiO_2		P_2O_5	
	List	Calc	List	Calc	List	Calc	List	Calc	List	Calc
LS-1	0.02	0.02	0.18	0.23	0.07	0.05	0.19	0.17	0.030	0.022
LS-2	0.03	0.03	1.34	1.39	1.19	1.19	4.47	4.47	0.100	0.093
LS-3	0.04	0.04	20.59	20.48	0.65	0.67	1.90	1.90	0.060	0.060
LS-4	0.01	0.02	0.34	0.38	0.03	0.03	0.15	0.11	0.010	0.010
LS-5	0.20	0.19	1.84	1.76	1.70	1.71	14.72	14.60	0.080	0.079
LS-6	0.32	0.35	2.52	2.43	5.07	5.04	14.11	14.22	0.200	0.202
LS-7	0.13	0.10	6.75	6.67	1.60	1.58	11.14	11.18	0.070	0.068
1-C	0.02	0.02	0.42	0.45	1.30	1.31	6.84	6.93	0.040	0.044
1-A	0.39	0.36	2.19	2.23	4.16	4.19	14.11	14.04	0.150	0.152
88-B	0.03	0.04	21.03	21.17	0.34	0.33	1.13	1.15	0.004	0.007
Unknowns										
D7	<u>0.12</u>	0.13	<u>2.02</u>	2.09	<u>2.96</u>	3.15	<u>13.86</u>	13.74	-	0.020
D13	<u>0.14</u>	0.13	<u>2.33</u>	2.17	<u>3.39</u>	3.21	<u>14.50</u>	14.46	-	0.030

Notes: <u>0.14</u> values received after analysis, not included in calibration
- certified (list) values not stated
*** values determined gravimetrically**

Table 2a: Analysis of limestones and dolomites by X-ray fluorescence

Sample ID	SO_3		K_2O		CaO		TiO_2		MnO	
	List	Calc	List	Calc	List	Calc	List	Calc	List	Calc
LS-1	0.04	0.03	0.01	0.03	55.04	54.99	0.01	<0.01	0.007	0.007
LS-2	0.35	0.36	0.24	0.21	50.14	50.14	0.10	0.08	0.028	0.034
LS-3	<0.01	<0.01	0.05	0.05	30.25	30.13	0.05	0.06	0.042	0.042
LS-4	0.09	0.09	0.01	0.03	55.44	55.41	0.01	< 0.01	0.007	0.008
LS-5	0.05	0.07	0.80	0.71	42.96	43.05	0.24	0.22	0.007	0.008
LS-6	0.73	0.72	0.98	0.94	39.98	40.04	0.28	0.26	0.035	0.036
LS-7	0.44	0.44	0.50	0.55	39.06	39.15	0.17	0.14	0.035	0.035
1-C	-	<0.01	0.28	0.30	50.30	50.34	0.07	0.09	0.025	0.024
88-B	-	<0.01	0.10	0.08	29.95	29.88	0.02	0.02	0.016	0.012
Unknowns										
D7	<u>0.51</u>	0.48	<u>0.72</u>	0.74	<u>42.48</u>	42.40	-	0.11	-	0.020
D13	<u>0.45</u>	0.40	<u>0.79</u>	0.78	<u>41.37</u>	41.28	-	0.10	-	0.020

Notes: <u>0.14</u> values received after analysis, not included in calibration
- certified (list) values not stated
* values determined gravimetrically

Table 2b: Analysis of limestones and dolomites by X-ray fluorescence

Sample ID	Fe_2O_3		SrO		LOI*	Total	
	List	Calc	List	Calc	List	List	Calc
LS-1	0.06	0.06	0.01	0.02	44.01	99.68	99.64
LS-2	1.19	1.16	0.16	0.16	40.64	99.98	99.96
LS-3	0.17	0.19	0.02	0.01	45.83	99.65	99.46
LS-4	0.19	0.19	0.12	0.11	43.56	99.97	99.95
LS-5	1.16	1.16	0.08	0.08	35.90	99.74	99.54
LS-6	1.55	1.57	0.20	0.21	34.26	100.23	100.27
LS-7	1.25	1.24	0.11	0.10	38.44	99.69	99.69
1-C	0.55	0.57	0.03	0.02	39.90	99.77	100.00
1-A	1.63	1.63	-	<0.01	34.95	99.81	99.83
88-B	0.28	0.23	0.01	0.01	46.98	99.89	99.73
Unknowns							
D7	<u>1.48</u>	1.43	-	0.10	36.03	100.18	100.44
D13	<u>1.59</u>	1.62	-	0.12	35.67	100.23	99.99

Notes: <u>0.14</u> values received after analysis, not included in calibration
- certified (list) values not stated
* values determined gravimetrically

Table 2c: Analysis of limestones and dolomites by X-ray fluorescence

APPENDIX A

Listing of Standards and Source

Standard	Geologic Formatiom	Region	Source
LS-1	Burlington	Missouri	Ash Grove Cement Company
LS-2	Raytown	Kansas	Ash Grove Cement Company
LS-3	Squamish	British Columbia	Ash Grove Cement Company
LS-4	Kimswick	Missouri	Ash Grove Cement Company
LS-5	Jacksonburg	Pennsylvania	National Bureau of Standards
LS-6	Jacksonburg	Pennsylvania	Hercules Cement Company
LS-7	Farley	Nebraska	Ash Grove Cement Company

APPENDIX B

Typical Limestone Spectra

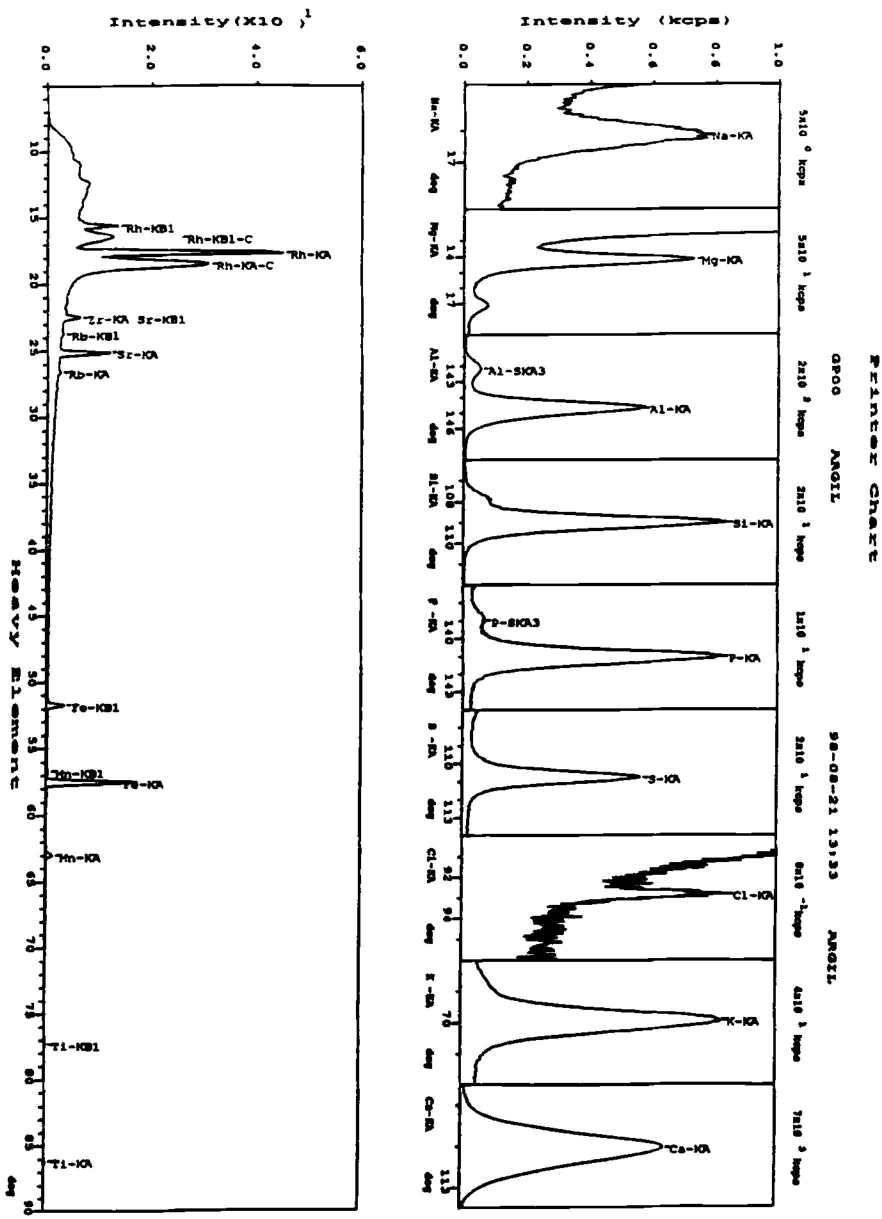

Printer Chart
GP00 ARGIL
98-08-21 13:33 ARGIL
Intensity (kcps)
Intensity(X10)
Heavy Element
Na-KA
Mg-KA
Al-SKA3
Al-KA
Si-KA
P-SKA3
P-KA
S-KA
Cl-KA
K-KA
Ca-KA
Rh-KB1
Rh-KB1-C
Rh-KA
Rh-KA-C
Zr-KA Sr-KB1
Rb-KB1
Sr-KA
Rb-KA
Fe-KB1
Mn-KB1
Fe-KA
Mn-KA
Ti-KB1
Ti-KA

APPENDIX C

Calibration Curves

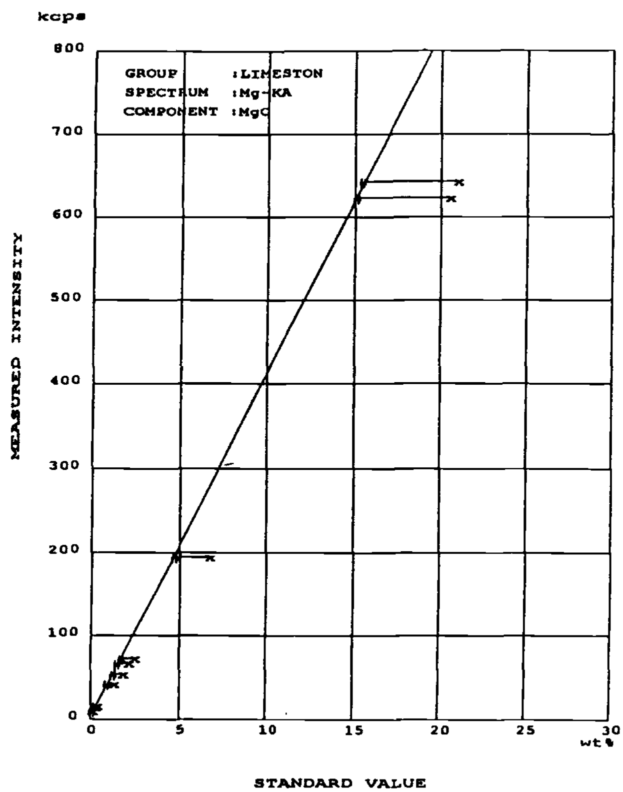

CALIBRATION CONSTANT

A = 0.00000e+000
B = 2.43732e-002
C = -9.35173e-002
ACC 8.64510e-002

MATRIX CORRECTION

*A[Na2O]= 1.75454e-002
*A[Al2O3]= 8.87632e-004
*A[SiO2]= 2.10712e-003
*A[P2O5]= 2.83472e-003
*A[SO3]= 3.82316e-003
*A[K2O]= 4.67165e-003
*A[CaO]= 5.98080e-003
*A[TiO2]= 8.15373e-003
*A[MnO]= 1.52718e-002
*A[Fe2O3]= 1.69987e-002
*A[SrO]= 8.20895e-003
*A[LOI]= 3.64352e-003

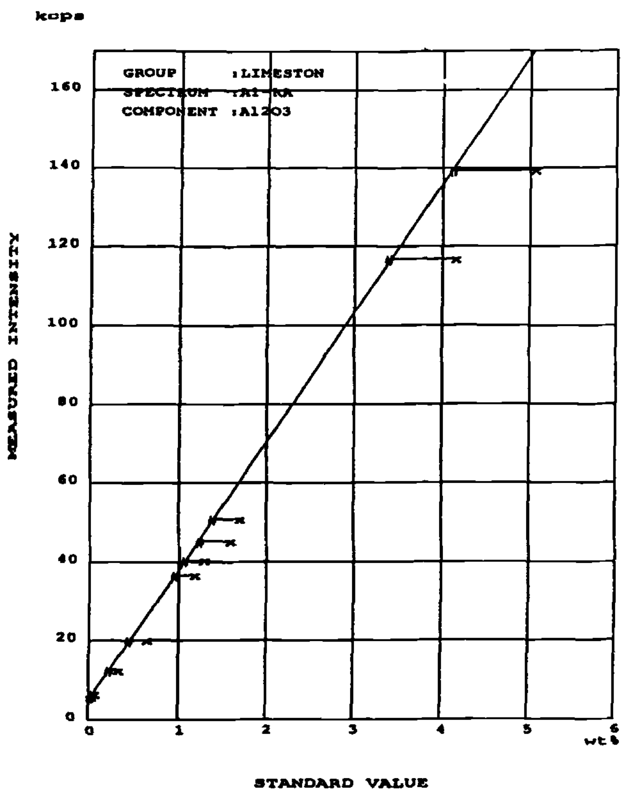

CALIBRATION CONSTANT

A = 0.00000e+000
B = 3.05543e-002
C = -1.52822e-001
ACC 1.84716e-002

MATRIX CORRECTION

*A[Na2O]= 1.26274e-002
*A[MgO]= 1.50826e-002
*A[SiO2]= 4.82174e-004
*A[P2O5]= 1.02900e-003
*A[SO3]= 1.83876e-003
*A[K2O]= 2.06084e-003
*A[CaO]= 3.03190e-003
*A[TiO2]= 4.86224e-003
*A[MnO]= 1.10208e-002
*A[Fe2O3]= 1.24812e-002
*A[SrO]= 7.28007e-003
*A[LOI]= 9.28514e-004

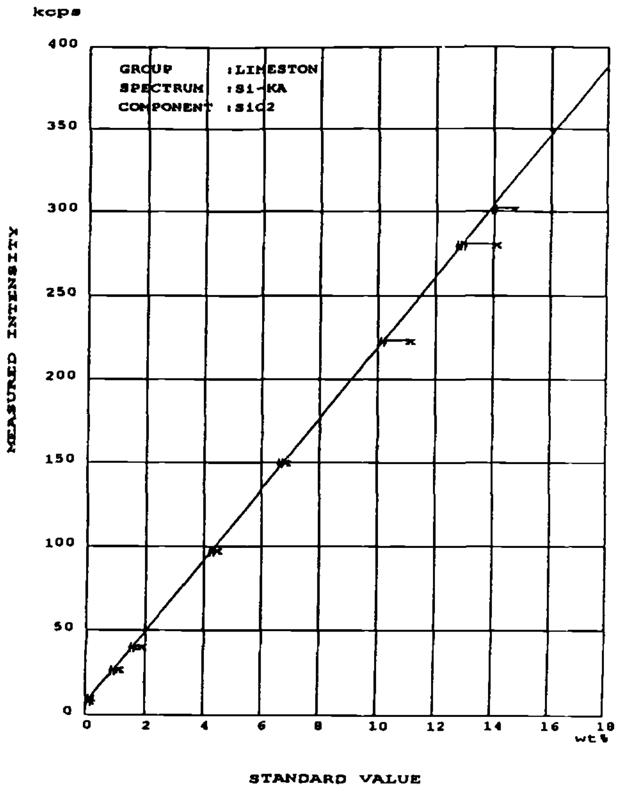

CALIBRATION CONSTANT

A = 0.00000e+000
B = 4.71361e-002
C = -3.23767e-001
ACC 7.56902e-002

MATRIX CORRECTION

*A[Na2O]=	8.79250e-003
*A[MgO]=	1.02542e-002
*A[Al2O3]=	1.16722e-002
*A[P2O5]=	-1.57557e-004
*A[SO3]=	6.01909e-004
*A[K2O]=	-3.10181e-006
*A[CaO]=	8.55060e-004
*A[TiO2]=	2.58508e-003
*A[MnO]=	7.95108e-003
*A[Fe2O3]=	9.15774e-003
*A[SrO]=	7.17607e-003
*A[LOI]=	-1.10580e-003

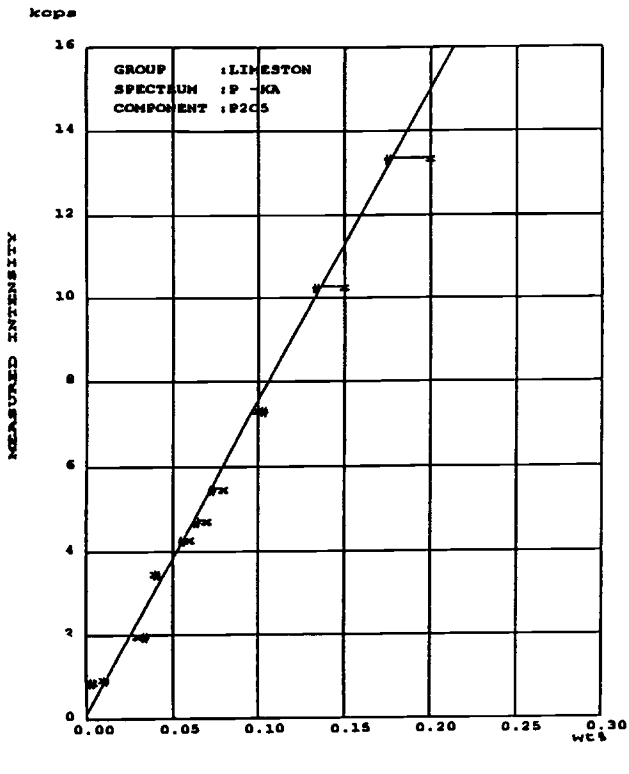


```
CALIBRATION CONSTANT
A =    0.00000e+000
B =    1.34022e-002
C =   -1.54642e-003
ACC    4.93211e-003
MATRIX CORRECTION

*A[Na2O    ]=  6.62350e-003
*A[MgO     ]=  8.06214e-003
*A[Al2O3   ]=  9.28864e-003
*A[SiO2    ]=  1.06289e-002
*A[SO3     ]=  4.23812e-005
*A[K2O     ]= -1.10709e-003
*A[CaO     ]= -4.76285e-004
*A[TiO2    ]=  1.03518e-003
*A[MnO     ]=  5.83409e-003
*A[Fe2O3   ]=  7.00432e-003
*A[SrO     ]=  3.81126e-002
*A[LOI     ]= -2.37499e-003
```

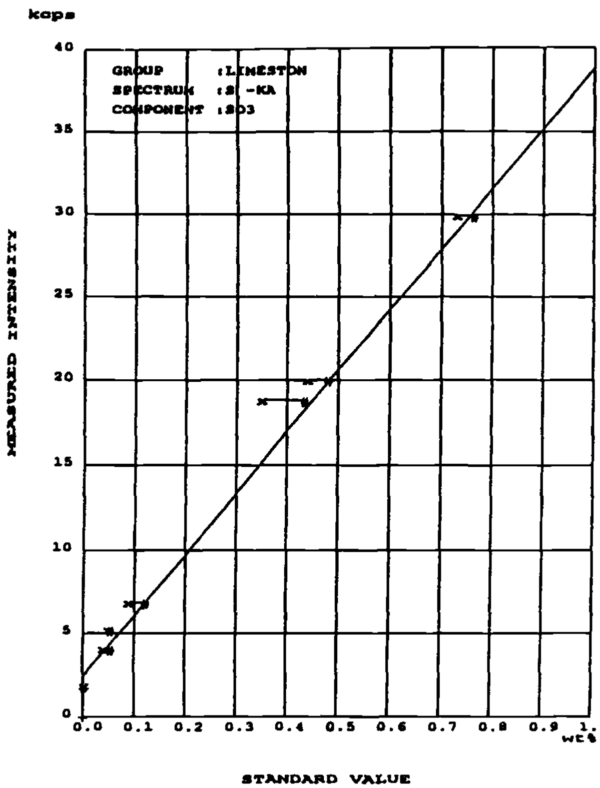

CALIBRATION CONSTANT

A = 0.00000e+000
B = 2.74817e-002
C = -6.70949e-002
ACC 1.35298e-002

MATRIX CORRECTION

*A[Na2O]= 3.93704e-003
*A[MgO]= 5.24525e-003
*A[Al2O3]= 6.26632e-003
*A[SiO2]= 7.58249e-003
*A[P2O5]= 8.18862e-003
*A[K2O]= -2.43079e-003
*A[CaO]= -2.04092e-003
*A[TiO2]= -8.02799e-004
*A[MnO]= 3.24580e-003
*A[Fe2O3]= 4.28969e-003
*A[SrO]= 3.11786e-002
*A[LOI]= -3.76786e-003

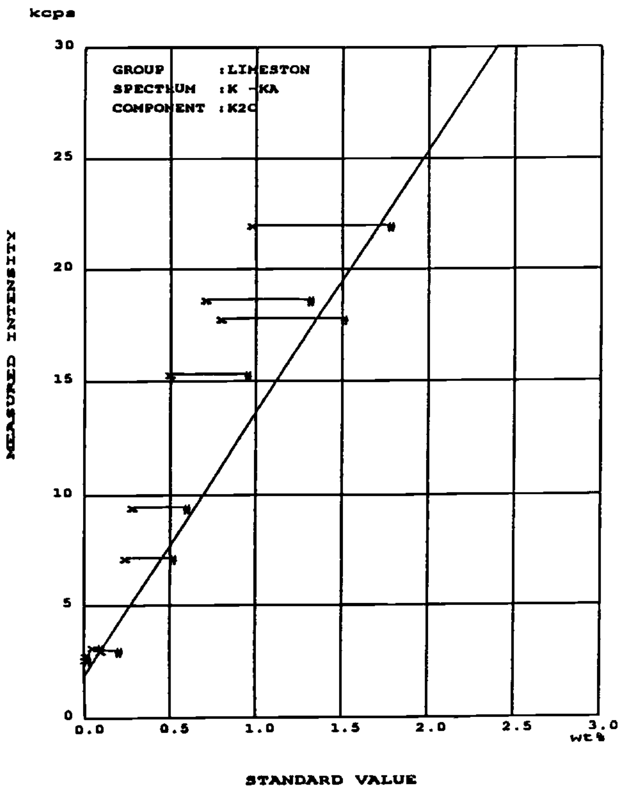

CALIBRATION CONSTANT

A = 0.00000e+000
B = 8.50044e-002
C = -1.58211e-001
ACC 5.82077e-002

MATRIX CORRECTION

*A[Na2O]= -2.40421e-003
*A[MgO]= -1.54273e-003
*A[Al2O3]= -9.54530e-004
*A[SiO2]= 3.25359e-005
*A[P2O5]= 5.98483e-004
*A[SO3]= 1.69522e-003
*A[CaO]= -5.20325e-003
*A[TiO2]= -4.58611e-003
*A[MnO]= -2.97620e-003
*A[Fe2O3]= -2.40618e-003
*A[SrO]= 1.36451e-002
*A[LOI]= -6.81258e-003

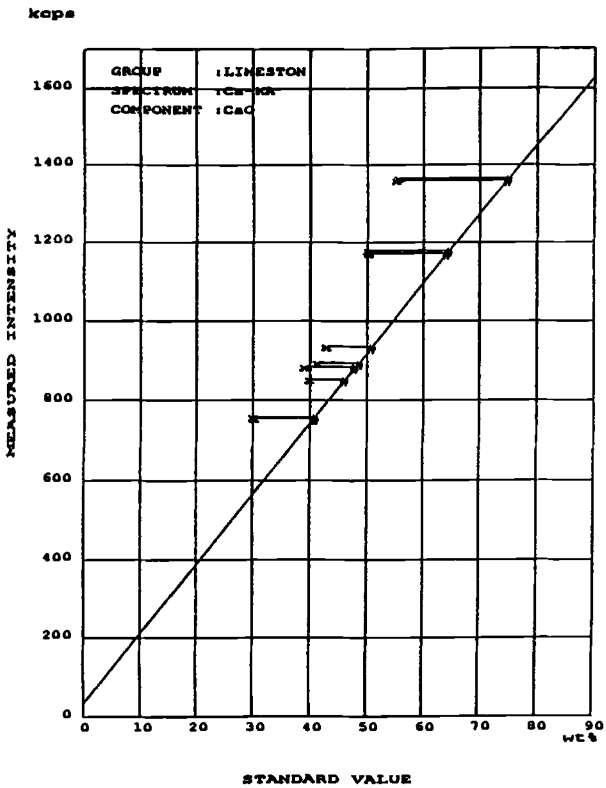

CALIBRATION CONSTANT

A = 0.00000e+000
B = 5.63635e-002
C = -1.83940e+000
ACC 7.59523e-002

MATRIX CORRECTION

*A(Na2O)= -6.07239e-004
*A(MgO)= 5.04786e-004
*A(Al2O3)= 1.25427e-003
*A(SiO2)= 2.55604e-003
*A(P2O5)= 3.33598e-003
*A(SO3)= 4.67018e-003
*A(K2O)= 2.60275e-002
*A(TiO2)= -2.85336e-003
*A(MnO)= -1.37479e-003
*A(Fe2O3)= -8.99624e-004
*A(SrO)= 1.94987e-002
*A(LOI)= -6.10834e-003

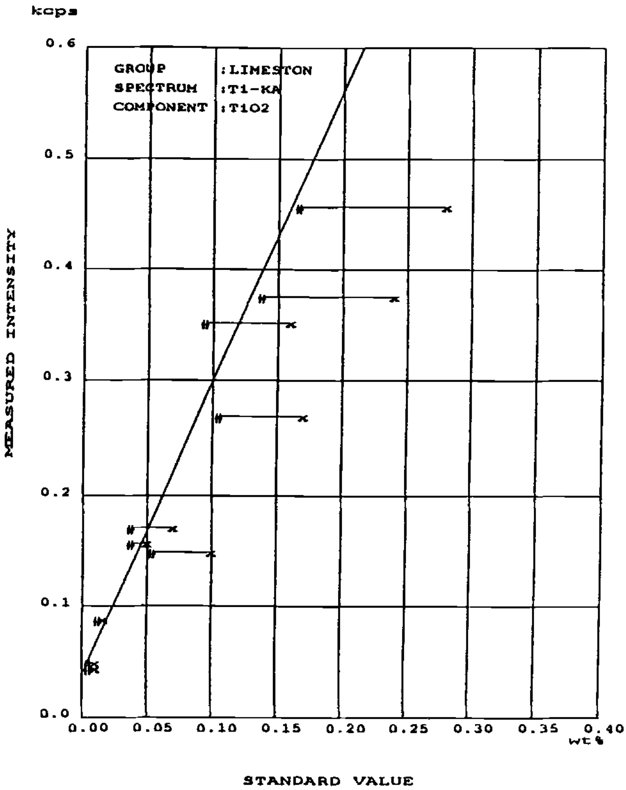


```
CALIBRATION CONSTANT

A =    0.00000e+000
B =    3.82096e-001
C =   -1.47423e-002
ACC    2.33548e-002
MATRIX CORRECTION

*A(Na2O    )= -2.38141e-003
*A(MgO     )= -1.40803e-003
*A(Al2O3   )= -7.54134e-004
*A(SiO2    )=  4.23494e-004
*A(P2O5    )=  1.18577e-003
*A(SO3     )=  2.24799e-003
*A(K2O     )=  2.17244e-002
*A(CaO     )=  2.26391e-002
*A(MnO     )= -5.02340e-003
*A(Fe2O3   )= -4.75039e-003
*A(SrO     )=  1.33815e-002
*A(LOI     )= -6.94084e-003
```

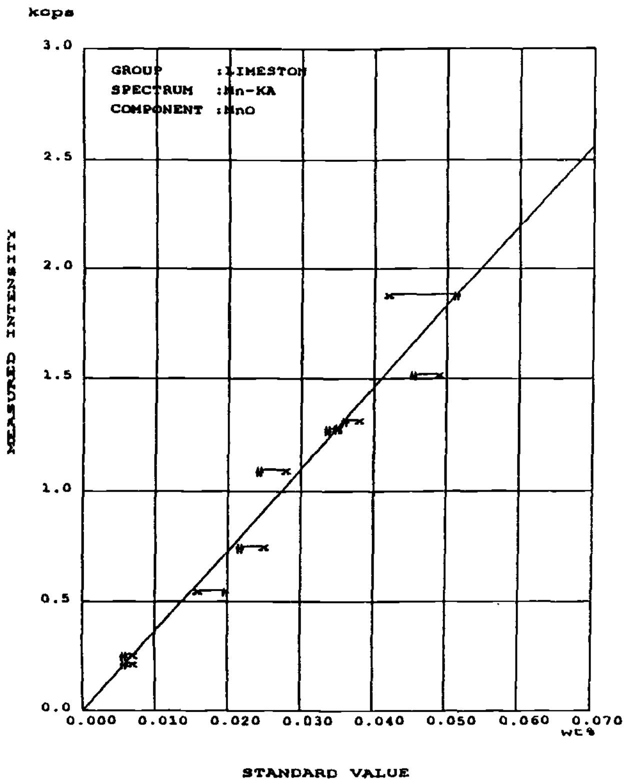


```
CALIBRATION CONSTANT

A -    0.00000e+000
B -    2.72994e-002
C -    0.00000e+000
ACC    2.93314e-003
MATRIX CORRECTION

*A[Na2O    ]= -5.63751e-003
*A[MgO     ]= -5.03370e-003
*A[Al2O3   ]= -4.61346e-003
*A[SiO2    ]= -3.86586e-003
*A[P2O5    ]= -3.33744e-003
*A[SO3     ]= -2.72203e-003
*A[K2O     ]=  9.95887e-003
*A[CaO     ]=  1.02155e-002
*A[TiO2    ]=  9.87657e-003
*A[Fe2O3   ]= -1.86424e-003
*A[SrO     ]=  2.68604e-003
*A[LOI     ]= -8.29845e-003
```

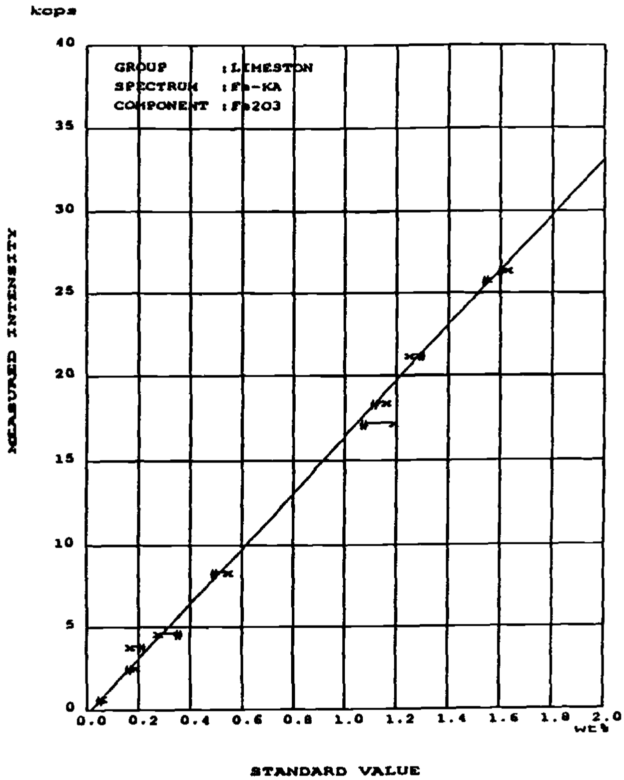

CALIBRATION CONSTANT

A = 0.00000e+000
B = 5.99927e-002
C = 1.48629e-002
ACC 2.55242e-002

MATRIX CORRECTION

*A(Na2O)= -5.88174e-003
*A(MgO)= -5.30036e-003
*A(Al2O3)= -4.88855e-003
*A(SiO2)= -4.16579e-003
*A(P2O5)= -3.64250e-003
*A(SO3)= -3.05478e-003
*A(K2O)= 9.32704e-003
*A(CaO)= 9.51587e-003
*A(TiO2)= 9.30177e-003
*A(MnO)= -4.44588e-004
*A(SrO)= 1.31251e-003
*A(LOI)= -8.40431e-003

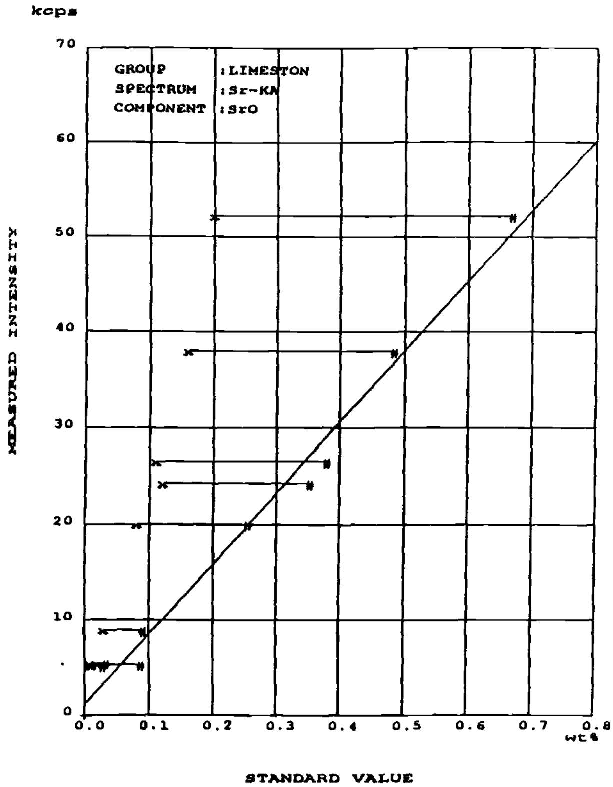

CALIBRATION CONSTANT

A = 0.00000e+000
B = 1.35456e-002
C = -1.53442e-002
ACC 8.85715e-003

MATRIX CORRECTION

*A[Na2O]= -8.97122e-003
*A[MgO]= -8.81334e-003
*A[Al2O3]= -8.67204e-003
*A[SiO2]= -8.47997e-003
*A[P2O5]= -8.30961e-003
*A[SO3]= -8.12682e-003
*A[K2O]= -4.38103e-003
*A[CaO]= -4.30648e-003
*A[TiO2]= -4.12987e-003
*A[MnO]= 1.25597e-004
*A[Fe2O3]= 8.04325e-004
*A[LOI]= -9.58517e-003

References

[1] Dwiggins, C.W, Jr., and Dunning, N.H., "Quantitative Determination of Traces of Vanadium, Iron, and Nickel in Oils by X-ray Spectrography", *Analytical Chemistry,* 32, 1137, 1960.

[2] Brown, O.E. "Use of X-ray Emission Spectroscopy in the Analysis of Cement, Raw Materials, and Raw mix", ASTM Annual Meeting, 1963.

[3] Moore, C., "Suggested Method for Spectrochemical Analysis of Portland Cement by Fusion with Lithium Tetra Borate Using an X-ray Spectrometer" *ASTM Report No. E-2, 5M10-26.*

[4] Harvy, P.K., Taylor, D.M., Hendry, R.D., and Brancroft., F "An Accurate Fusion Method for the Analysis of Rocks and Minerals and Chemically Related Materials by X-ray Fluorescence", *X-ray Spectrometry, 2, 33-34,* 1972.

[5] Claisse, F., "Accurate X-ray Fluorescence Analysis Without Standards", *Norelco Reporter 4,* 1957.

[6] Wheeler, B.D., "Cement Raw Mix Control Through X-ray Emission Spectrography *Proceedings of the Third Forum on the Geology of Industrial Minerals,* Special Distribution 34, University of Kansas, 1967.

[7] Hooper, P.R., "Rapid Analysis of Rocks and Minerals by X-ray Fluorescence" *Analytical Chemistry,* 36,1964.

[8] Wheeler, B.D., "Accuracy in X-ray Spectrochemical Analysis as Related to Sample preparation" *Spectroscopy,* vol. 3, No. 3, pp 24-33, March, 1998.

[9] Kester, B., AIEE Cement Industry Conference, Milwaukee, Wisconsin, 1960.

[10] Wheeler, B.D., "Chemical Analysis of Mg-Cr Refractories by X-ray Fluorescence, Fall Meeting of the American Ceramic Society, Refractories Division, Paper # 13-RI-76F, October 9. 1972

[11] LaChance,G.R., and Traill, R.J., "A Practical Solution to the Matrix Problem in X-ray Analysis", *Canadian Spectroscopy,* vol. 11, nos. 2-3, March-May, 1966.

[12] Lucus-Tooth, H.J., and Price, B.J., "A Mathematical Method for the Investigation of Interelemnt Effects in X-ray Fluorescence Analysis", *Metalurgia,* vol. LXIV, no. 383, Dept., 1961.

[13] Rasberry, S.D., and Heinrich, K.F.J., "Calibration of Interelement Effects in X-ray Fluorescence Analysis", *Analytical Chemistry,* vol. 46, no. 1, Jan., 1974.

[14] Hasler, M.R., and Kemp, J.W., "Suggested Practice for Spectrochemical Computations", ASTM Committee E-3, Report SM 2-3, American Society for Testing and Materials, Philadelphia, PA, pp 72-82, 1957.

[15] Sherman, J., "The Correlation Between Fluorescent Intensity and the Chemical Composition", *ASTM Special Publication*, no. 157, pp 27-33, 1954.

[16] Burnstein, F., "Particle Size and Mineralogical Effects in Mining Applications of X-ray Analysis", Denver Research Institute, University of Denver, 1962.

[17] Campbell, W.J., and Thatcher, D., *Advances in X-ray Analysis*, vol. 2, University of Denver, 1958.

[18] National Bureau of Standards, Washington, DC.

[19] Ash Grove Cement Company, Kansas City, MO.

[20] Hercules Cement Company, Bethlehem PA.

[21] Medusa Cement Company, Dixon, IL.

L. K. Crouch,[1] Marcus L. Knight,[2] R. Craig Henderson,[3] and William A. Sneed, Jr.[4]

UNBONDED CAPPING FOR CONCRETE MASONRY UNITS

REFERENCE: Crouch, L. K., Knight, M. L., Henderson, R. C., and Sneed, W. A., Jr., **"Unbonded Capping for Concrete Masonry Units,"** *Masonry: Materials, Testing, and Applications, ASTM STP 1356,* J. H. Brisch, R. L. Nelson, and H. L. Francis, Eds., American Society for Testing and Materials, 1999.

ABSTRACT: Due to the manufacturing process, the bearing surfaces of concrete masonry units are often somewhat rough and uneven. Therefore, concrete masonry units must be capped when tested in compression according to ASTM C 140-96, Standard Test Methods of Sampling and Testing Concrete Masonry Units. Capping of concrete masonry units is time consuming and expensive. Several studies of compression tests on concrete cylinders indicate that the use of elastic pads in rigid retaining caps give similar compressive strength results to approved capping methods. An unbonded capping system for concrete masonry units similar to that described in ASTM C 1231-93, Standard Practice for Use of Unbonded Caps in Determination of Compressive Strength of Hardened Concrete Cylinders, was developed. The average compressive strength results obtained when using the unbonded capping system ranged from 92-94% of the average compressive strength results obtained when using ASTM C 140-96 approved methods. Further, use of the unbonded capping system was found to increase productivity and substantially reduce testing cost.

KEYWORDS: concrete masonry units, compressive strength, loadbearing, unbonded cap, neoprene

---

Performance requirements for most masonry materials are determined by structural design considerations and environmental exposure conditions. Appropriate masonry units are selected for the desired application based on engineering properties such as compressive strength and durability. Routine quality control tests are necessary to assure

---

[1]Associate Professor of Civil Engineering, Tennessee Technological University, Cookeville, TN 38505.

[2]Graduate teaching assistant, Civil and Environmental Engineering Department, Tennessee Technological University.

[3]Assistant Professor of Civil Engineering, Tennessee Technological University, Cookeville, TN 38505.

[4]President, WASCO, Nashville, Tennessee.

that the delivered masonry units conform to the engineering property specifications determined in the design process [1]. The research described herein involved the experimental evaluation of a new capping technique for concrete masonry compressive strength evaluation.

Research Significance

Compressive strength of individual concrete masonry units is among the most common routine quality control tests. However, difficulties exist in adequately characterizing the compressive strength of concrete masonry units (CMU). Due to the manufacturing process, CMU often have rough and irregular surfaces. When the CMU are tested in compression, the surface roughness and irregularities lead to stress concentrations which often cause the unit to fail at a lower strength. To avoid erroneous low strength results, ASTM C 140-96 specifies that all CMU tested in compression shall be capped with either sulfur mortar or high-strength gypsum capping compound. Capping ensures that the loaded faces of the masonry unit are plane and perpendicular to the axis on which the stress is applied and that the load is distributed uniformly over the surface of the specimen.

Background and Literature Review

Materials under a uniaxial compressive load tend to expand in the transverse direction due to Poisson's effect. The expansion tendency is influenced by the unit's height-to-length ratio, the loading platens, and capping material used. If the expansion is restrained, transverse confining stresses build up near the platens. The effect of this restraint is to place a portion, the extent of which depends on the unit's height-to-length ratio, of the material being tested in a triaxial state of stress. The triaxial state of stress may increase or decrease the observed strength of the material near the platens depending on the strength and stiffness of the capping material, the platen configuration, and material properties [2].

Since typical CMU have a low height-to-length ratio, effectively subjecting virtually the entire unit to the triaxial stress state, extreme measures, such as brush platens [2], to reduce the effects of platen confinement may be justified for research work. However, extreme measures are not practical for routine quality control testing. Figure 1 shows the approximate extent of the triaxial stress state in Portland Cement Concrete (PCC) cylinders and facing brick compressive strength specimens.

To address the problem of low strength capping materials decreasing the observed strength of the material being tested, ASTM C 617-94, Standard Practice for Capping Cylindrical Concrete Specimens, requires that the compressive strength of all materials used for capping of concrete cylinders be not less than the cylinder strength. Due to the two-to-one length-to-diameter ratio, a portion of the PCC cylindrical specimens remains in uniaxial compression and no upper strength limit is needed for capping materials.

It appears the ideal capping material for CMU would have the same strength and stiffness as the material being tested. The ideal capping material would smooth aspirates on the surface of the CMU, be unrestrained by the loading platen, and also be easy to use and economical. Considering the range of strengths and stiffness of available CMU, it appears unlikely that such an ideal capping material will be available in the near future.

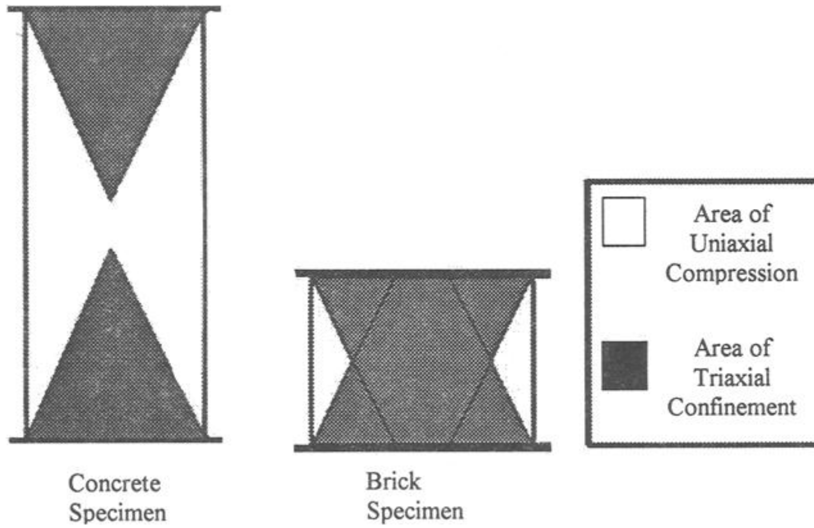

FIG. 1—*Approximate extent of triaxial stress.*

Further, capping of CMU with capping materials currently approved by ASTM is time consuming and expensive. Toxic fumes and the necessity of heating sulfur mortar create air pollution and safety considerations. ASTM C 140-96 requires a minimum 2 hour hardening period for sulfur-mortar caps or high-strength gypsum caps before compression testing. Unfortunately, neither capping material is reusable, due the possibility of toxic fumes with reused sulfur mortar and the irreversible chemical reaction that high-strength gypsum undergoes to harden.

Finally, researchers differ on the effect of capping materials on the observed strength of masonry units. Kelch and Emme [*3*] concluded that strength difference between sulfur-mortar and gypsum capped clay masonry units will be small in magnitude. Dodd and McGee [*4*] reported only small differences in bricks capped with a wide variety of materials such as cardboard, plasterboard, insulating wallboard, portland cement, and dental plaster. However, Drysdale, Hamid and Baker [*2*] report that "soft capping" materials such as fiberboard or plywood reduce the observed compressive strength of masonry units. Further, the National Concrete Masonry Association [*5*] reports observed compressive strength reductions from using fiberboard capping for concrete masonry units which vary from twenty to forty percent and are directly proportional to unit strength.

One possible solution may come from portland cement concrete technology. ASTM C 1231-93 and the American Association of State Highway and Transportation Officials, AASHTO T22-92 [*6*] currently allow the use of elastic pads in rigid retaining caps to be used for capping concrete compressive strength test cylinders. Several studies [*7, 8, 9, 10*] of concrete testing indicate that the use of elastic pads in rigid retaining caps give similar compressive strength results to sulfur capping while eliminating the hazards and delays associated with sulfur or gypsum capping. In addition, the use of these unbonded capping systems is more economical since the caps can be reused.

Experimental Program

To determine if an unbonded capping system for CMU similar to that described in ASTM C 1231-93 was viable, CMU from the same lot were tested for compressive strength using currently approved ASTM capping methods as well as the newly developed unbonded capping system. Since CMU manufacturers often use oriented strand board caps for routine compressive strength monitoring, it was decided to also include this method of capping in the study.

Viability of the unbonded capping system was determined by statistical comparison of the compressive strengths obtained. Desirability of the unbonded capping system was determined by comparing productivity, cost, and method safety with approved capping methods.

Materials

A sample of 250 concrete masonry units from the same lot, nominally 203 mm by 203 mm by 203 mm, were obtained from a local supplier. Upon arrival, these units were separated into two distinct groups. The two groups were composed of the units that had sash grooves, and the units that did not. This was done to minimize variability in the results due to differences in the units.

Nine units were selected from each group. These nine units were used to perform three tests for absorption, unit weight, and net area on each type of unit. These tests were completed in accordance with the requirements set forth in ASTM C 140-96. The material properties were used to determine the type of unit delivered from the manufacturer and compliance with ASTM C 90-96a, Standard Specification for Loadbearing Concrete Masonry Units. Also, and perhaps most importantly for this research, the average net area that was determined for each type of unit was used in calculating the respective net area compressive strengths of the units tested in compression.

The results of the material property tests on sash units and non-sash units are shown in Tables 1 and 2, respectively. Both sash units and non-sash units were determined to be normal weight units complying with ASTM C 90-96a. Absorption requirements were also met.

TABLE 1—*Material properties – sash units.*

Test #	Unit Weight kg/m^3	Absorption kg/m^3	Net Area Mm^2
1	2 080	169	21 781
2	2 060	176	22 052
3	2 073	172	22 103
Average	2 071	173	21 981

TABLE 2—*Material properties - non-sash units.*

Test #	Unit Weight kg/m^3	Absorption kg/m^3	Net Area mm^2
1	2 059	179	22 548
2	2 050	181	22 735
3	2 058	178	22 381
Average	2 056	179	22 555

The sulfur mortar used for capping in the study was a proprietary product called Rediron 9000. The product came in the form of flakes that were ready to be added to a melting pot. The initial time required to melt this material was approximately two hours. Three 50.8 mm cubes of the sulfur mortar were fabricated to assure that the strength of the sulfur mortar yielded an average compressive strength of 34.5 MPa at 24 hours. The average compressive strength of the sulfur cubes was found to be 76 MPa.

The high-strength gypsum cement used for capping was a proprietary product called Hydrostone. ASTM C 140-96 requires that gypsum cement gaged with water attain a minimum compressive strength of 24.1 MPa at 2 hours. A neat gypsum cement paste with a water-gypsum cement ratio of 0.26 produced a workable capping material. The average compressive strength of three 50.8 mm cubes at two hours was 38.3 MPa.

The oriented strand board used for the project was purchased at a local building materials establishment and engineering properties for the material were not available.

Procedure

To facilitate comparison of the unbonded capping system to each ASTM approved capping method as well as the commonly used non-approved oriented strand board technique the testing parameters shown in Table 3 were used. Each test series consisted of tests on three units.

TABLE 3—*Testing parameters.*

Designation	Unit Type	Capping Method	# of Tests
N*	Non-sash	Original Neoprene	10
N	Non-sash	Corrected Neoprene	8
W	Non-sash	Oriented Strand Board	8
H	Non-sash	Hydrostone	8
SN	Sash	Corrected Neoprene	12
SW	Sash	Oriented Strand Board	12
SS	Sash	Sulfur Mortar	12

Prior to testing each unit the center of gravity was determined and the unit was marked in accordance with ASTM C 140-96. For hydrostone and sulfur mortar approved capping methods, ASTM procedures were followed without exception. A sulfur mortar capping alignment jig was developed to ensure that sulfur mortar caps were perpendicular to the loading axis and as consistent in thickness as possible. The capping alignment jig is shown in Figure 2.

For oriented strand board capping, oriented strand board plates, 203 mm by 203 mm by 6.35 mm were used as caps for the specimens. The specimens were centered on oriented strand board plates placed above and below. Thereafter, the entire assembly was centered between the loading platens and loaded to failure at a rate of approximately 133 to 178 kN/min, the approximate rate used for other capping methods. The oriented strand board plates were not reused due to extensive damage during loading.

CMU tested with the unbonded capping system were prepared in the same manner and loaded at approximately the same rate as CMU's capped with other methods. The loading rate was in compliance with ASTM C 140-96.

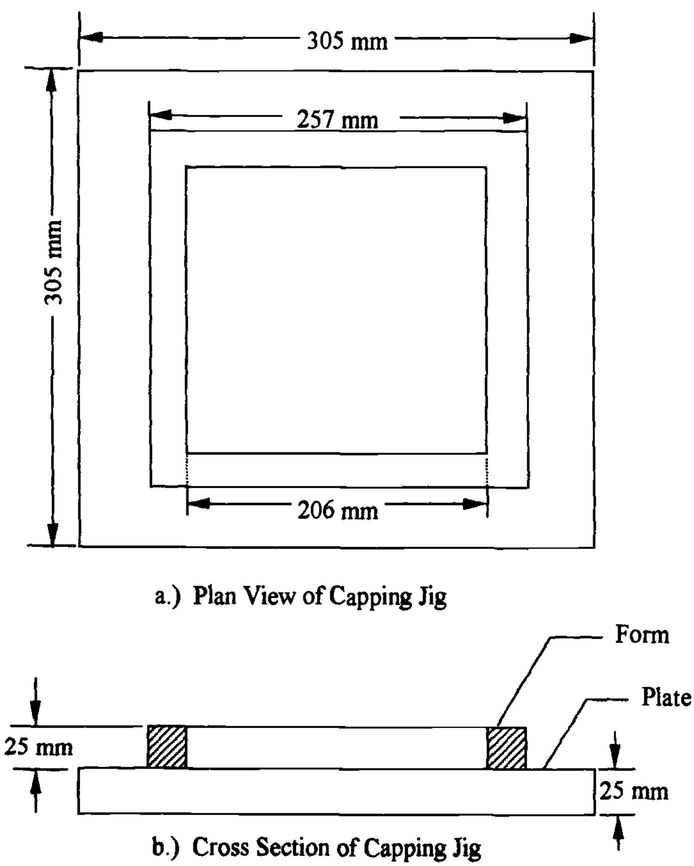

FIG. 2—*Sulfur capping jig.*

Development of the Unbonded Capping System

ASTM C 1231-93 and ASTM C 140-96 were used as guides for developing the unbonded capping system. The unbonded capping system was comprised of retainers with cavities to contain the neoprene pads.

The retainers were made of steel and subsequently hardened to comply with ASTM C 140-96 requirements. The cavity size was chosen to be 203 mm by 203 mm by 29 mm resulting in overall retainer dimensions of 254 mm by 254 mm by 50.8 mm to comply with ASTM C 1231-93 requirements. Both a plan view and a cross section of the steel retainers are shown in Figure 3. The circular holes in the corners of the retainers were bored so that the machine shop would have easier access for milling the corner sections of the steel retainers.

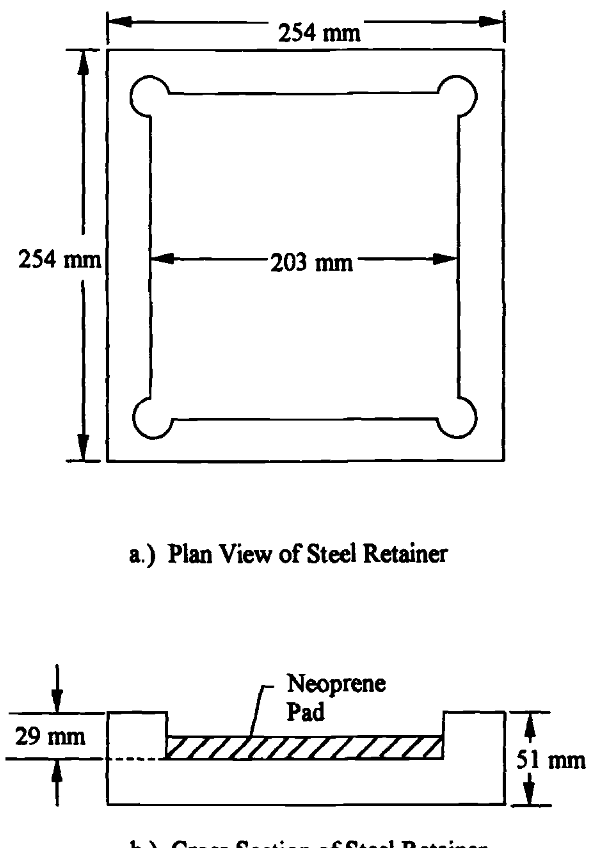

FIG. 3—*Plan and cross section of steel retainer.*

The dimensions of the neoprene pads were selected to be 201.6 mm by 201.6 mm by 12.7 mm to comply with ASTM C 1231-93 requirements. Neoprene pads with a Shore A durometer hardness of 70 were selected in lieu of durometer 50 neoprene to prevent excessive wear on the pads.

Initial Results

After completing the first 10 compression tests on the non-sash units using the original neoprene capping system, it was noticed that the compressive strength results were considerably lower than the compressive strengths obtained with the approved Hydrostone capping method. That is, the compressive strengths when using the original neoprene capping system were only about 84 percent of those using the Hydrostone capping method [*11*]. A graphical representation of the strength difference is shown in Figure 4. After careful observation, the reason for the lower compressive strengths was thought to be the fact that the corners of the units were breaking off during testing.

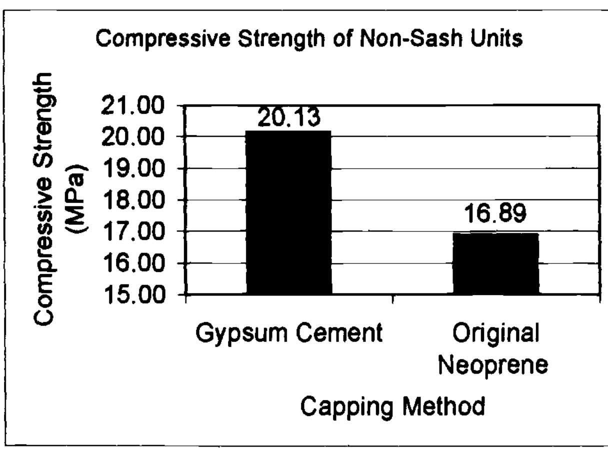

FIG. 4—*Initial compressive strength results.*

Adjustments to the Unbonded Capping System

It appeared that the corners of the units were breaking off during testing due to excessive expansion of the neoprene pads as the compressive load was applied. As shown in Figure 5, the neoprene was cut square, and not to fit the round corners of the steel retainers. Therefore, during testing, the corners of the pads were allowed to spread into the open space in the corners of the retainers. This expansion of the neoprene pads applied a lateral tensile load on the bearing surface of the unit, especially at the corners. The tensile load apparently caused the corners to break off during compression testing. The combination of tensile load applied at the bearing surface of the unit, along with the reduced bearing surface area of the unit, were the most likely reasons for premature failure and low observed compressive when using the original neoprene capping system.

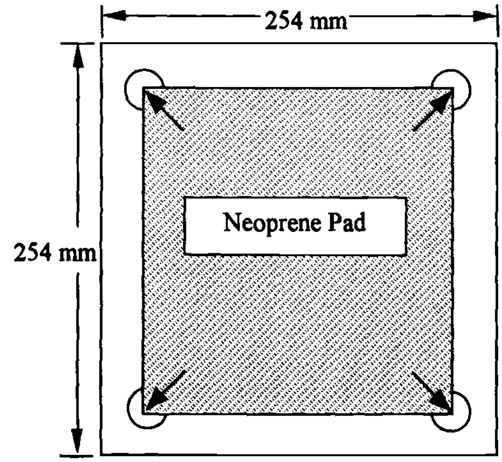

FIG. 5—Original steel retainer.

To alleviate this problem, the corners of the retainers were filled. This was accomplished by fabricating steel plugs that were slightly larger than the holes in the retainers. The plugs were driven into the holes in the plates. Next, the plugs were milled off flush with the top of the plate. The plugs were also milled out of the inside corners of the retainers so that a radius of 9.53 mm was obtained. A sketch of the improved retainers is shown in Figure 6. After repairing the retainers in this manner, new neoprene pads were prepared so that a tight fit was obtained around the entire perimeter of the pad.

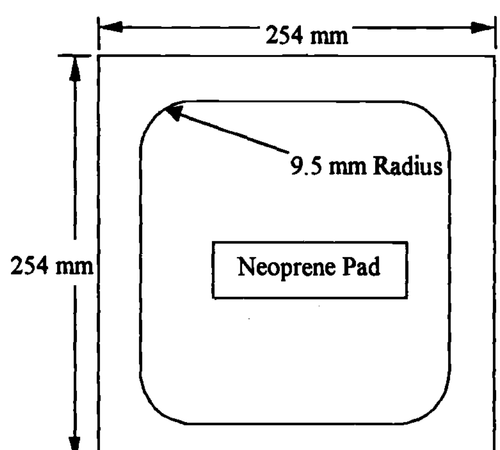

FIG. 6—*Corrected steel retainer.*

Final Results

The average compressive strength test results for each capping method are shown in Table 4 for non-sash units and in Table 5 for sash units.

TABLE 4—*Compressive strength results – non-sash units.*

Capping Technique	Average Compressive Strength (MPa)
Gypsum Cement	20.13
Oriented strand board	15.72
Corrected Neoprene	18.89
Original Neoprene	16.89

TABLE 5--*Compressive strength results – sash units.*

Capping Technique	Average Compressive Strength (MPa)
Sulfur	20.27
Oriented strand board	15.03
Corrected Neoprene	18.75

Analysis of Results

The results of all compressive strength tests, regardless of unit type or capping method exceeded ASTM C 90-96a requirements for minimum compressive strength of individual units (11.7 MPa) and average of three units (13.1 MPa). Average compressive strengths, standard deviations and coefficients of variation are shown in Table 6.

TABLE 6--*Statistical analysis.*

Method	Compressive Strength (MPa)	Std. Dev. (MPa)	Coeff. Of Var. (%)
N*	16.89		
N	18.89	0.59	3.1
W	15.72	0.62	4
H	20.13	2.13	10.6
SN	18.75	1.24	6.6
SW	15.03	0.76	5.1
SS	20.27	1.22	6

As shown in Table 4, the average compressive strength obtained when using oriented strand board as a capping material was only 74% of the observed compressive strength of sulfur mortar for sash units. Similarly, the average compressive strength obtained when using oriented strand board as a capping material was only 78% of the observed compressive strength of non-sash units capped with Hydrostone [*11*]. These results are in good agreement with the results reported by National Concrete Masonry Association [*5*]. Although the results from the units tested with oriented strand board caps show low standard deviations and coefficients of variation, the strength differences listed above show why oriented strand board is not an approved method.

The compressive strength results obtained using the corrected unbonded capping system were only 1.52 MPa less than sulfur mortar capping for the sash units and 1.24 MPa less than Hydrostone capping for the non-sash units. A two tailed t-test was used to determine if a significant statistical difference existed between the results obtained using the unbonded capping system and ASTM C 140-96 approved methods. When using a two tailed t-test, a significant difference was found to exist at the 0.05 confidence interval between sash units capped with sulfur mortar and sash units capped with the corrected unbonded capping system. However, a similar t-test revealed no significant difference in compressive strength at the 0.05 confidence interval between non-sash units capped with Hydrostone and the corrected unbonded capping system. Although the statistical results appear inconclusive, there is little practical difference in strength between the corrected unbonded capping system and the ASTM approved methods. The corrected unbonded capping system produced observed compressive strengths which were 92.5 and 93.8 percent of the observed compressive strengths of the approved methods for sash and non-sash units respectively [*11*]. Further, the corrected unbonded capping system produced similar or better coefficients of variation than approved methods.

Compressive strengths resulting from use of the unbonded capping system may be closer to the actual CMU strengths than those produced by the approved methods. The Hydrostone capping material had approximately twice the strength of the CMU while the sulfur mortar had approximately four times the compressive strength of the CMU. Higher strength capping materials may over restrict the bearing surfaces, thus increasing the extent of triaxial confinement and thereby increasing observed compressive of the CMU. Since neoprene's stiffness is strain dependent, it may produce a cap with stiffness which is closer to that of the CMU being tested.

Productivity

The time it takes to cap a CMU with the unbonded capping system is negligible. However, for this comparison, it will be conservatively assumed that it takes one technician five minutes to cap a CMU with the unbonded capping system. In this research, it required two technicians working together for 45 minutes to cap a CMU with either of the approved capping methods. Therefore, the unbonded capping system is at least 18 times as fast as the approved capping methods [*11*].

Economic Comparison

For this comparison, it was assumed that the labor cost associated with capping a

CMU with the unbonded capping system and the material cost associated with capping a CMU with an approved capping method could both be neglected. Therefore, the cost associated with the unbonded capping system included the cost of steel retainers and the neoprene pads. It was assumed that if steel retainers were in commercial production, a set could be purchased for $500. A set of neoprene pads used in this research cost approximately $30. Therefore, the total up-front cost of the unbonded capping system would be about $530. After viewing the neoprene pads from this research, it was determined that the pads had a useful life of about 50 tests [*11*]. It was assumed that the steel retainers would last indefinitely. Therefore, assuming 50 tests were completed with each set of pads, and ignoring any labor cost, the cost per compressive strength test using the unbonded capping system was found to be approximately $10.60. Likewise, the cost of capping a CMU with an approved capping technique was found to be $15.00 per unit assuming a technician hourly rate of $10.00 per hour. Thus capping a CMU with the unbonded capping system cost only about two-thirds as much as capping with an approved method, even assuming the steel retainer cost is spread over only the first 50 tests [*11*].

Conclusions

Based on the limited results of this study, the following conclusions can be drawn.

1. The average observed compressive strengths of hollow CMU capped with the unbonded capping system ranged from 92.5 to 93.8 percent of units from the same lot capped with ASTM-approved capping methods.
2. Statistical comparisons of observed compressive strength yielded inconclusive results. When using a two-tailed t-test to compare the unbonded capping system with approved methods, sash units capped with sulfur mortar showed a significant difference to unbonded caps and non-sash units capped with Hydrostone showed no significant difference compared to CMU capped with the unbonded capping system.
3. The unbonded capping system produced coefficients of variation in compressive strength testing similar to or less than those of ASTM-approved methods.
4. The unbonded capping system was found to be 18 times faster and cost only 70% as much as capping with either ASTM-approved capping method.

Acknowledgements

The authors express their appreciation to the Tennessee Technological University Faculty Research Program and the Tennessee Technological University Center for Electric Power for their financial support of the project. Many thanks to Richard Maxwell, TTU civil engineering technician, who assisted in the design and fabrication the capping jig. The authors wish to thank the Masonry Institute of Tennessee and WASCO for donating the concrete masonry units for the study and for their continued support of the civil engineering program at Tennessee Technological University. Special thanks to Mr. Verble Wilson of Mallory Controls and Mr. Doug Boles of Quality Mold Shop Incorporated, who donated the labor and materials for the bearing plate and steel retainers used in the study.

References

[1] Scheirhorn, C., "Masonry Testing - Problems and Solutions," *Masonry Construction*, February 1995, pp. 83-87.

[2] Drysdale, R. G., Hamid, A. A., and Baker, L. R., *Masonry Structures, Behavior and Design*, Prentice Hall. 1994, Englewood Cliffs, NJ.

[3] Kelch, N. W. and Emme, F. E., "Effect of Type, Thickness, and Age of Capping Compounds on the Apparent Compressive Strength of Brick," in *ASTM Bulletin # 230*, May 1958, pp.# 38-41.

[4] Dodd, C.M. and McGee, T.D., " A Comparison of Various Methods of Capping Brick, Structural Tile and Concrete Block for Compressive Strength Tests," *in The Iowa State University Bulletin*, Vol. LIX, No. 17, September 21, 1960, pp. 1-11.

[5] National Concrete Masonry Association, "Concrete Masonry Unit – Testing Variables," *NCMA-TEK* 18-7, 1992. Herndon, Va.

[6] "Standard Specifications for Transportation Materials and Methods of Sampling and Testing, Part II Tests," Seventeenth Edition, 1995, American Association of State Highway and Transportation Officials, pp. 11-17. Washington D.C.

[7] Carrasquillo, P.M. and Carrasquillo, R.L., "Effect of Using Unbonded Capping Systems on the Compressive Strength of Concrete Cylinders," ACI Materials Journal, Vol.# 85, No.17, May-June 1988, pp. 141-147.

[8] Richardson, David N., "Effects of Testing on the Comparison of Neoprene Pad and Sulfur Mortar-Capped Concrete Test Cylinders," ACI Materials Journal, Vol.# 87, No.# 52, Sept.-Oct. 1990, pp. 489-495.

[9] Ozyildirim, Celik, "Neoprene Pads for Capping Concrete Cylinders," Cement, Concrete, and Aggregates, CCAGDP, Vol. 7, No.# 1, Summer 1985, pp. 25-28.

[10] Crouch, L. K. and Pearson, John B., "Neoprene Capping for Static Modulus of Elasticity Testing," *ACI Materials Journal*, Vol.# 92, No.# 6, Nov.-Dec. 1996, pp. 643-648.

[11] Knight, Marcus L., "Development of an Unbonded Capping System for Concrete Masonry Units". Master of Science Thesis in Civil Engineering, Tennessee Technological University, May 1998, Cookeville, TN.

R. Craig Henderson,[1] G. Scott Wilson,[2] L.K. Crouch,[3] William A. Sneed, Jr.[4]

COMPARISON OF ACTUAL AND ALLOWABLE STRESS VALUES FOR OUT-OF-PLANE SHEAR ON MASONRY WALLS

REFERENCE: Henderson, R. C., Wilson, G. S., Crouch, L. K., and Sneed, W. A. Jr., **"Comparison of Actual and Allowable Stress Values for Out-of-Plane Shear on Masonry Walls,"** *Masonry: Materials, Testing, and Applications, ASTM STP 1356,* J. P. Brisch, R. L. Nelson, and H. L. Francis, Eds., American Society for Testing and Materials, 1999.

ABSTRACT: This paper presents research results from the testing of 16 masonry wall specimens in direct out-of-plane shear. The wall specimens were two courses high and 1.2 m (48 in.) long. The walls were nongrouted and were constructed with face-shell bedding only. The testing apparatus was configured such that failure mechanisms other than direct out-of-plane shear (i.e., those resulting from flexural and axial loads) were minimized. Shear stress values from the 16 wall tests are compared with allowable shear stress values obtained in ACI 530 / ASCE 5 / TMS 402.

These results show that the code allowable shear stress values appear to be unconservative for this application of out-of-plane shear. It was found that the walls tested failed in out-of-plane shear at an average shear force of 69.8 kN (15,696 lb). This force produced an average shear stress of 0.349 MPa (50.65 psi) based on a parabolic stress distribution and 0.885 Mpa (128.36 psi) for pure shear stress.

KEYWORDS: masonry walls, out-of-plane shear, in-plane shear, mortar, concrete masonry units

In design, engineers must frequently assess the out-of-plane shear resistance of masonry walls. However, national masonry codes provide little guidance on the calculation of allowable shear values for out-of-plane loads. Often, the equations used to calculate the allowable shear stresses are intended for in-plane shear. For example, ACI 530 / ASCE 5 / TMS 402 provides allowable shear stress values for only *in-plane* shear

[1] Assistant Professor of Civil Engineering, Tennessee Technological University, Cookeville, TN 38505.
[2] Graduate research assistant, Department of Civil and Environmental Engineering, Tennessee Technological University, Cookeville, TN 38505.
[3] Associate Professor of Civil Engineering, Tennessee Technological University, Cookeville, TN 38505.
[4] President, WASCO, Nashville, TN.

but recommends that in the absence of suitable research data these values be used for out-of-plane shear as well [*1*].

Since the behavior of a masonry element subjected to out-of-plane shear differs significantly from that of in-plane shear, the code-specified values are likely to produce inaccurate results for loads perpendicular to the face of a wall. This is especially true for walls constructed with face-shell bedded mortar only. However, partially grouted walls are similarly affected due to the ambiguity regarding the effective area that resists the out-of-plane shear forces.

Background and Literature Review

In reference to the allowable shear equations provided in ACI 530-95 / ASCE 5-95/ TMS 402-95, the commentary states that there is an absence of suitable research for limiting out-of-plane shear stresses. The allowable values given in the code are based on recent research, and four sources for this research are referenced.

Woodward and Ranking [*2*], tested eight hollow core walls. Loads on the specimens were applied in-plane, and the emphasis of the research was on the influence of vertical compressive stress on the lateral in-plane load resistance of the walls. Lateral in-plane displacements were applied to the top surface of wall specimens while maintaining a constant compressive vertical stress. The following equation was derived from the test data:

$$v = 69.3 + 0.376a \text{ (psi)}$$

where

v = maximum shear stress of masonry joint and
a = compressive stress normal to shear surface.

A three-block prism setup was the basis for research conducted by Pook, Stylianou, and Dawe [*3*]. Forty-three hollow core prisms constructed of concrete masonry units were tested. The prisms were set up in the test frame and loaded in-plane to cause a double-shear failure at the joints. From the data obtained, they concluded that with increasing compressive stress, the failure shear load increases proportionally after the initial bond strength of the joint is exceeded. Equations similar in form to those of Woodward and Ranking were developed for the prediction of in-plane capacity

The research of Hamid, Drysdale, and Heidebrecht included the in-plane testing of forty-six specimens constructed of hollow core concrete masonry units [4]. They employed a four-unit setup that eliminated the effects of flexural stresses during testing. Their findings included a consistent failure pattern of shear slip of the mortar joints. This failure was initiated by a debonding at the block-mortar interfaces. The data also showed that the variable most significantly affecting the shear strength of concrete masonry is the level of normal compressive stress.

Nuss, Noland, and Chinn conducted prism research which included the development of a new type of couplet test method [5]. For these tests, four-brick-high prisms were constructed. When the specimens were loaded in the longitudinal direction, shear and compression were produced on the mortar joint faces. All the shear specimens (a total 115 were tested) failed in-plane along the top of the mortar joint, the bottom of the mortar joint, or a combination of the two. Several variables and their effect on the shear strength of the joints were looked at in this research; so the relationship between normal stress and ultimate shear stress was not strictly examined.

As indicated by the research discussed, a good deal of study has been done on the shear strength of masonry systems, particularly how the shear strength is affected by an applied, normal compressive load. However, none of the research related to allowable masonry shear stresses included out-of-plane shear tests. Only in-plane shear was investigated. Thus, there is a lack of suitable data on the out-of-plane shear resistance of masonry elements.

Research Objective and Overview

The intent of the research described herein is to focus on the correlation of the actual out-of-plane shear resistance of tested unreinforced concrete masonry walls to the allowable shear stress values obtained in ACI 530 / ASCE 5 / TMS 402.

In order to compare actual versus allowable shear stress, 16 masonry wall specimens were subjected to out-of-plane loading, producing an isolated shear failure at the bed joints. Effort was made to prevent other failure mechanisms. The test setup (Fig. 1) was designed such that a uniform shear force was applied to the top course of the masonry wall specimens. Each specimen was two courses high and was subjected to a uniform axial load so as to compensate for the bending component resulting from the applied lateral force. Both the lateral and axial forces were applied to the center of the specimens and distributed over the entire length through rigid wide-flange sections (Fig. 2). A gypsum cement cap was placed on the wall specimens to ensure a flat surface for axial loading and eliminate eccentric forces and nonuniform stresses. A steel cap plate, 6.35 mm (1/4 in.) thick, rested between the gypsum cap and the wide-flange. The steel cap plate and wide-flange surfaces were well lubricated to allow lateral displacement of the top course of the wall specimens and to minimize the friction force between the surfaces as compared to the applied shear. The bottom course of the wall was prevented from lateral displacement by another rigid wide-flange beam opposite the one that applied the lateral load.

The sixteen wall specimens tested were constructed of nominal 203 mm by 203 mm by 406 mm (8 in. by 8 in. by 16 in.) concrete masonry units. Each wall was nominally 1.2 m (48 in.) long and two courses high. Type S Portland Cement Lime mortar, proportioned similar (1: 0.5: 1.67 by volume) to the specification requirements in ASTM Standard for Mortar for Unit Masonry C 270-96a, was used for the mortar. Units for the first course were laid in a full mortar bed while the second course was laid in running bond using faceshell bedding only. The mortar joint thickness was 9.5 mm (3/8 in.). The same experienced mason, using consistent quality workmanship, constructed each wall.

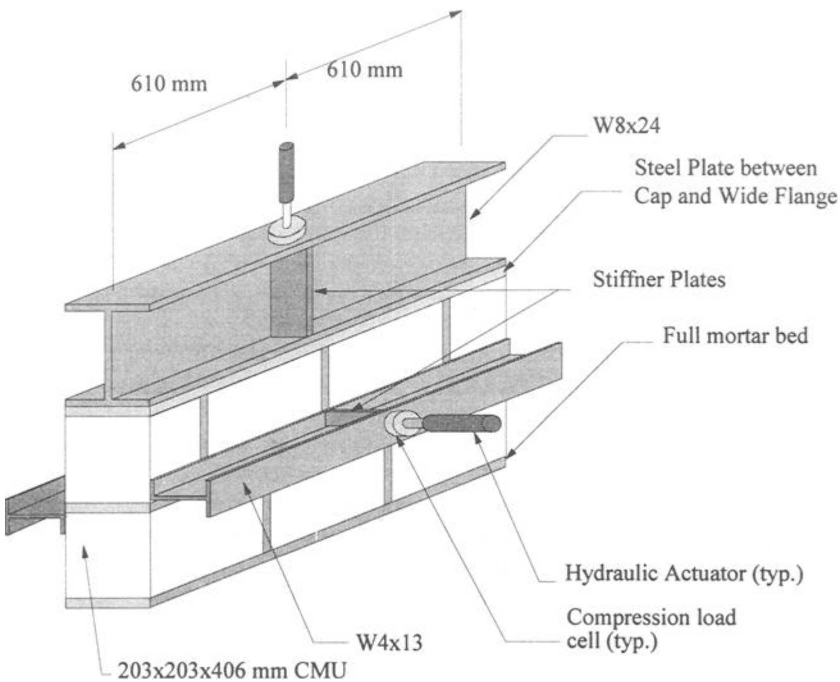

FIG. 1--*Out-of-plane shear setup.*

Loads were applied to the wall specimens using an adjustable load frame (Fig. 2). A vertical load of 22.2 kN (5000 lb) was applied through a 489 kN (55-ton) actuator connected to the W18x86 upper beam of the load frame. The lateral load was applied using a 890 kN (100-ton) actuator connected to one of the W14x30 columns of the load frame. Each actuator was connected to an appropriately sized load cell, and load data was obtained and recorded using a Measurements Group data acquisition system.

Initially, a 22.2 kN (5000 lb) vertical load was applied to the wall. After this precompression load, the dial indicators were zeroed. Lateral load was then applied to the wall's top course and displacements at incremental loads were determined until shear failure along the bed joint occurred. Because of the lubrication applied to the wide-flange and cap plate surfaces, the friction forces were small and, thus, the compression stress distribution was nearly uniform with expected gradients of less than five percent.

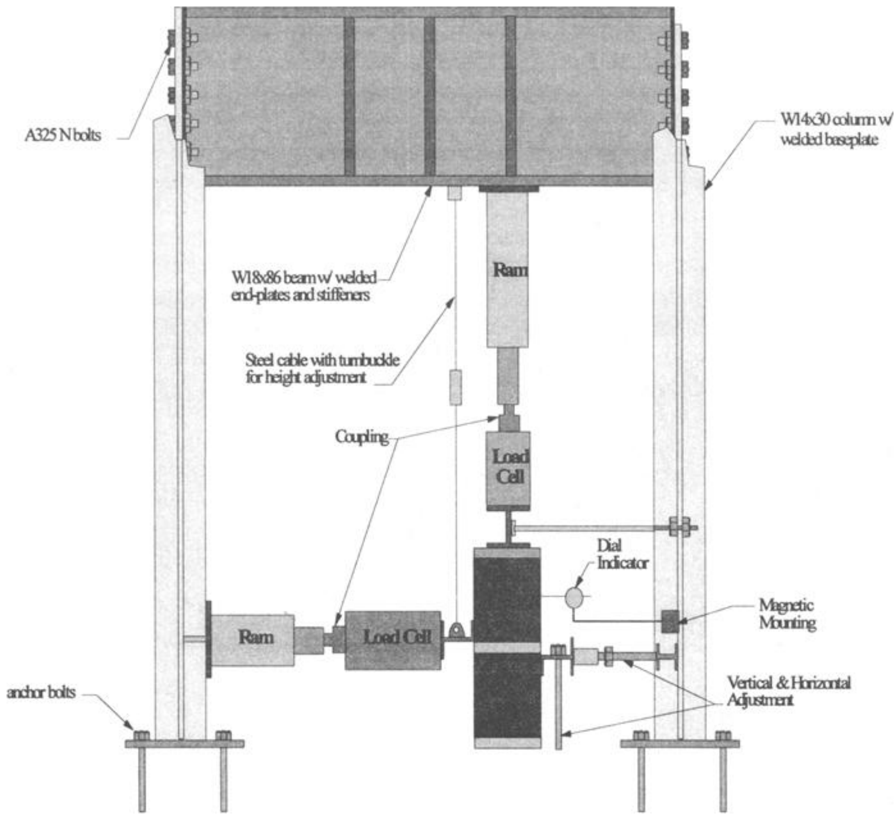

FIG. 2--*Setup with wall specimen and load frame.*

The loads applied to the wall specimen were obtained by the use of load cells at the vertical and lateral rams. The load cells relayed electrical data that was translated into force units by the data acquisition system. The data acquisition system was set to record data continuously; thus, the lateral load of the wall specimen at failure was attained.

Displacement dial indicators were mounted to the W14x30 column of the load frame that was opposite the application of the lateral load. These indicators were precise to 0.025 mm (0.001 in.) and were fixed so as to measure the displacement at mid-height of the top course of the wall. Three indicators were used, and the displacements at quarter points along the wall were measured (Fig. 2).

Results

Allowable Stress

Using the net area compressive strength of 21.86 MPa (3170 psi) obtained from unit testing and a Type S mortar, the net area compressive strength of the masonry, f'm, was calculated to be 15.13 MPa (2195 psi) from Table 1 of ACI 530.1-95. This value for f'm was then used in the calculation of the allowable shear stress. From ACI 530, Section 6.5.2, allowable shear stress, Fv, shall not exceed:

(a) $1.5\sqrt{f'm}$

(b) 0.83 MPa (120 psi)

(c) $v + 0.45\dfrac{N_v}{A_n}$

where

$f'm$ = compressive strength of masonry,
v = 0.26 MPa (37 psi) for masonry in running bond that is not grouted solid,
N_v = force acting normal to shear surface, and
A_n = actual net cross-sectional area.

Actual Stress

From ACI Section 6.5.1, the actual shear stress on an unreinforced masonry wall, where some degree of bending exists, is calculated for a parabolic stress distribution as

$$f_v = \frac{VQ}{Ib} \tag{1}$$

where

V = design shear force, or in this case the maximum out-of-plane shear force a wall specimen obtained,
Q = first moment about the neutral axis of that portion of the cross section lying between the neutral axis and the extreme fiber,

I = moment of inertia, and
b = width of the section; assumed to be the full length of the wall; 1.2 m (48 in.).

The bed joint cross section (through which shear stresses were transmitted) for the wall specimens in this research can be seen in Fig. 3. The faceshell mortar provides for the transmission of stresses from course to course. The bed joint length is 1.2 m (48 in.) and the thickness of each line of mortar is 31.8 mm (1.25 in.). It is with this area of mortar that all the stress calculations were made.

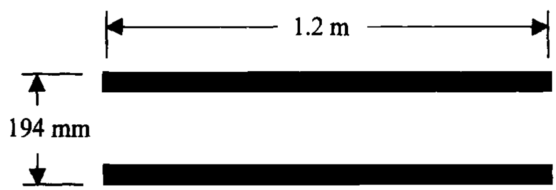

FIG. 3--*Faceshell mortar.*

If the average shear stress distribution is assumed (as in the case of direct shear), actual stress is calculated as

$$f_v \quad \frac{V}{A} \tag{2}$$

where

V = design shear force, or in this case the maximum out-of-plane shear force a wall specimen obtained and
A = net cross-sectional area.

Comparison of Allowable and Actual Stress

Table 1 shows the axial load applied to the specimens, the actual shear and code allowable shear, and the actual shear stress and code allowable shear stress. The axial load generally increased for each specimen as the tests progressed due to some bending resulting from the applied loads. The actual shear values (V, act) were determined directly from the testing (i.e., the load applied to the specimen from the actuator). The code allowable shear (V, code) was calculated from ACI 530 Equation 6-7 by setting f_v equal to F_v from the controlling equation of Section 6.5.2. Actual shear stress (f_v, act) and allowable shear stress (F_v, code) are calculated directly from sections 6.5.1 and 6.5.2, respectively. It should be noted that the applied axial load affects the code allowable shear stress (F_v, code) when ACI 530 Equation 6.5.2 (c) controls. This equation is a function of the applied axial load, N_v, and the net cross-sectional area, A_n and controlled for all specimens except Wall 1 where ACI 6.5.2 (a) controlled.

Using a ratio of the allowable code shear values to those obtained from testing, a factor of safety for the design was tabulated. As shown, the walls failed in out-of-plane shear at an average shear force of 69.8 kN (15,696 lb). This force produced an average shear stress at failure of 0.349 MPa (50.65 psi) according to ACI 530-95, Equation 6-7. From ACI 530-95, section 6.5.2, the controlling average allowable shear stress to be used for design would be 0.421 MPa (61.01 psi). This results in an average factor of safety of 0.830.

TABLE 1—*Actual stress (parabolic) versus code allowable.*

Wall	Axial Load (N)	V, act (N)	V, code (N)	f_V, act (MPa)	F_V, code (MPa)	Factor of Safety
1	42 256	77 840	96 883	0.389	0.485[1]	0.803
2	27 355	78 730	82 798	0.394	0.414	0.951
3	28 245	77 840	83 832	0.389	0.419	0.929
4	24 019	60 715	78 921	0.304	0.395	0.769
5	34 694	73 837	91 327	0.369	0.457	0.808
6	33 805	78 507	90 294	0.393	0.452	0.869
7	27 355	67 667	82 798	0.338	0.414	0.817
8	29 802	66 444	85 641	0.332	0.428	0.776
9	25 354	67 387	80 472	0.337	0.402	0.837
10	23 797	56 992	78 662	0.285	0.393	0.725
11	28 690	59 661	84 349	0.298	0.422	0.707
12[2]	27 355	48 986	82 798	0.245	0.414	0.592
13	31 136	82 733	87 192	0.414	0.436	0.949
14	22 240	63 273	76 853	0.316	0.384	0.823
15	26 688	67 721	82 022	0.339	0.410	0.826
16	24 464	67 890	79 438	0.340	0.397	0.855
Avg.	28 660	69 816	84 099	0.349	0.421	0.830
Std. Dev.	5 193	7 973	5 462	0.04	0.03	0.07
Coef. of Var.	18.12	11.42	6.49	11.42	6.49	8.81

[1] ACI 530 Section 6.5.2 Equation (a) controls.

[2] Not used in statistical calculations due to possible predamage.

Table 2 lists the results from the wall tests and the shear stress calculated as pure shear. The failure shear force and the controlling code allowable shear stress are unchanged at 69.8 kN (15,696 lb) and 0.421 MPa (61.01 psi), respectively. However, the average stress at failure for this case is 0.902 MPa (130.83 psi). This results in an average factor of safety, as compared to the code-allowable shear stress, of 2.14.

TABLE 2—*Actual stress (pure shear) versus code allowable.*

Wall	Axial Load (N)	V, act (N)	V, code (N)	f_V, act (MPa)	F_V, code (MPa)	Factor of Safety
1	42 256	77 840	37 513	1.005	0.485(1)	2.075
2	27 355	78 730	32 059	1.017	0.414	2.456
3	28 245	77 840	32 459	1.005	0.419	2.398
4	24 019	60 715	30 558	0.784	0.395	1.987
5	34 694	73 837	35 362	0.954	0.457	2.088
6	33 805	78 507	34 961	1.014	0.452	2.246
7	27 355	67 667	32 059	0.874	0.414	2.111
8	29 802	66 444	33 160	0.858	0.428	2.004
9	25 354	67 387	31 158	0.870	0.402	2.163
10	23 797	56 992	30 458	0.736	0.393	1.871
11	28 690	59 661	32 659	0.771	0.422	1.827
12(2)	27 355	48 986	32 059	0.633	0.414	1.528
13	31 136	82 733	33 760	1.069	0.436	2.451
14	22 240	63 273	29 757	0.817	0.384	2.126
15	26 688	67 721	31 759	0.875	0.410	2.132
16	24 464	67 890	30 758	0.877	0.397	2.207
Avg.	28 660	69 816	32 563	0.902	0.421	2.143
Std. Dev.	5 193	7 973	2 115	0.10	0.03	0.19
Coef. of Var.	18.12	11.42	6.49	11.42	6.49	8.81

(1) ACI 530 Section 6.5.2 Equation (a) controls.

(2) Not used in statistical calculations due to possible predamage.

Using the stress equations provided in ACI 530, based on the existence of some bending in the wall specimens, a designer would meet code requirements if he calculated the walls in this research to attain an out-of-plane ultimate strength of 84.1 kN (18,907 lb). However, the walls failed at an average of 69.8 kN (15,696 lb), achieving only 80.3% of the design strength (Table 1). Similarly, if the actual shear stress is calculated assuming pure shear an average safety factor of 2.14 results (Table 2).

Though measures were taken to produce pure shear, all flexural stresses can rarely be completely eliminated. Therefore, factors of safety between 0.83 and 2.14 may be expected for similar applications. Safety factors of 3 and above are common when masonry is designed using working stress in ACI 530-95. For example, when considering bending, the allowable compressive stress, F_b, is 1/3 that of the specified strength of masonry, f'm. (i.e., a factor of safety of 3). An overall factor of safety of 4 is incorporated in the allowable equations for combined axial compression and flexure. Similarly, when considering the slenderness effects on axial compressive strength, the code allows only axial load stresses not exceeding 1/4 of the failure stresses. Using a factor of safety of 3.0 as a guide with the data obtained in these tests, the maximum allowable shear stress used in design would be 0.116 MPa (16.9 psi) for a parabolic stress distribution and 0.300 MPa (43.5 psi) for pure shear.

A likely reason for the lower failure stresses resulting from this application of out-of-plane shear as compared to the allowable stresses obtained from ACI 530 is that the mode of failure for in-plane and out-of-plane shear is different (Fig. 4 and Fig. 5). Figure 4 shows the displaced shape that the wall specimens in this research would have if they were tested to failure through the application of in-plane shear. Similarly, the displaced shape that the walls for this application of out-of-plane shear attained is shown in Figure 5.

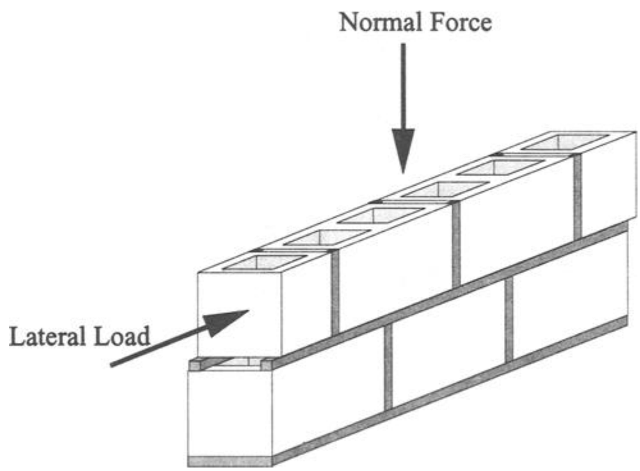

FIG. 4--*Displaced shape at failure for in-plane loading.*

To cause the top course of the wall specimen to mobilize as the lateral load is applied in-plane, the lateral force must overcome the bond along the entire length of the wall specimen. However, as lateral load is applied out-of-plane to the wall specimen, the length of bond that the load must overcome is only the thickness of the mortar joints. As the top course is mobilized, the area of bond between the mortar and the top and bottom courses is more significantly reduced in the out-of-plane failure mode. For example, load-displacement data indicate that each wall specimen displaced between 2.54 mm (0.1 in.) and 5.08 mm (0.2 in.) before failure occurred. The initial bed joint cross section as shown in Figure 3 has an area of bond equal to 77,419 mm^2 (120 in.^{2}). If the top course is displaced 2.54 mm (0.1 in.) through the application of in-plane loading (i.e., before shear failure occurs), this area of bond is reduced to 77,260 mm^2 (119.75 in.^{2}) – a reduction in area of 0.2%. However if the top course is mobilized 2.54 mm (0.1 in.) through the application of out-of-plane loading, the area of bond is reduced to 71,226 mm^2 (110.4 in.^{2}) – a reduction in area of 8.7%.

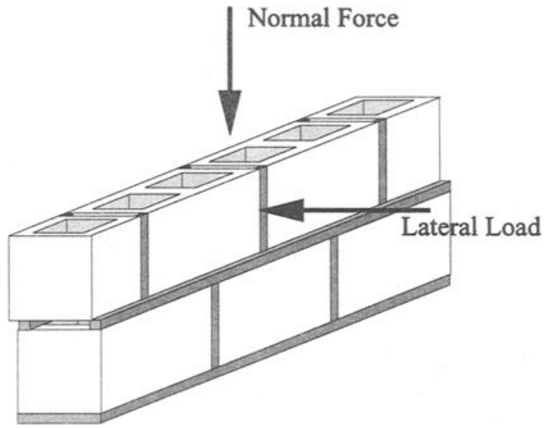

FIG. 5--*Displaced shape at failure for out-of-plane loading.*

Statistical data are also listed in Table 1 for the walls tested. The standard deviation for the ultimate out-of-plane shear load was calculated to be 8.0 kN (1792 lb). The standard deviation for the maximum out-of-plane shear stress attained was found to be 0.04 MPa (5.78 psi). The data obtained show a coefficient of variation for this test series of 11.42 percent. This value is considered reasonable for the sample size, and it is believed that if more samples were included in the statistical base, the coefficient of variation would drop to below 10 percent (considered good). With a larger sample size, statistical data are less sensitive to the maximum and minimum values obtained. In fact, if the maximum and minimum shear stress values of the walls analyzed are not considered in the statistical analysis (i.e., Wall 11 and Wall 13, respectively), the coefficient of variation becomes 10.32 percent.

Figure 6 shows a typical load-displacement graph for the walls tested. The displacement at the ends of the wall specimens was consistently greater than the displacement at the middle of the walls. This may be a result of additional confinement at the center of the wall specimens and, therefore, greater difficulty in mobilizing the upper course at the location of the middle displacement gage.

Along with each out-of-plane shear test, companion mortar cube compression testing was also done. For each wall specimen, three 50.8 mm by 50.8 mm by 50.8 mm (2 in. by 2 in. by 2 in.) mortar cubes were made during construction. Results of the compression tests can be seen in Table 3. Also, flow tests were performed on the mortar for the last eight walls tested. These tests were done in accordance with ASTM Standard Test Method for Compressive Strength of Hydraulic Cement Mortars (ASTM C 109/ C 109M-95). There does not seem to be a direct correlation between flow of plastic mortar and ultimate out-of-plane shear attained for a companion wall specimen. However, the wall that attained the highest shear load had the mortar with the lowest flow.

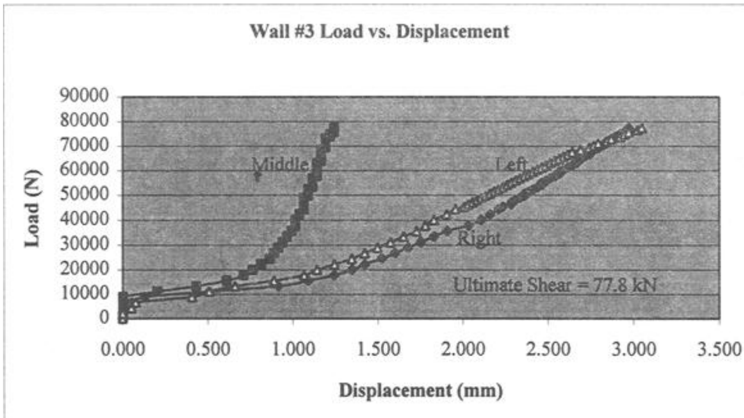

FIG. 6–*Typical load displacement curves.*

TABLE 3--*Mortar test data.*

Wall	Average Cube Compr. Str. (MPa)	Shear Load Obtained (N)	Flow (%)
1	11.121	77 844	---
2	11.818	78 734	---
3	19.112	77 844	---
4	16.940	60 718	---
5 (Spec Mold)	17.602	73 840	---
6	12.011	78 511	---
7	10.508	67 671	---
8	11.052	66 448	---
9	14.838	67 391	111
10	11.983	56 995	106
Spec. Mold	16.816	---	---
11	12.921	59 664	102
12	10.646	48 988	106
13	21.987	82 737	85
14	16.327	63 276	94
Spec. Mold	31.282	---	---
15	19.519	67 724	103
16	19.092	67 893	103
Average	15.031	69 819	---
Std. Deviation	---	7,971	---
Coef. of Variation	---	11.42	---

Conclusions

The objective of this research was to focus on the correlation of the actual out-of-plane shear resistance of unreinforced concrete masonry walls to the allowable shear stress values given in ACI 530-95. This objective was accomplished by performing experimental testing on sixteen concrete masonry wall specimens. Along with the testing of the wall specimens, other correlative tests were conducted, including masonry unit properties, plastic mortar flow characteristics, and hardened mortar cube compression tests. With the information obtained from this research, the following conclusions can be drawn.

1. The walls failed in out-of-plane shear at an average shear force of 69.8 kN (15,696 lb). This translates into an average shear stress at failure of 0.349 MPa (50.65 psi). From ACI 530-95, the controlling average allowable shear stress to be used for design would be 0.421 MPa (61.01 psi), based on a parabolic stress distribution. This results in an average factor of safety of 0.830. Thus, the walls failed at a lower stress than was allowed by the code.
2. If the failure of the wall specimens is calculated to be a pure shear failure, the average shear stress at failure can be calculated to be 0.902 MPa (130.83 psi). This results in an average factor of safety, as compared to the code-allowable shear stress, of 2.14.
3. The code allowable shear value appears to be somewhat unconservative for this application of out-of-plane shear. Safety factors of 3.0 and above are common when masonry is designed using working stress in ACI 530-95. For example, when considering bending, the allowable compressive stress, F_b, is 1/3 that of the specified strength of masonry, $f'm$ (i.e., a factor of safety of 3). An overall factor of safety of 4 is incorporated in the allowable equations for combined axial compression and flexure. Similarly, in considering the slenderness effects on axial compressive strength, the code allows only axial stresses not exceeding 1/4 of the failure stresses.
4. Load-displacement curves are linear over the full range of loading for each of the wall specimens. Hence, the walls failed in the elastic region, typical of shear failure on unreinforced masonry elements.
5. There does not appear to be a clear correlation between mortar cube compressive strength and ultimate out-of-plane shear attained for a specimen. Also, there does not seem to be a direct correlation between flow of plastic mortar and ultimate out-of-plane shear attained for a companion wall specimen.
6. Although a good deal was gained from this research, follow-up studies would be helpful in quantifying allowable values. Walls that are partially and fully grouted as well as walls with varying amounts of reinforcement should also be tested. With a larger base of experimental data, then, equations specifically for out-of-plane shear could be developed.

References

[1] ACI 530/ASCE 5/TMS 402, "Building Code Requirements for Masonry Structures," 1995.

[2] Woodward, K. and Ranking, F., "Influence of Vertical Compressive Stress on Shear Resistance of Concrete Block Masonry Walls," U.S. Department of Commerce, National Bureau of Standards, Washington, D.C., 1984.

[3] Pook, L.L., Styliano, M.A., and Dawe, J.L., "Experimental Investigation of the Influence of Compression on the Shear Strength of Masonry Joints," *Proceedings of the Fourth Canadian Masonry Symposium*, Fredericton, New Brunswick, Canada, 1986, pp. 1053-1062.

[4] Hamid, A.A., Drysdale, R.G. and Heidebrecht, M., "Shear Strength of Concrete Masonry Joints," *Proceedings of the American Society of Engineers*, New York, 1979, pp. 1227-1240.

[5] Nuss, L.K, Noland, J.L. and Chinn, J., "The Parameters Influencing Shear Strength Between Clay Masonry Units and Mortar," *Proceedings of the North American Masonry Conference*, University of Colorado, Boulder, CO, 1978.

Lucas G. Ponce,[1] Richard E. Klingner,[2] and John M. Melander[3]

Use of Ruggedness Testing to Develop an Inter-Laboratory Testing Protocol for Mortar-Cement Mortar

REFERENCE: Ponce, L. G., Klingner, R. E., and Melander, J. M., "**Use of Ruggedness Testing to Develop an Inter-Laboratory Testing Protocol for Mortar-Cement Mortar,**" *Masonry: Materials, Testing, and Applications, ASTM STP 1356,* J. H. Brisch, R. L. Nelson, and H. L. Francis, Eds., American Society for Testing and Materials, West Conshohocken, PA, 1999.

ABSTRACT: In 1996, ASTM approved a specification for a new product, called mortar cement, intended for use in applications requiring masonry with high tensile bond strength. An inter-laboratory testing program is planned; the objectives will include the determination of intra- and inter-laboratory coefficients of variation of bond-wrench results for that product. Prior to conducting the inter-laboratory testing program, it is necessary to set the test procedures and variables to be used. Some of those procedures (such as the precise control of flow, the use of jigs, templates and drop hammers to construct prisms, and bag curing), have already been found to reduce the variability of bond-wrench results, are included in ASTM C1329-96, Standard Specification for Mortar Cement, and ASTM C1357-96, Standard Test Methods for Evaluating Bond Strength, and will be used in the inter-laboratory study. However, other test procedures must still be established. To do so, and prior to the inter-laboratory study, a pilot "ruggedness study" was conducted; the objective was to determine which additional factors should be controlled during the inter-laboratory study. In this paper, the conduct and results of that ruggedness study are presented and discussed in the light of current bond-wrench testing procedures, and specific changes are recommended to ASTM bond-wrench testing standards.

KEYWORDS: bond, masonry, mortar, mortar cement, ruggedness

Introduction

Background

In 1996, ASTM approved a specification for a new product, called mortar cement, which is intended for use in areas requiring masonry with high tensile bond strength. It is desired to conduct an inter-laboratory testing program to determine intra- and inter-laboratory coefficients of variation of bond-wrench results for this product.

[1] Former Graduate Research Assistant, The University of Texas at Austin.
[2] Phil M. Ferguson Professor in Civil Engineering, The University of Texas at Austin.
[3] Program Manager, Masonry, Portland Cement Association, Skokie, Illinois.

Bond-wrench testing is described in general in ASTM C1072-94, Standard Test Method for Measurement of Masonry Flexural Bond Strength. Recent studies (Hedstrom et al. 1991, Melander et al. 1993) have also found that coefficients of variation from bond-wrench testing can be significantly reduced by careful control of experimental procedures. These include the precise control of flow; the use of jigs, templates and drop hammers to construct prisms; and bag curing. Those procedures have been included in ASTM C1329-96, Standard Specification for Mortar Cement, and ASTM C1357-96, Standard Test Methods for Evaluating Bond Strength, and will be used in the inter-laboratory study. To eliminate variations due to differences among bond-wrench testing machines, the inter-laboratory study will be conducted using a single type of bond-wrench machine.

However, other test procedures must still be established. To do so, and prior to the inter-laboratory study, it is desired to conduct a "ruggedness study," whose objective is to determine which additional factors should be controlled during the inter-laboratory study.

Design of Ruggedness Testing

"Ruggedness testing" is a systematic procedure for determining the influence of different variables on a test result, and is prescribed in ASTM E1169-89, Standard Guide for Conducting Ruggedness Tests. The variables may be related to the specimens themselves, or to the testing conditions. In ruggedness testing, the variables (termed "main effect variables") are first identified, and results are then obtained for specimens and test conditions corresponding to different combinations of those variables selected in a particular arrangement.

The following 7 main effect variables were proposed. The letters A through G identifies them; some are explained further below:

(A) couplets versus prisms (C versus P)

(B) target mortar flow (low [120-123] versus high [127-130] (L versus H). A single mortar design was used, and flow was changed by changing water content.

(C) moisture content of units (low [20%] versus high [35%]) (L versus H).

(D) delay time between joints (1 minute versus 6 minutes) (1 versus 6). Variable D refers to the method of building prisms. Some laboratories build one prism at a time, leading to about a 1-minute delay between successive joints of each prism. Others build 6 prisms at a time, leading to about a 6-minute delay between successive joints of each prism.

(E) curing temperature (low [74 F] versus high [88 F]) (L versus H)

(F) conditioning (conditioning versus no conditioning) (Y versus N). Variable F refers to conditioning the specimens in laboratory air for 24 hours after removing them from bag curing.

(G) loading rate (low versus highest rate of ASTM C1072) (L versus H)

Consideration of these factors leads to the Plackett-Burman design shown in Table 1.

Table 1 - Plackett-Burman design for ruggedness testing

MEASUREMENT	FACTOR						
	A Specimen	B Flow	C Moisture	D Delay	E Curing T	F Condition	G Rate
1A, 1B	C	L	H	1	H	N	L
2A, 2B	P	L	H	6	L	Y	L
3A, 3B	P	H	H	6	H	N	H
4A, 4B	C	H	L	6	H	Y	L
5A, 5B	P	L	L	1	H	Y	H
6A, 6B	C	H	H	1	L	Y	H
7A, 7B	C	L	L	6	L	N	H
8A, 8B	P	H	L	1	L	N	L

In Table 1, each measurement (1A, 2A, and so forth) represents a set of 30 joints whose variables are arranged as shown in the table. For example, Measurement 1A represents a set of 30 joints with the following variables:

Specimen	couplets
Flow	low
Unit Moisture Content	high
Delay in Laying	1 minute
Curing Temperature	high
Conditioning	no
Loading Rate	low

Two replicates of each measurement were conducted. These are termed Measurements 1B, 2B, and so forth. In this design, one factor (construction delay) cannot be varied when couplets are used, since couplets involve only a single joint.

Bond-Wrench Testing Program

Masonry couplets and prisms were constructed of standard concrete masonry units. A single mortar design (consisting of mortar cement, graded Ottawa sand, and 20/30 Ottawa sand) was used throughout the construction. The mortar proportions used are given in Table 2. Water was varied to control the flow. Mortar tests included the measurement of

Table 2 Mortar batch proportions

Mortar Type	Proportions by Volume		Batch Weights, kg		
	Mortar Cement	Sand	Mortar Cement	20-30 Sand	Graded Sand
S	1	3	6.80	11.00	11.00

flow, density, gravimetric air content, cone penetration, and compressive strength at 28 days of 2-inch cubes. Bond-wrench testing was performed on prisms and couplets 28 days after their construction.

Mortar was mixed using the procedure outlined in ASTM C780-96, Test Method for Preconstruction and Construction Evaluation of Mortars for Plain and Reinforced Unit Masonry. Prisms were constructed in accordance with ASTM C1357. Bond wrench tests were performed according to ASTM C1072 and ASTM C1357. The standard bond wrench apparatus is shown in Figure 1. To facilitate prism testing, a mechanism was installed on the bond wrench so that the height of the prism base support could be adjusted by one person.

Before the main test series, baseline tests were conducted to establish the expected strength values for a common combination, and to standardize testing techniques. Each test involved three 6-high prisms, with no special moisture control, no conditioning, and upper-limit testing rate.

Test results for all specimens (construction histories, batching quantities, mortar properties, prism dimensions, bond-wrench results, and corresponding strength) are given in Ponce et al. (1997).

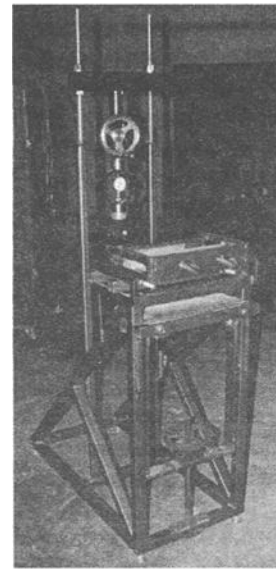

Figure 1 - Standard bond wrench testing apparatus

Table 3 Raw numerical results from ruggedness testing

SERIES	**REPLICATE A**		**REPLICATE B**	
	Mean Bond Strength, psi	**COV, %**	**Mean Bond Strength, psi**	**COV, %**
1	69.5	0.18	92.8	0.21
2	73.5	0.22	48.9	0.19
3	105.3	0.15	134.5	0.13
4	89.1	0.19	143.4	0.23
5	69.2	0.25	104.6	0.21
6	60.4	0.14	86.2	0.10
7	100.8	0.20	112.3	0.21
8	119.0	0.17	118.2	0.18

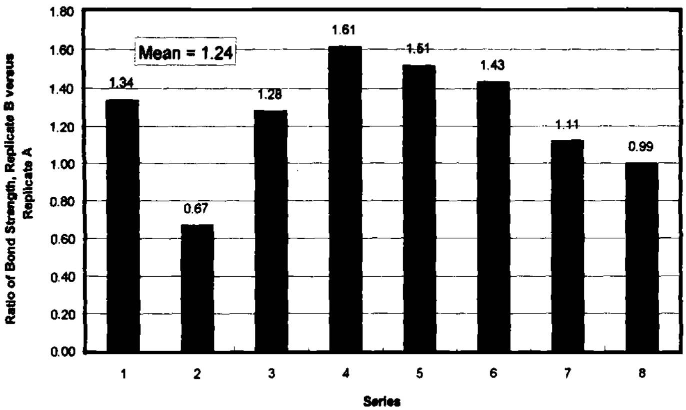

Figure 2 *Changes in mean bond strength from Replicate A to Replicate B*

Significance of Bond-Wrench Test Results

Preliminary Evaluation of Bond-Wrench Test Results

Raw numerical results from ruggedness testing are shown in Table 3. It is apparent that the mean bond strength from the second replicate is consistently higher than that from the first replicate (Figure 2). At the same time, there seems to be no consistent difference in coefficients of variation between the two replicates (Table 3), nor any consistent change in bond strength or coefficient of variation over time, as might be suggestive of a learning effect.

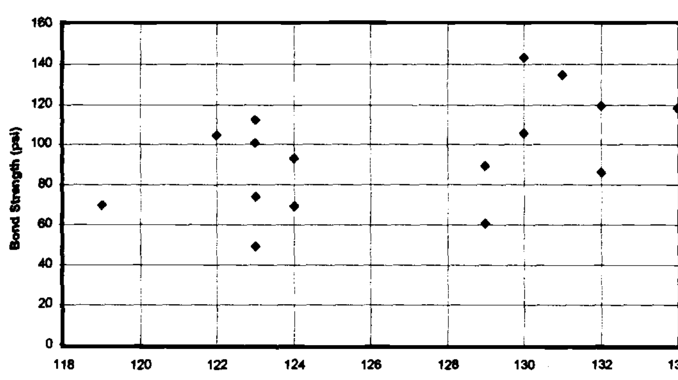

Figure 3 *Bond strength versus flow*

Examination of Variation within Replicates

To examine the variation of bond strength within replicates, the bond strength of each specimen was plotted versus flow as shown in Figure 3. Bond strength increases significantly with increasing flow.

Figure 4 shows the high, low, and mean daily temperatures in Austin, Texas during the construction period. Table 4 shows the construction date of each specimen, along with the low, high, and mean temperatures for that day. Figure 4 and Table 4 show that the "low" first replicates appeared to coincide with a string of tests on specimens that had been constructed during times of significantly lower temperature. To investigate this, the bond strengths were also plotted versus the mean temperature at the construction date (Figure 5).

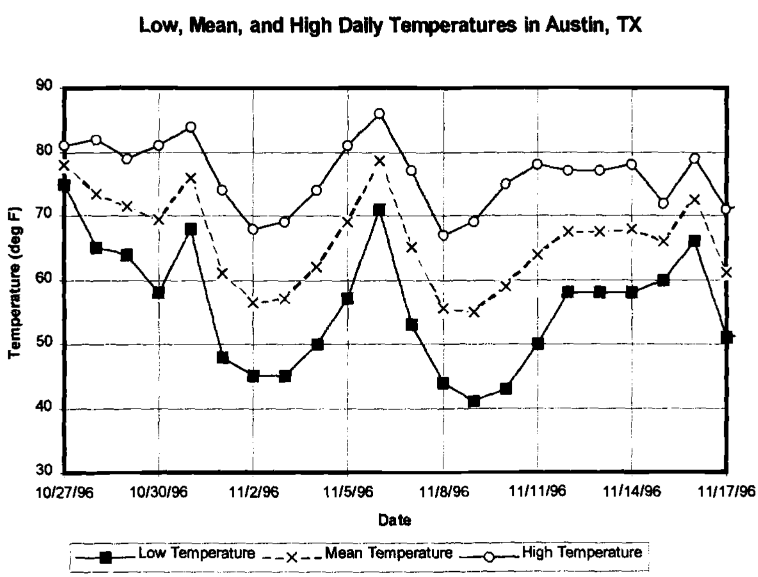

Figure 4 Low, mean, and high daily temperatures in Austin, Texas

This temperature is representative of the temperature of the mortar during mixing. A tendency for bond strength to increase with the mean temperature during construction is evident as shown in Figure 5.

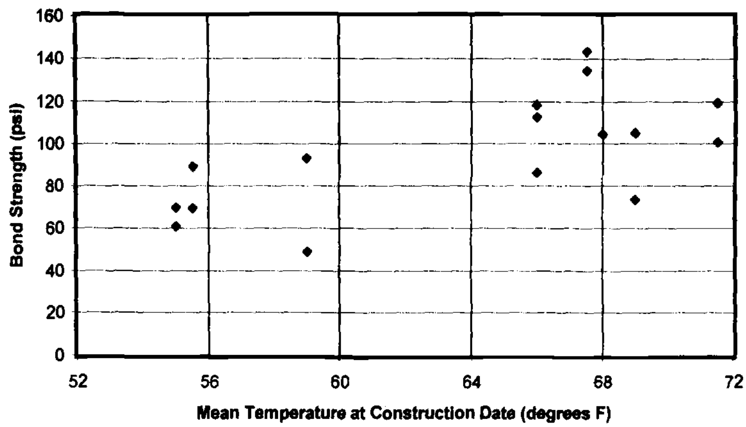

Figure 5 *Bond strength versus mean temperature at construction date*

Table 4 *Flow, mean bond strength, and temperatures for specimen construction dates*

Specimen	Construction Date	Flow	Bond Strength (psi)	Temperature (F)		
				Low	Mean	High
1A	11/8/96	119	69.5	44	55.5	67
2A	11/5/96	123	73.5	57	69.0	81
3A	11/5/96	130	105.3	57	69.0	81
4A	11/8/96	129	89.1	44	55.5	67
5A	11/9/96	124	69.2	41	55.0	69
6A	11/9/96	129	60.4	41	55.0	69
7A	10/29/96	123	100.8	64	71.5	79
8A	10/29/96	132	119.0	64	71.5	79
1B	11/10/96	124	92.8	43	59.0	75
2B	11/10/96	123	48.9	43	59.0	75
3B	11/12/96	131	134.5	58	67.5	77
4B	11/12/96	130	143.4	58	67.5	77
5B	11/14/96	122	104.6	58	68.0	78
6B	11/15/96	132	86.2	60	66.0	72
7B	11/15/96	123	112.3	60	66.0	72
8B	11/15/96	134	118.2	60	66.0	72

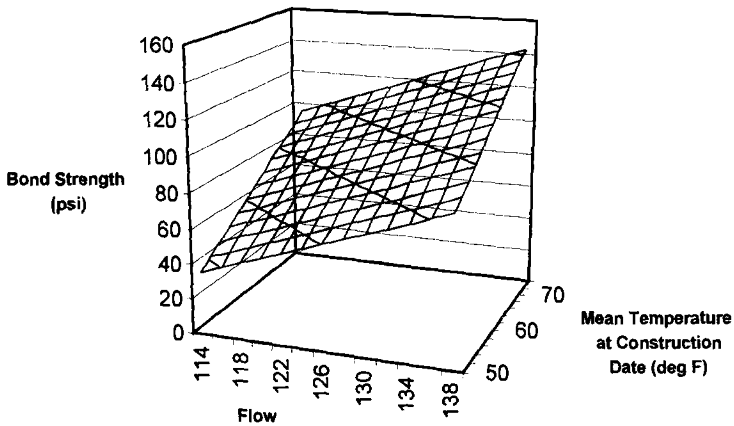

Figure 6 *Bond strength versus flow and mean temperature at construction date*

Normalization of Results for Effects of Flow and Temperature

To remove the effects of the differences in flow and construction temperature within each set of replicates, the following procedure was used:

1) A multivariable linear regression analysis was performed to determine the best fit to the bond strength as a function of flow and mean daily temperature (F) on the date of construction. The results indicate that the bond strength can be predicted as:

$$Strength = 2.01 * flow + 2.44 * temperature - 315 \qquad \text{(Eq.1)}$$

The plane represented by this equation is shown in Figure 6.

2) Using Equation (1), the raw bond strength results were normalized to a flow of 125 and a temperature of 68°F.

Table 5 contains the resulting mean bond strengths after normalization to a flow of 125 and a temperature of 68°F. The variation of bond strengths within replicates was again obtained. Figure 7 shows that the difference in strength within replicates still remains, but is significantly reduced.

Table 5 Mean bond strengths after normalization with respect to flow and temperature

SERIES	MEAN NORMALIZED BOND STRENGTH, PSI	
	Replicate A	Replicate B
1	112.1	116.8
2	75.0	74.9
3	92.8	123.7
4	111.6	134.5
5	103.0	110.6
6	84.1	77.0
7	96.2	121.2
8	96.4	105.0

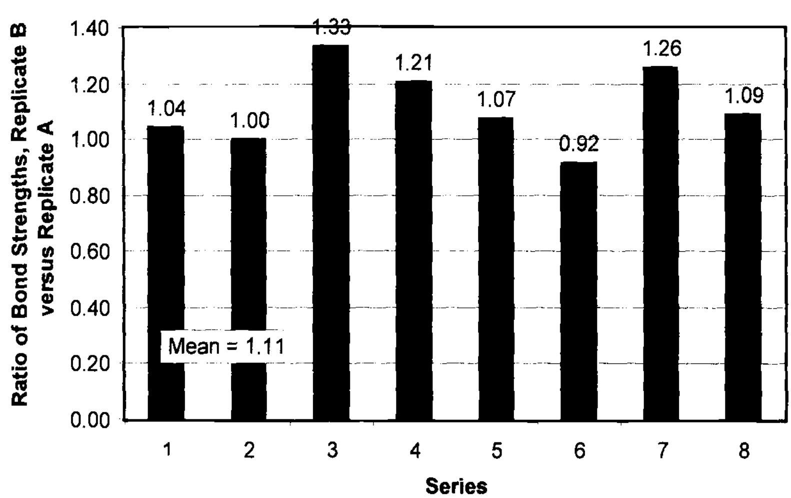

Figure 7 Changes in mean bond strength within replicates after normalization with respect to flow and temperature

Changes due to Each Main Effect Variable Using Normalized Bond Strengths

Table 6 shows the average change due to each main effect variable calculated using the normalized bond strengths. In general, the significance of each main effect variable is similar for both replicates. Because all values in Table 6 have been normalized to a single flow of 125, that table no longer contains any information about the change in bond strength experienced when going from low- to high-flow specimens.

Table 6 Average change due to each Main Effect Variable after normalization with respect to flow and temperature

VARIABLE	AVERAGE CHANGE DUE TO EACH VARIABLE, PSI (NORMALIZED BOND STRENGTHS)	
	Replicate A	Replicate B
Couplets versus Prisms	-9.2	-8.8
Low versus High Flow	-0.4	4.2
Low versus High Moisture	-10.8	-19.8
1-Minute versus 6-Minute Delay	-5.0	11.2
Low versus High Curing Temperature	16.9	26.9
Unconditioned versus Conditioned	-6.0	-17.4
Low versus High Testing Rates	-4.7	0.3

The results in Table 6 suggest the following about each Main Effect Variable:

A) Bond strength is somewhat consistently higher for couplets than prisms.
C) Low versus high moisture is quite significant. Standard units with a higher moisture content had significantly lower bond strength.
D) Bond strength is not significantly affected by the delay time between courses.
E) Bond strength increases significantly with higher curing temperature.
F) Conditioning for 24 hours in laboratory air prior to testing consistently and significantly reduces bond strength.
G) As determined previously, rate of loading does not seem to significantly affect bond strength.

These qualitative conclusions were confirmed by "t-tests" on normalized data (ASTM E1169).

Supplementary Tests to Study Influence of Flow

Previously discussed study results clearly indicate the importance of flow as a Main Effect Variable. It was therefore desired to perform additional tests to examine the effects of flow more closely. Five more sets of 30 joints each were constructed and tested, using flows of 120, 125, 130, 135, and 140).

Table 7 Test matrix for supplementary tests to study the influence of flow

Specimen	Target Flow
9A,B	120
10A,B	125
11A,B	130
12A,B	135
13A,B	140

Table 8 *Values of remaining main effect variables in supplementary tests to study the effect of flow*

Main Effect Variable	Value
Couplets versus Prisms	Prisms
Flow	varied as noted above
Unit Moisture Content	Low
Delay in Laying	6 minutes (lay one course at a time)
Curing Temperature	Normal
Conditioning	No
Loading Rate	High

Two replicates were used for each flow. All materials (units, sand, mortar cement and water) were at laboratory temperature prior to mixing. All prisms were cured under those same laboratory conditions. Cone penetrometer readings were closely compared with flow table readings, and care was taken to control the physical techniques used in the penetrometer measurements.

The test matrix for the supplementary tests to study the influence of flow is shown in Table 7. In those supplementary tests, the remaining Main Effect Variables were set to the values shown in Table 8. Flow was controlled to within ±2 for each specimen.

Table 9 *Results of supplementary tests to study the effect of flow*

Specimen	Date made	Date tested	Flow	Bond Strength, psi	COV
9A	10/23/97	11/20/97	118	72.0	0.21
9B	10/23/97	11/20/97	122	72.4	0.19
10A	10/23/97	11/20/97	124	76.1	0.14
10B	10/24/97	11/21/97	125	75.7	0.23
11A	10/16/97	11/13/97	130	78.2	0.30
11B	10/24/97	11/21/97	128	60.4	0.28
12A	10/18/97	11/15/97	134	91.6	0.20
12B	10/21/97	11/18/97	135	94.5	0.23
13A	10/18/97	11/15/97	139	97.3	0.21
13B	10/18/97	11/15/97	142	103.6	0.20

Bond strength results from the supplementary tests to study the effect of flow are summarized in Table 9 and Figure 8. The results shown in Table 9 and Figure 8 are reasonably linear, with a correlation coefficient of about 0.7. However, the results for both replicates with a flow of 130 (Specimens 11A and 11B) fall noticeably below that trend, and the respective coefficients of variation (0.28 and 0.30) are considerably higher than obtained for the other specimens.

Examination of the complete results in Appendix B of Ponce (1997) shows that several prisms in 11A and 11B were lower than the others. On that basis, the same data are plotted in Figure 9 without the results from Specimens 11A and 11B. The slope of the curve is almost exactly the same, and the correlation coefficient is quite close to 1.0.

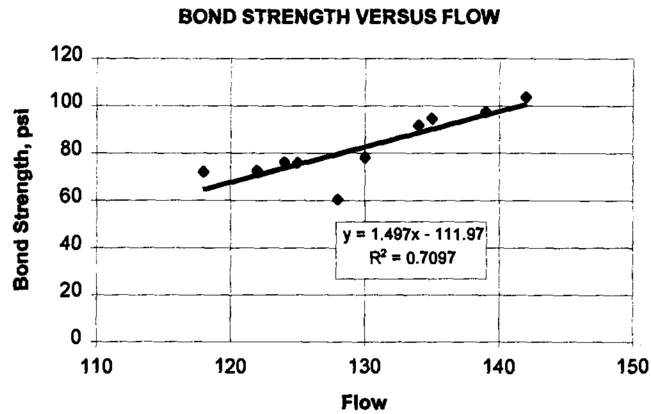

Figure 8 *Results of supplementary tests to study effect of flow*

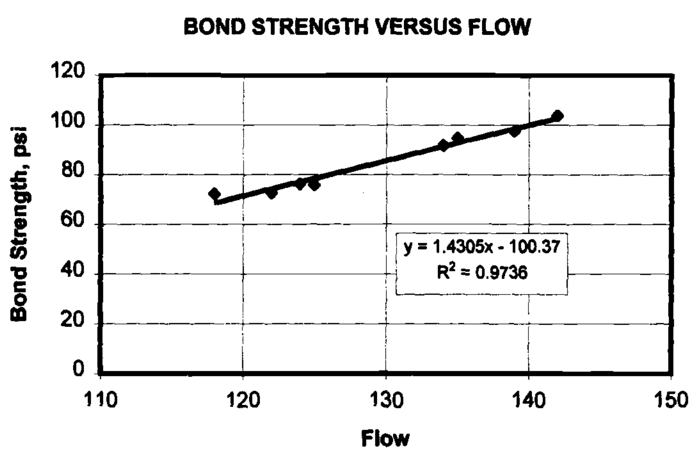

Figure 9 *Results of supplementary tests to study the effect of flow, omitting results from Specimens 11A and 11B*

Significance of Results from Supplementary Tests to Study the Effect of Flow

It is clear from Figure 9 that for these supplementary tests, tensile bond strength is essentially an increasing linear function of flow. These results are consistent with the results obtained in the previously tested specimens of this study. For those previous specimens, a multivariable regression analysis gave the relationship of Equation 1. That equation suggests that at constant temperature, the best-fit line of bond strength as a function of flow will have a slope of 2.01. Figure 9, however, indicates that at the mean laboratory temperature of 68 F, the best-fit slope is about 1.45. This suggests that the bond strength is not a linear function of flow and mean temperature, and that the best-fit multivariable regression equation of Equation 1 is only an approximation to the actual nonlinear relationship.

Consistency of Results from Supplementary Tests to Study the Effect of Flow

The consistency of results from the supplementary tests can be evaluated in terms of the relationship between replicates. Previous comparisons between replicates showed the necessity of normalizing the replicates for flow. Using a slope of 1.43 (Figure 8), the raw bond strength results from each specimen are normalized (corrected) to what they would have been at the target flow (120, 125, and so forth) for that specimen. The resulting bond strength values, normalized for flow, are shown in Table 10.

Table 10 Results of supplementary tests to study the effect of flow

Specimen	Flow	Bond Strength, psi	Target Flow	Normalized Bond Strength, psi
9A	118	72.0	120	74.9
9B	122	72.4	120	69.5
10A	124	76.1	125	77.5
10B	125	75.7	125	75.7
12A	134	91.6	135	93.1
12B	135	94.5	135	94.5
13A	139	97.3	140	98.8
13B	142	103.6	140	100.7

Figure 10 shows the ratios obtained by dividing the mean normalized bond strength obtained from the second replicate of each specimen, by the mean normalized bond strength obtained from the first replicate. Because both replicates of Specimen 12 had anomalous bond-strength values, those replicates are not plotted in Figure 10.

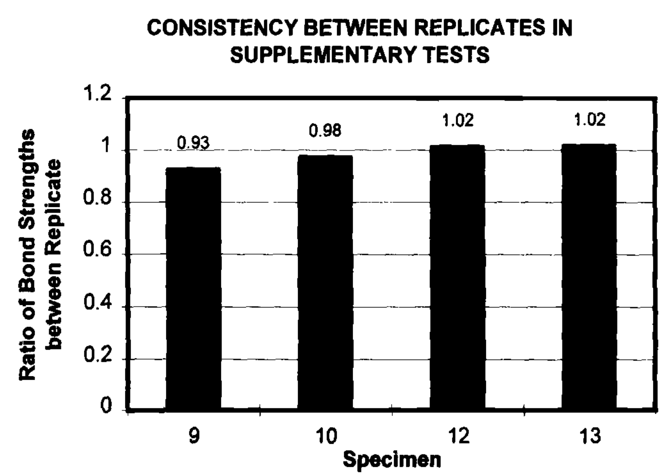

Figure 10 Ratios between normalized bond strengths of replicates

Summary, Conclusions, and Recommendations

Summary

The objectives of this ruggedness study were to identify the variables that should be controlled in inter-laboratory bond-wrench testing involving mortar-cement mortar. Two replicates of the following 7 main effect variables were used:

(A) couplets versus prisms (C versus P)
(B) mortar flow (low versus high) (L versus H)
(C) unit moisture content (low versus high permissible) (L versus H)
(D) delay time between joints (1 minute versus 6 minutes) (1 versus 6)
(E) curing temperature (low versus high) (L versus H)
(F) conditioning prior to testing (conditioning versus no conditioning) (Y versus N)
(G) loading rate (low ASTM versus high ASTM) (L versus H)

Preliminary examination of the bond wrench data showed discrepancies between the results of the first and second replicates. These discrepancies appeared to be unrelated to testing technique. Further examination revealed that in addition to the main effect variables included here, bond strength appeared to decrease significantly with decreasing ambient temperature on the day of construction. The bond strengths were normalized (corrected) to remove those effects, using a multivariable regression analysis with flow and construction temperature as the independent variables. Using the normalized data, discrepancies between the results of the first and second replicates were significantly reduced. A similar normalization procedure should be used in evaluating bond strength results from other studies.

A supplementary study was conducted to evaluate the effects of mortar flow only. All tests were conducted inside the laboratory, using prisms, low moisture content, a 6-minute delay time, low curing temperature, and no conditioning. Although no specimens from the supplementary study had exactly the same combination of main effect variables as the specimens of the supplementary study, the results were reasonably similar, and showed quite similar trends.

The results of the supplementary study indicate that if all variables except flow are controlled, and if all testing is done in laboratory-conditioned space, good correlation and repeatability are possible.

Conclusions

Examination of the normalized results leads to the following conclusions regarding the main effect variables:

1) Couplets are slightly stronger than prisms. This variable should ideally be controlled. However, couplets are more costly and time-consuming to test than prisms. If all labs test either couplets or prisms, results will be useful.
2) Bond strength increases significantly with flow, within the range of 120 to 130. Flow should be controlled to within ± 3, and bond strength results should be normalized for the effects of flow within that range.

3) Bond strength decreases significantly with increasing moisture content of units, between 20% and 35% of total absorption. This variable should be controlled.
4) Bond strength is not significantly affected by the delay time between courses. Between 1 and 6 minutes, this variable need not be controlled. From a practical construction viewpoint, it is believed more convenient to construct the prisms with a 6-minute delay between courses (that is, construct 6 prisms, one course at a time).
5) Bond strength is significantly increased by higher curing temperature, within a range of 60 to 80 F. This variable should be controlled by curing the specimens inside temperature-controlled space.
6) Bond strength is significantly decreased by 24-hour conditioning in laboratory air prior to testing. This variable should be controlled.
7) Bond strength is not significantly affected by rate of testing, within the low and high rates currently permitted by ASTM C1072. This variable need not be controlled.

Recommendations for Inter-Laboratory Bond-Wrench Testing

For inter-laboratory bond-wrench testing, the following variables should be controlled:

1) Use all prisms, or all couplets, but not both.
2) Control flow to within ±3, and normalize the bond-strength results with respect to flow within that range.
3) Use units stored in air to achieve a moisture content equal to about 20% of total absorption.
4) Construct prisms in temperature-controlled space, and normalize the results for the effects of temperature on the day of construction if necessary.
5) Construct prisms one course at a time, rather than one prism at a time.
6) Cure all specimens inside controlled space, and normalize the results for the effects of temperature if necessary.
7) Do not condition specimens prior to testing.

Acknowledgments

The research reported in this paper (PCA R&D Serial Number 2144a) was conducted by the University of Texas at Austin, with the sponsorship of the Portland Cement Association (PCA Project Index No. 95-06). The contents of this paper reflect the views of the authors, who are responsible for the facts and accuracy of the data presented. The contents do not necessarily reflect the views of the Portland Cement Association.

References

Hedstrom et al. (1991): Hedstrom, E. G., Tarhini, K. M., Thomas, R. D., Dubovoy, V. S., Klingner, R. E., and Cook, R. A., "Flexural Bond Strength of Concrete Masonry Prisms Using Portland Cement and Hydrated Lime Mortars," *The Masonry Society Journal*, Vol. 9, No. 2, February 1991.

Melander et al. (1993): Melander, J. M., Ghosh, S. K., Dubovoy, V. S., Hedstrom, E. G., and Klingner, R. E., "Flexural Bond Strength of Concrete Masonry Prisms Using Masonry Cement Mortars," *Masonry: Design and Construction, Problems and Repair, ASTM STP 1180*, J. M. Melander and L. R. Lauersdorf, Eds., American Society for Testing and Materials, Philadelphia, PA, 1993.

Ponce et al. 1998): Ponce, L. G., Klingner, R. E., Holser, P., Johnson, B., Mastraccio, A., and Placencia, P., "Use of Ruggedness Testing to Develop an Inter-Laboratory Testing Protocol for Mortar-Cement Mortar," PCA R&D Serial No. 2144, Portland Cement Association, 1998.

L.K. Crouch,[1] R. Craig Henderson,[2] and William A. Sneed, Jr.[3]

DEVELOPMENT OF AN UNBONDED CAPPING SYSTEM FOR CLAY MASONRY PRISMS

REFERENCE: Crouch, L. K., Henderson, R. C., and Sneed, W. A. Jr., **"Development of an Unbonded Capping System for Clay Masonry Prisms,"** *Masonry: Materials, Testing, and Applications, ASTM STP 1356,* J. H. Brisch, R. L. Nelson, and H. L. Francis, Eds., American Society for Testing and Materials, 1999.

ABSTRACT: To ascertain if an unbonded capping system was feasible for clay masonry prisms, the compressive strengths of thirty clay masonry prisms capped with an unbonded capping system modeled after ASTM C 1231 were compared with those of thirty masonry prisms capped with ASTM C 67 approved high-strength gypsum cement at the ages of 7 and 28 days. All prisms were constructed by a professional mason using Grade SW, Type FBS cored face brick from the same lot and ASTM C 270 Type S PC-lime mortar. There was no significant difference in mean compressive strength for the two capping methods at either age. In addition, capping with the unbonded capping system was faster and easier. Further, 28-day results obtained using the unbonded capping system had a lower coefficient of variation and higher mean compressive strength than those obtained with high-strength gypsum.

KEYWORDS: masonry prism, compressive strength, masonry, masonry prism strength, neoprene, unbonded cap, elastomeric, compressive strength of masonry, specified compressive strength of masonry, prisms

---

[1]Associate Professor of Civil Engineering, Tennessee Technological University, Cookeville, TN 38505.

[2]Assistant Professor of Civil Engineering, Tennessee Technological University, Cookeville, TN 38505.

[3]President of Wasco, 1138 Second Avenue North, Nashville, TN 37208.

The requirements for all masonry materials are determined by structural design considerations and environmental exposure conditions. Appropriate masonry units are selected for the desired application based on engineering properties such as compressive strength and durability. Routine quality control tests are necessary to ensure that the completed masonry configurations conform to the engineering property specifications determined in the design process. The research described herein involved the experimental evaluation of the effect of two capping techniques on masonry prisms in determining compressive strength.

Research Significance

Compressive strength of individual facing brick is among the most common routine quality control tests. However, difficulties exist in adequately characterizing the compressive strength of masonry prisms based on the brick and mortar properties that make up the prism. Due to the manufacturing process, masonry prisms often have rough and irregular surfaces. When the masonry prisms are tested in compression the surface roughness and irregularities lead to stress concentrations which often cause the assembly to fail at an artificially low stress. This reduced stress value is unrelated to the strength of the assembly, but rather a failure in the testing procedure. To avoid these erroneous results, ASTM Standard Test Method for Constructing and Testing Masonry Prisms Used to Determine Compliance with Specified Compressive Strength of Masonry (C 1314-95) specifies that all masonry prisms tested in compression shall be capped with either sulfur mortar or a high-strength gypsum cement capping compound. Capping ensures that the loaded faces of the masonry prisms are plane and perpendicular to the axis on which the stress is applied and that the load is more uniformly distributed over the surface of the specimen. Several studies of concrete cylinders indicate that the use of elastic pads in rigid retaining caps gives similar compressive strength results to sulfur and high-strength gypsum cement capping systems while eliminating the hazards and delays associated with other capping methods. In addition, the use of these unbonded capping systems is more economical since the caps can be reused. In the development of an unbonded capping system for masonry brick prisms, a neoprene capping procedure was introduced and compared with a commercially available high-strength gypsum cement.

Literature Review

The testing of clay masonry prisms using bonded and unbonded capping techniques has been the interest of engineers and construction industry professionals for many years. Published literature on the testing of masonry prism systems has been limited for research and review. Most prism testing over the years was usually conducted for private use.

The most recognized property studied and tested for prisms has been compressive strength. Compressive strength of a prism is obtained by dividing the ultimate compressive load attained in uniaxial compression by the cross-sectional area of the prism.

The compressive strength of masonry prisms must equal or exceed the compressive strength of masonry used in the structural design. Building codes limit allowable stresses in masonry to a percentage of the compressive strength [*1*]. Constraints on time and money have usually necessitated only strength tests to determine if the prism will withstand the loads, stresses, and strains placed on it.

When studying the compressive strengths for masonry prisms, two methods can be used to verify the compressive strength of masonry. According to the Specification for Masonry Structures (ACI 530.1 / ASCE 6 / TMS 602), these two methods are the unit strength method and the prism test method [*2*]. The unit strength method takes into account compressive strength of the units and the mortar types used. The prism test method determines the compressive strength of the masonry by testing masonry prisms representative of the loaded structure [*1*]. The prisms are usually constructed in stacked bond fashion with full mortar bedding and a minimum of two units high.

Different factors affect the compressive strength of masonry prisms. The compressive strength of the units, the type of mortar used, workmanship, and curing are the major factors involved in compressive strength of masonry, and these factors are reflected in the prism tests. Therefore, prism test results are more representative of actual in-place performance of masonry than are tests of component masonry materials [*1*]. The prism test method provides quality control checks on workmanship and curing.

It has been found that testing capped prisms gives results closer to actual masonry wall strengths than prisms tested without capping. Capping a specimen provides a smooth, plane bearing surface for the application of the compressive test load. The capping material can be either sulfur or high-strength gypsum cement.

According to ACI 530.1 / ASCE 6 / TMS 602, the compressive strength of masonry is based on the average of three prism strengths, but shall not be taken as more than the strength of the masonry units used in the construction of the prisms [*2*]. Appropriate correction factors for prism geometry from tables in the ACI Code or ASTM Procedure are applied to the average prism strength to get the actual compressive strength of the masonry prisms. Current masonry codes encourage the use of correction factors for prism geometry based on the h/t ratio. These correction factors enable conversion of the strength of a prism of a particular geometry to that of a standard 5-course prism [*3*]. The variables "h" and "t" denote prism height and least lateral dimension, respectively. The correction factor is multiplied by the compressive strength of the prism to obtain a more accurate strength measurement. The correction factors imply that a 5-course prism is a more realistic geometry.

Factors that influence strength include the types of portland cement and lime used, the proportions of the cement, lime, and sand in the mortar batch, the amount of entrained air in the mortar, curing conditions, size and shape of the specimens, expertise of the lab technician, slight changes in sand gradation, and consistency of the mix.

The main concept to remember about mortar strength is that higher strengths do not make the best mortar. Portland cement and lime need to be balanced to obtain the desired mortar for the job. A clear understanding of the proper proportions needed when mixing mortar is of the utmost importance.

Brick unit compressive strengths have been found to range from 11 720 kPa to 248 220 kPa [*4*]. Brick strength is much higher in compression than in tension, similar to concrete masonry units or cylinders. The strength of brick is greater than the strength of mortar, but the strength of the prism is between the two. Brick is vital to the prism system; however, the key to understanding prism performance is to understand the brick and mortar bond.

Bond between the brick and mortar is one of the primary factors in sound masonry practice. A good cohesive bond between and mortar increases the strength and durability of the wall system. Walls with strong, durable bond remain watertight and strong enough to withstand stresses from high winds, vibrations, etc [*5*].

Many factors exert influences on the bond of mortar to masonry. Factors affecting bond include the type of mortar, the type of masonry unit, water content of mortar, and workmanship. One of the primary aspects of mortar study is bond strength. Mortars with lime have been found to exhibit good bond strength. It has been discovered over time, that the brick and mortar bond highly influences the strength of the wall. One of the prevailing opinions among researchers in masonry study is the substantiated need for both lime and portland cement in a well balanced, all-purpose mortar. High lime mortars contribute to producing a tight, durable bond which is resistant to water, but they usually have moderate to low tensile bond strengths. High cement mortars have high bond strengths, but have a lower extent of bond and have a tendency to develop separation cracking. It has been shown that cement based mortars tend to be stiff and unworkable leading to joints that are incompletely filled and characterized by frequent voids and holes that lead to permeable masonry. Lime's superiority over portland cement in producing adhesive and durable bond is due to its higher degree of plasticity and water retention, and its greater fineness and inherent stickiness, which permit joints to be filled more readily and completely [*5*]. Mortars with the right concentrations of lime and portland cement produce the durability and bond needed to protect against water and cracking while strength is maintained.

A solid understanding of Poisson's ratio increases the knowledge of how brick wall systems function. Poisson's ratio is the ratio of the lateral strain to longitudinal strain for longitudinal loading [*6*]. Compressive loading on a specimen produces expansion at right angles to the applied force. When studying brick prisms, modulus of elasticity can be considered at the joints where mortar and brick meet. Compressive loading on brick prisms will cause lateral expansion of the mortar between the bricks. The mortar will expand more because its modulus of elasticity is lower than that of the brick. This is a strong indicator that the majority of prism failures will be along the brick and mortar joints.

Materials

A 525-count cube of Grade SW, Type FBS, cored facing brick was donated by the Masonry Institute of Tennessee for use in the study. The brick (M/S Seton Hall Regent Brick, # 031-10-284-0) were manufactured by General Shale Brick of Atlanta Georgia. The average dimensions of the facing brick units were 194 mm x 89 mm x 57 mm. The results of three ASTM Standard Test Methods for Sampling and Testing Brick and Structural Clay Tile (C 67-96) absorption tests are shown in Table 1. All absorption test results met ASTM Standard Specification for Facing Brick (Solid Masonry Units Made from Clay or Shale) (C 216-95a) requirements for Grade SW facing brick. Three brick compressive strength tests were conducted in accordance with ASTM C 67-96 and are found in Table 2. The facing brick had three cores, all of which were approximately the same size, and together produced a 20.69% void area as determined by ASTM C 67-96 procedures.

TABLE 1--*Absorption data*

Test Number	Avg Oven Dry Wt (g)	Avg Wt 24-hr Saturated (g)	Avg Wt 5-hr Boil (g)	Avg Abs. Cool %	Avg Abs. Boil %	Saturation Coefficient
1	789.6	822.0	850.9	4.10	7.76	0.529
2	808.5	841.4	870.7	4.07	7.69	0.529
3	802.7	837.5	866.6	4.34	7.96	0.545

TABLE 2--*Brick compressive strength*

Test Number	Length Avg (cm)	W Avg (cm)	Area (cm^2)	Load (Newtons)	Strength (kPa)
1	9.6	8.9	85.4	694 484	81 320
2	9.8	8.8	86.2	682 635	79 190
3	9.4	8.8	82.7	672 867	81 360
Average					80 620

ASTM Standard Specification for Mortar for Unit Masonry (C 270-96a) Type S mortar was used. This mortar was specified by the proportion method and consisted of a Portland Cement / Lime combination. Mortar compressive strength and flow properties were conducted in accordance with ASTM Standard Test Method for Compressive Strength of Hydraulic Cement Mortars (Using 2-in. or [50.8 mm] Cube Specimens) (C 109M-95) and are found in Table 3 and Table 4 indicating 7-day and 28-day tests respectively. Determination of flow was conducted on each batch of mortar produced in accordance with ASTM C 109M-95. From each batch, three 50.8 mm cubes were constructed for compressive strength testing of the hydraulic cement mortar. The strength specimens were tested at 7 and 28 days in accordance with ASTM C 109M-95. The 7-day 50.8 mm specimens were older than the specified 20-24 hours when they were to be submerged in the noncorroding tank of saturated lime water. The 28-day 50.8 mm specimens were cured in accordance with ASTM C 109M-95. This deviation from specification may have been substantial in the low strengths of the 7-day 50.8 mm cubes.

TABLE 3--*7-day mortar properties.*

Test Age	Batch Number	Flow %	Cubes Constructed	Average Cube Strength (MPa)	Within Test Coeff. of Variation
7	1.0	96	3	10.8	8.3
7	2a	92	3	9.9	3.1
7	2b	100	3	8.8	3.8
7	3a	88	3	11.0	3.0
7	3b	97	0	...	...

TABLE 4--*28-day mortar properties.*

Test Age	Batch Number	Flow %	Cubes Constructed	Average Cube Strength (MPa)	Within Test Coeff. of Variation
28	1	91	3	13.6	5.0
28	2	92	3	21.6	4.1
28	3	95	3	18.7	3.8
28	4	99	3	17.5	5.9

A commercially available high-strength gypsum cement, which was ASTM C 67-94 approved, was used for the project to cap the brick prisms. A water-gypsum cement ratio of 0.26 was used for the capping procedure. The average compressive strength of three 50.88 mm cubes of high-strength gypsum mixture at twenty-four hours was 36.9 MPa. A commercially available 70 durometer neoprene was also used for a capping material for the brick prisms. The neoprene was used as an experimental capping method for this project.

Procedure

The average dimensions of the brick units were measured and used to size the steel retainer caps which were modeled after ASTM Standard Practice for Use of Unbonded Caps in Determination of Compressive Strength of Hardened Concrete Cylinders (C 1231-93) relating to the brick dimensions. The inside dimensions of the steel retainer caps were 203 mm x 98 mm x 25 mm (Figure 1). The outside dimensions of the steel retainer caps were 251 mm x 152 mm x 51 mm. The size of the neoprene pads were modeled after ASTM C 1231-93 and were cut to specifications with relation to brick dimensions rather than cylinder dimensions.

There were no significant deviations from the testing procedures observed during the testing of the brick specimens. Commercially available high-strength gypsum cement was used to cap the half-brick compressive strength specimens.

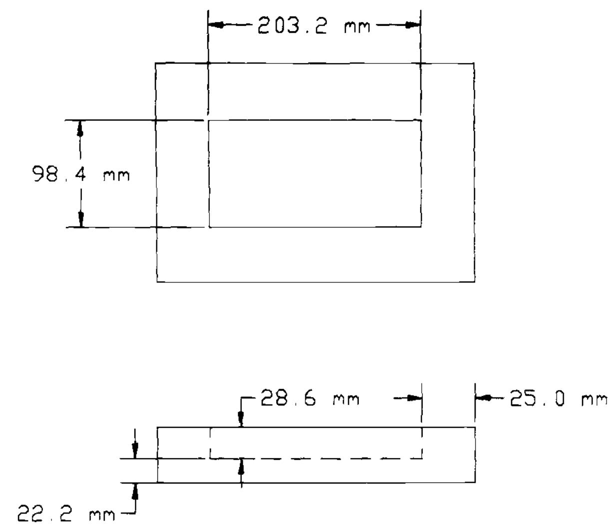

FIG. 1—*Schematic of steel retainer cap.*

Construction of the brick prisms were conducted for 7 and 28 day tests and were in accordance with ASTM C 1314-95. Sixty prisms were constructed for each test age. Each masonry brick prism consisted of three clay masonry brick units because of the allowable clearance of the compression loading frame. A professional mason was engaged to construct the masonry brick prisms.

Each constructed prism was placed in a moisture-tight bag and stored until specified removal. There was a slight deviation from specifications preceding the 7-day testing. The prisms were to be removed from the moisture-tight bags two days prior to the test, however the prisms were removed one day before testing and the significance is estimated to be minute. The curing procedure was in accordance with ASTM C 1314-95. The prisms were measured prior to the capping procedure. Commercially-available high-strength gypsum was used to cap thirty prisms, while neoprene pads were used for the remaining thirty. High-strength gypsum capping was done in accordance with ASTM C 1314-95. Neoprene capping was performed in relation to ASTM C 1231-93. The gypsum capped prisms were tested in accordance with ASTM C 1314-95. Neoprene capped prisms were tested in relation to ASTM C 1231-93 and at the same loading rate that was used for the testing of gypsum capped prisms. Although the loading rates for the different capping methods remained constant, the 7-day loading rate was approximately 124 550 Newtons per minute while the 28-day loading rate was approximately 169 032 Newtons per minute, due to the increase in the strength of the specimens.

Results

The compressive strengths obtained for both 7-day and 28-day tests are shown in the following tables (Table 5 and Table 6). Corrected and uncorrected values are shown for each capping method at each age.

TABLE 5--*7-day compressive strength.*

Test	High-strength gypsum cement		Unbonded capping system		
	Uncorrected strength, kPa	Corrected strength, kPa	Uncorrected strength, kPa	Corrected strength, kPa	Corrected percent diff.
1	24 270	24 661	19 720	20 041	-18.7
2	23 236	23 581	21 650	22 041	-6.5
3	22 133	22 501	23 926	24 224	7.7
4	21 375	21 719	21 581	21 972	1.2
5	22 202	22 547	18 754	19 007	-15.7
6	21 375	21 650	20 133	20 386	-5.8
7	22 340	22 708	20 961	21 237	-6.5
8	23 788	24 178	22 685	23 052	-4.7
9	21 306	21 581	23 236	23 581	9.3
10	23 995	24 293	22 064	22 340	-8.0
Average	22 602	22 942	21 471	21 788	-5.0

TABLE 6--*28-day compressive strength.*

Test	High-strength gypsum cement		Unbonded capping system		
	Uncorrected strength, kPa	Corrected strength, kPa	Uncorrected strength, kPa	Corrected strength, kPa	Corrected percent diff.
1	31 096	31 579	26 477	26 891	-14.8
2	29 580	29 993	25 236	25 580	-14.7
3	28 545	28 959	29 304	29 649	2.4
4	26 753	27 028	29 717	30 131	11.5
5	20 616	20 961	29 373	29 855	42.4
6	30 614	31 028	27 856	28 201	-9.1
7	28 132	28 545	27 787	28 132	-1.5
8	26 684	27 166	24 270	24 615	-9.4
9	26 339	26 684	27 097	27 511	3.1
10	24 684	25 029	27 925	28 270	12.9
Average	27 304	27 697	27 504	27 884	0.7

Analysis of Results

The uncorrected compressive strength values shown were multiplied by the height-to-thickness correction factor for masonry prism compressive strength found in ASTM C 1314 Table 1 to obtain the corrected values. Analytical discussion of the results is focused on the corrected values obtained.

The average 7-day compressive strength of the prisms capped with high-strength gypsum cement was found to be 22 942 kPa. These results show a standard deviation of 1161 kPa and a coefficient of variation of 5.061. The average 7-day compressive strength for the prisms capped with neoprene was found to be 21 788 kPa. The standard deviation for these prisms was calculated to be 1640 kPa with a coefficient of variation of 7.527. The average percent difference in compressive strength between the prisms capped with high-strength gypsum cement and those capped with neoprene was found to be -5.0%.

The average compressive strength for the prisms capped with high-strength gypsum cement at 28 days was found to be 27 697 kPa. The standard deviation of these tests was calculated to be 3127 kPa with a coefficient of variation of 11.29. For the prisms capped with neoprene, the average 28-day compressive strength was found to be 27 884 kPa. The standard deviation for these tests was calculated to be 1810 kPa and the coefficient of variation was determined to be 6.491. The average percent difference in compressive strength between the prisms capped with high-strength gypsum cement and those capped with neoprene was found to be 0.7%.

The expected value for 28-day compressive strength obtained from Table 1 page S-10 in ACI 530.1 / ASCE 6 / TMS 602, was found to be 22 857 kPa. (2) The average 28-day compressive strength obtained from testing with neoprene pads was found to be 5 027 kPa greater than the conservative value interpolated from the code.

Utilizing a two-tailed t-test, assuming a two sample equal variance, the 7 and 28-day results achieved a 95% confidence interval. This confidence interval showed that there was no statistical significance between the results obtained from prisms capped with high-strength gypsum and those capped with neoprene.

The mode of failure was consistent throughout the testing process regardless of the capping technique employed. In each prism, regardless of capping technique, the failure was found to be due to expansion of the mortar. As the mortar tried to expand outward, tensile stress was developed and cracks formed at the corners. This tensile stress and the resulting cracks were the typical modes of failure for the prisms. The extent of failure, however, was different between the two capping techniques. The prism failures using neoprene were much more extensive and explosive. A possible reason for this occurrence is that as the prisms were loaded, strain energy was built up in the neoprene pads. As the prisms reached their ultimate strength and the mortar expansion caused cracking at the corners, the prisms could no longer resist this stored energy. At this point the stored energy was released into the prism and caused a more rapid and destructive failure and thus a disaggregation of the prism. However, this type of failure is consistent with the observed "more violent" failures noted in ASTM C 1231-93.

Based on the compressive strength values obtained (Table 6 and Table 8), the degradation of the neoprene pads was not severe enough to effect the ultimate strengths of the prisms through 10 full tests, 30 prisms. However, 30 prisms appears to be a limit on the maximum number of prisms that should be tested with one set of neoprene pads due to wearing of the material.

The time required to test an individual prism was found to be essentially equal regardless of the capping technique employed. However, capping with high-strength gypsum cement has to be done 24 hours prior to actual prism testing and required approximately 12 labor hours to cap 30 individual prisms, 10 complete tests. Neoprene capping required approximately five minutes to cap all 30 specimens.

The use of an unbonded capping system proved to be a logistically better and more economical approach to the capping of masonry prisms. The 70-durometer neoprene pads were estimated to cost approximately $14.00 per set. Assuming thirty tests per set of neoprene pads, an approximate cost for the capping involving the high-strength gypsum cement was $7.00. A labor rate of only $0.60 per hour would be required to offset the higher material cost of the neoprene pads. The steel retainers for the neoprene pads would have an initial cost of approximately $250.00. Assuming a pay rate of $10.00 per labor hour, only 63 prisms need to be capped to offset the initial cost of the steel retainers.

Conclusions

Based on the results of this study, the following conclusions can be drawn.

1. Due to statistical analysis, the use of unbonded capping systems is found to be an adequate capping method for masonry brick prisms based on a lower standard deviation than the prisms capped with high-strength gypsum cement for the 28-day results.

2. The use of unbonded capping systems is also found to be an adequate capping method for masonry brick prisms based on a two-tailed t-test, assuming a two-sample equal variance data set. This test was based on a 95% confidence interval. This test showed that there was no significant difference in the means of the high-strength gypsum cement-capped prisms and the neoprene capped prisms for both the 7- and 28-day tests.

3. The use of unbonded capping systems proved to be a less time-consuming capping method for the masonry brick prisms. The prisms capped with the high-strength gypsum cement had to be capped 24 hours prior to testing, and the capping also involved approximately 12 labor hours during the capping process for 30 prisms.

4. The use of an unbonded capping system proved to be a logistically better and more economical approach to the capping of masonry prisms.

Recommendations

1. The research should be repeated with standard 5-brick solid unit prisms with a compression loading frame that has adequate clearance.

2. The testing of unbonded capping methods should be performed on various other masonry prism configurations to provide further evidence of compliance.

3. In order to achieve greater statistical results, a larger sample consisting of more than 30 tests should be performed on masonry brick prisms.

4. The unbonded capping system described herein should be considered for ASTM approval based on logistical, statistical and economical factors.

Acknowledgments

The authors gratefully acknowledge Mr. Joe Williams for constructing the prisms tested. They would like to thank Mr. Rick Maxwell and Mr. Perry Melton for their technical assistance, and the Masonry Institute of Tennessee for donating the bricks used in the research. The authors wish to recognize Mr. Barry Wilson at Mid-South Machine and Supply for the fabrication of the steel retainer caps, and also to thank the following individuals for the lab work and technical assistance they provided for the project:

Mr. Jason B. Burgess, Mr. Marcus L Knight, Ms. Heather J. Sauter, Mr. Jeffery D. Stevens, Mr. Barry N. Whitten, and Mr. G. Scott Wilson.

References

[1] "Compressive Strength of Masonry," *Masonry Information*, Portland Cement Association, IS276.01M, 1993, pp. 1-3.

[2] *Specification for Masonry Structures*, Masonry Standards Joint Committee, Detroit, 1995.

[3] Hegemier, G. A., Krishnamoorthy, G., Nunn, R. O., and Moorthy, T. V., "Prism Tests for the Compressive Strength of Concrete Masonry," *Proceedings of the North American Masonry Conference*, Aug. 1978, pp. 18-23.

[4] "Single Wythe Bearing Walls," *Technical Notes on Brick Construction*, Brick Institute of America, 11490 Commerce Park Dr., Reston VA 22091 Sept. 1994, 26 Revised, p. 3.

[5] Boynton, R. S., and Gutschick, K. A., "Bond of Mortar to Masonry Units," *Masonry Mortar Technical Notes # 3*, National Lime Association, Sept.1964, p.1.

[6] Buchanan, George R., *Mechanics of Materials*, Holt, Rinehart and Winston, Inc., New York, 1988.

Joel S. Weinstein[1] and Wayne A. Hostetler[2]

The Importance of Testing to Evaluate the Effect Masonry Walls Have on High-Rise Building Stiffness

REFERENCE: Weinstein, J. S. and Hostetler, W. A., **"The Importance of Testing to Evaluate the Effect Masonry Walls Have on High-Rise Building Stiffness,"** *Masonry: Materials, Testing, and Applications, ASTM STP 1356,* J. H. Brisch, R. L. Nelson, and H. L. Francis, Eds., American Society for Testing and Materials, 1999.

ABSTRACT: A structural investigation was undertaken to evaluate the stiffening effect that unreinforced masonry core walls have on an existing high-rise building. Numerous unknowns about the masonry walls made it difficult to meaningfully apply to the study information available in the literature about typical masonry construction and strengths. A testing program, which consisted of an on-site investigation, in-place tests on representative masonry walls, and laboratory tests on representative masonry units and mortar joints, was implemented to evaluate the masonry directly. In conjunction with structural analysis, the testing program played a crucial role in determining that the masonry walls do indeed add substantial stiffness to the building.

KEYWORDS: masonry walls, high-rise buildings, in-place testing, shear tests, building stiffness

Introduction

It has long been known in the construction industry that masonry walls can add substantial stiffness to low-rise buildings, even when they are not intended for structural purposes. However, much less is known about the stiffening effect that nonstructural masonry has on high-rise buildings. By testing and analysis, it was determined that the high-rise building, whose case study is presented herein, is significantly stiffened by its masonry core walls. The testing program played a vital role in reaching this conclusion, as it provided information that was essential to the building stiffness analysis.

[1]Senior Vice President, LZA Technology, 641 Avenue of the Americas, New York, NY 10011.

[2]Project Director, LZA Technology, 641 Avenue of the Americas, New York, NY 10011.

Background

A structural analysis of the steel moment frames of a high-rise office building constructed in Houston, Texas, circa 1970, indicated very large building deflections. However, this did not correlate well with the building's history of satisfactory performance during all types of wind conditions, including a major hurricane. As a result, an investigation was conducted to determine whether the building's concrete masonry core walls are significantly stiffening the building.

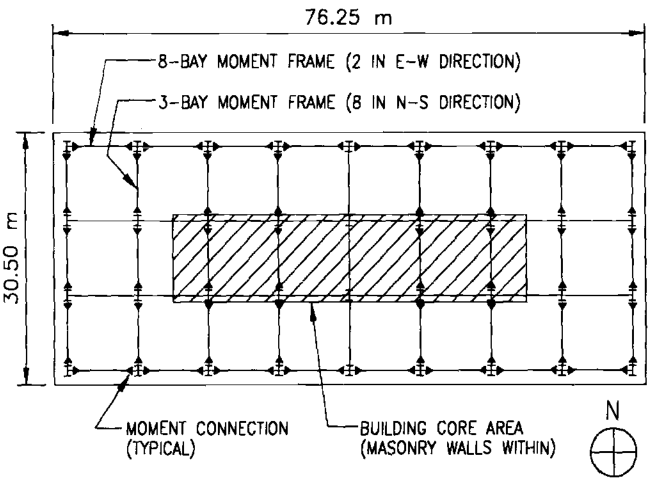

FIGURE 1--*Schematic plan of building moment frames and core area.*

Description of Structure

The building is 35 stories tall, with each story having a floor area of approximately 2 300 square meters. The typical floor is constructed of a one-way composite concrete slab on metal deck, which is supported by steel beams and girders. The beams and girders are supported by steel columns located on nine column lines lying in the north-south direction and four column lines lying in the east-west direction. Eight moment frames lie in the north-south direction, and two moment frames lie in the east-west direction (Figure 1). All the moment frames extend the full height and length or width of the building.

Elevator, stair and mechanical shaft openings at the building core are enclosed with 150-mm or 200-mm thick unreinforced concrete masonry walls. The steel beams are concrete encased where they frame openings; the masonry walls are tight to the underside of the concrete encasement. Mechanical rooms, bathrooms and closets, located at the core area, are enclosed with 150-mm or 100-mm unreinforced concrete masonry walls that typically extend to the overhead structure, but are not tight against it.

Investigation Summary

Two three-dimensional finite element computer models were created to compute building deflections due to wind loads. These models served as the primary tools for the building stiffness analysis. One model had elements for only the steel moment frames. The other model had elements for both the steel moment frames and the masonry walls.

By comparing the building deflections computed with and without the masonry walls, it would be possible to evaluate the effect of the masonry walls on the building stiffness. However, lack of available documentation regarding the construction, strength and condition of the existing masonry walls made it difficult to properly account for the masonry walls in the building stiffness analysis. Consequently, a masonry testing program was implemented to obtain the needed information.

It is important to note that around the same time as this investigation, a wind tunnel test program was performed to confirm the design force wind loads specific to the building. The results indicated wind loads similar in magnitude to those prescribed by the governing code.

Masonry Testing Program

On-Site Investigation

The first step of the testing program was to verify the construction and condition of the existing masonry walls, by investigative probing and observation. This step provided critical information needed to properly model the stiffness and connectivity of the masonry walls. Following are some of the key observations that were made:

1. The locations and thicknesses of the masonry walls generally comply with the building's architectural drawings.
2. The masonry walls are constructed of unreinforced hollow concrete masonry units.
3. Mortar joints are approximately 10 mm thick. Some bed joints are fully mortared on face shells and webs, and others are mortared only on face shells. Head joints are typically mortared on the face shells.
4. Steel beams framing around elevator, stair and mechanical shaft openings are concrete encased as shown on the structural drawings. Joints between masonry walls and concrete encased beams are mortared. Joints at tops of closet, bathroom, and mechanical room masonry walls are filled with spray fireproofing, not mortar.
5. No dowels or mechanical connectors were seen between the masonry walls and floor slab, or between the walls and overhead structure. However, locations were observed where the masonry walls are mechanically locked by way of bearing against the side of a perpendicular beam or bearing against termination points in the concrete encasement.

6. At junctures between perpendicular walls, the walls are connected with mechanical fasteners embedded in the bed joints; masonry units are not interlocked between perpendicular walls.
7. The masonry walls are generally of good construction and are in good condition. However, some locations were observed where joints are cracked or are not completely filled with mortar, especially at joints between the masonry and the underside of the concrete encasement. Some mortar joints, mostly in the stairwells and elevator shafts, appeared to have been repaired or filled with sealant. Some minor cracks were observed in the stairwell masonry walls at re-entrant corners of door openings.

Masonry Testing

An important part of the testing program was to evaluate how effective the unreinforced masonry walls are in resisting large forces. If a masonry wall in the building were to reach a stress level that caused it to crack, some load would shift from the wall to the steel frames. This would decrease the masonry wall's contribution to the building stiffness, and result in larger building deflections. Only with the correct masonry strength information would it be possible to analyze the structure in a manner that would incorporate the stiffening benefits of the masonry walls, but would not allow artificially high forces (that would cause cracking or movement) to exist in the masonry wall elements. Therefore, three types of tests were performed to evaluate the strength of the masonry walls in compression, tension, bending and shear.

TABLE 1--*Results of compressive strength tests (ASTM C 140).*

Set	Number of Masonry Units Tested	Width of Masonry Unit, mm	Average Net Area Strength, MPa
1	3	100	17.2
2	3	150	19.8
3	3	150	19.1
4	3	150	18.3
5	3	150	16.7
6	3	200	18.8

Compressive Strength Tests--Six sets of masonry units were carefully removed from representative walls scattered throughout the building, and were delivered to a laboratory. Testing on these masonry units was done in accordance with ASTM

Standard Test Methods of Sampling and Testing Concrete Masonry Units (ASTM C 140). Measurements were made, photographs were taken, and compressive strength tests were performed on the individual masonry units. The test results are summarized in Table 1.

The average net area compressive strength of all the units tested was 18.3 MPa. According to the ACI Specifications for Masonry Structures (ACI 530.1), the net area masonry compressive strength can be taken equal to about 12.3 MPa for masonry constructed of type N mortar and individual units having a strength of 18.3 MPa. A value of 12.3 MPa is a reasonably high net area masonry compressive strength for interior walls that appear to have not been intended for structural purposes.

Flexural Tensile Strength Tests--Nine masonry prisms, 400 mm wide by 600 mm high, were cut from representative walls and delivered to a laboratory. Testing was performed in accordance with ASTM Standard Method for Measurement of Masonry Flexural Bond Strength (ASTM C 1072). Measurements were made, photographs were taken, and tests were performed on the prisms to determine the masonry flexural tensile strength. The test results (Table 2) were used to evaluate the strength of the masonry walls in bending and tension.

TABLE 2--*Results of flexural tensile strength tests (ASTM C 1072).*

Prism	Number of Mortar Joints Tested	Width of Masonry Unit, mm	Average Net Area Strength, MPa
1	1	150	0.24
2	2	150	0.51
3	2	150	0.27
4	2	150	0.36
5	1	150	0.25
6	1	150	0.43
7	1	150	0.56
8	2	150	0.52
9	2	150	0.45

The average flexural tensile strength of all the prism mortar joints tested is 0.41 MPa. According to the ACI Building Code Requirements for Masonry Structures (ACI 530), an allowable flexural tensile stress of 0.13 MPa should be used for the design of masonry walls constructed of type N mortar and hollow masonry units. The tested ultimate strength of 0.41 MPa, as compared to the code prescribed allowable stress, is reasonably high for interior walls that appear to have not been intended for structural purposes.

In-Place Masonry Shear Tests--Three representative walls, located near the top, mid-height and bottom of the building, were tested in-place for masonry shear strength. Each wall was tested at three locations. The test methodology, based upon the Uniform Building Code Standard 21-6 In-place Masonry Shear Tests (UBC 21-6), involved removing masonry units to create openings on either side of a test unit, inserting a hydraulic ram into one of the openings, and pushing the test unit until the joints on top and bottom slipped (Figure 2). The results of these tests were used to evaluate the strength of the building's masonry walls in shear.

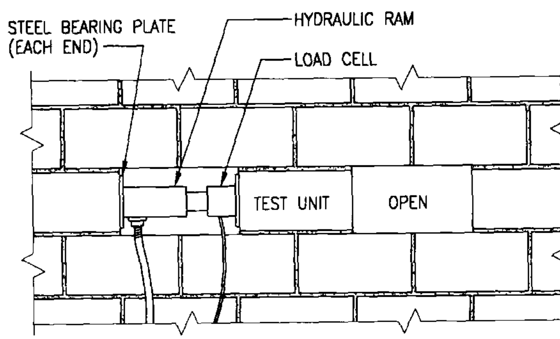

FIGURE 2--*Schematic of in-place masonry shear test.*

For each test, three loads were recorded: the maximum load, the sustained load, and the maximum re-load. The maximum load is the highest force exerted by the ram up until the unit began to slip; this force equals the bond shear strength of the mortar joints plus frictional shear resistance. The sustained load is the force that the test unit was able to sustain while slipping, as the ram continued to push. The maximum re-load is the highest force exerted by the ram, after unloading, up until the time the unit began to slip a second time; this force equals the frictional shear resistance at the mortar joints.

Table 3 summarizes the results of the shear tests. The average maximum load of the nine tests is 43.0 kN, which translates to 53.1 kN per meter of wall length. This is the average *bond strength plus frictional shear resistance* of the masonry walls. The average maximum re-load of the nine tests is 28.5 kN, which translates to 35.2 kN per meter of wall length. This is the average *frictional shear resistance* of the masonry walls. These test results provided a basis to limit the masonry wall shear forces to within realistic magnitudes in the building stiffness analysis.

TABLE 3--*Results of in-place masonry shear tests (UBC 21-6).*

Test Unit	Width of Masonry Unit, mm	Total Mortar Joint Length, m	Max Load, kN	Max Reload, kN	Max Load, kN/m	Max Reload, kN/m
1	150	0.81	44.1	31.0	54.4	38.3
2	150	0.81	43.7	33.4	54.0	41.2
3	150	0.81	37.8	22.8	46.7	28.1
4	150	0.81	33.6	20.5	41.5	25.3
5	150	0.81	56.1	39.1	69.3	48.3
6	150	0.81	37.8	22.1	46.7	27.3
7	150	0.81	34.2	27.8	42.2	34.3
8	150	0.81	45.0	29.0	55.6	35.8
9	150	0.81	54.3	30.9	67.0	38.1

Building Stiffness Analysis Results

Based upon the building stiffness analysis, which relied on the finite element computer models as well as the testing program results, the building is indeed stiffened significantly by the masonry core walls. The masonry walls provide the most substantial stiffening to the building when the wind loads are not too severe and the masonry walls are maintained in good repair. Under these normal conditions, the wind load deflections are about 15% lower in the north-south direction and about 50% lower in the east-west direction when the effects of the masonry walls are accounted for in the analysis, as opposed to when the frames are analyzed alone.

As may be evident from Figure 1, the steel moment frames' combined stiffness and the wind load are both substantially greater in the north-south direction than in the east west direction. On the other hand, the combined stiffness of the masonry walls does not differ as significantly as the steel frames do, between the two directions. Therefore, the effect of the masonry walls on building stiffness is much greater in the east-west direction than in the north-south direction.

The in-place masonry shear tests proved to be extremely helpful because they demonstrated that for the case study building, the mortar joints still provide significant frictional shear resistance after cracking. By accounting for this frictional resistance in the stiffness analysis, it was possible to determine the stiffening effect of the masonry walls even with the assumption that many of them had cracked. This was key to the investigation because according to analysis, the design force wind loads would cause cracking in the masonry walls throughout much of the building.

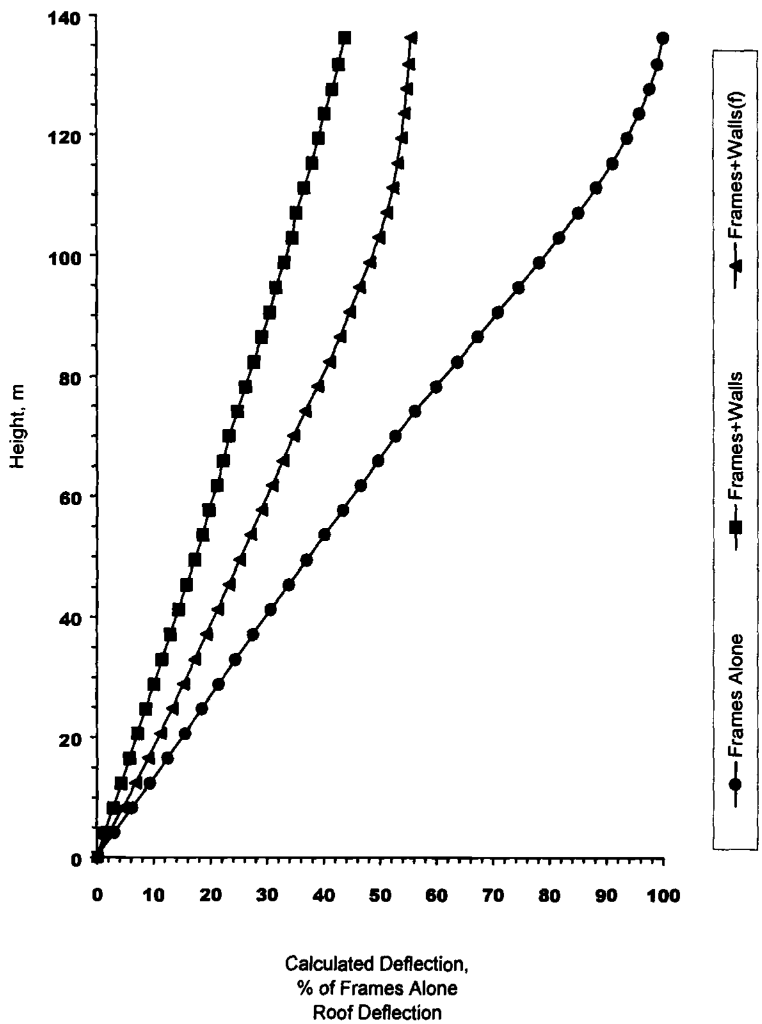

FIGURE 3--*Comparative plots of building deflections due to east-west wind.*

Figure 3 compares three deflection curves for wind in the east-west direction. The "frames alone" curve depicts the building's deflected shape, assuming only the steel moment frames resist the wind loads. The "frames+walls" curve depicts the building's deflected shape, assuming uncracked masonry walls assist the frames in resisting the wind loads. These two curves show the degree to which the building stiffness is enhanced by the masonry walls when the building is subject to normal wind loads that do not cause cracking in the masonry walls. The "frames+walls(f)" curve depicts the building's deflected shape, assuming cracked masonry walls assist the frames in resisting the wind loads by transferring shear through friction alone. This curve only applies to the most severe wind load conditions, similar in magnitude and recurrence to those prescribed by code. Comparison of this curve to that of the frames alone demonstrates the benefit that even cracked masonry walls have on the building stiffness.

Conclusions

Although it is not common for masonry walls to be utilized in the lateral systems of high-rise buildings, this investigation revealed that even unreinforced masonry walls can provide substantial stiffness to high-rise buildings, provided the walls are maintained in good repair.

The testing program served a critical role in this investigation, as it provided important information related to the construction, condition and strength of the existing masonry--information needed to accurately account for the masonry walls in the stiffness analysis. Without such information, it would not have been possible to determine with any certainty what effect the masonry walls have on the building stiffness.

As this case study demonstrates, a well planned testing program can be very important when evaluating the structural impact that in-place masonry has on existing structures.

Glenn R. Bell[1] and Brent A. Gabby[1]

In-Situ Evaluation of Compressed Brick Veneer Using the Flatjack Technique

REFERENCE: Bell, G. R. and Gabby, B. A., **"In-Situ Evaluation of Compressed Brick Veneer Using the Flatjack Technique,"** *Masonry: Materials, Testing, and Applications, ASTM STP 1356,* J. H. Brisch, R. L. Nelson, and H. L. Francis, Eds., American Society for Testing and Materials, West Conshohocken, PA, 1999.

ABSTRACT: The flatjack is a relatively nondestructive tool that allows engineers engaged in the repair and retrofit of masonry buildings (both historic and non-historic) to directly determine the in-situ state of compressive stress in masonry walls. The flatjack technique recently was used on a large modern apartment complex to quantify the compression in a brick veneer that was distressed and had questionable wind-load resistance. The compression in the veneer was due to a combination of concrete frame shrinkage and brick growth in a wall system that lacked horizontal control joints under the steel shelf angles. Although the compression caused spalling in the veneer, it also contributed beneficially to the walls' wind resistance. The amount of compression in the veneer was determined in several locations throughout the height of one elevation of the building using flatjacks. We found that the compression in the veneer was greater than the flexural tension produced by design wind loads (including a reasonable factor of safety), but below the compressive strength of the brick masonry. This finding allowed a repair solution that was modest relative to strengthening the wall for inadequate wind resistance. Prior to employing the flatjack in the field, we conducted in-house research to check the accuracy and reliability of the method, and develop our technique. We found that by altering gauge points from those locations prescribed by current ASTM standards to those recommended in recent research, greater accuracy could be obtained.

KEYWORDS: flatjack, brick masonry, compressive stress, flexural stress, control joints, shelf angles

Background and Description of Building Construction

Simpson Gumpertz & Heger Inc. was retained to investigate causes of distressed and falling masonry on a medium-rise apartment building in Baltimore, Maryland, and to develop recommendations for repairs. The building, constructed in 1961, is 14 stories high and is comprised of three wings arranged in a Y-shaped plan. The building frame is mostly reinforced concrete with some structural steel in the floor system. The exterior cavity walls consist of a 10 cm (4 in.) brick exterior wythe over a 10 cm (4 in.) block backup

[1]Principal and Staff Engineer, respectively, Simpson Gumpertz & Heger Inc., 297 Broadway, Arlington, MA 02474.

Figure 1 - Typical Wall Elevation

(nominal dimensions), and are of general construction typical of the 1950s and 60s. There are windows in punched openings at each floor level and continuous brick piers that run the full height of the building between the window openings (Figure 1). Each elevation is similar in its detailing and contains little or no ornamentation, other than cast stone head and sill elements that project from the face of the building.

The brick is supported by shelf angles, which align with the window heads. The shelf angles are supported by hangers, which are welded to steel plates cast into the edges of the concrete slabs above. The block back-up generally rests on the floor slab at each floor level (Figure 2). Over the window heads, there are additional inward-facing lintels that support the block over the window openings.

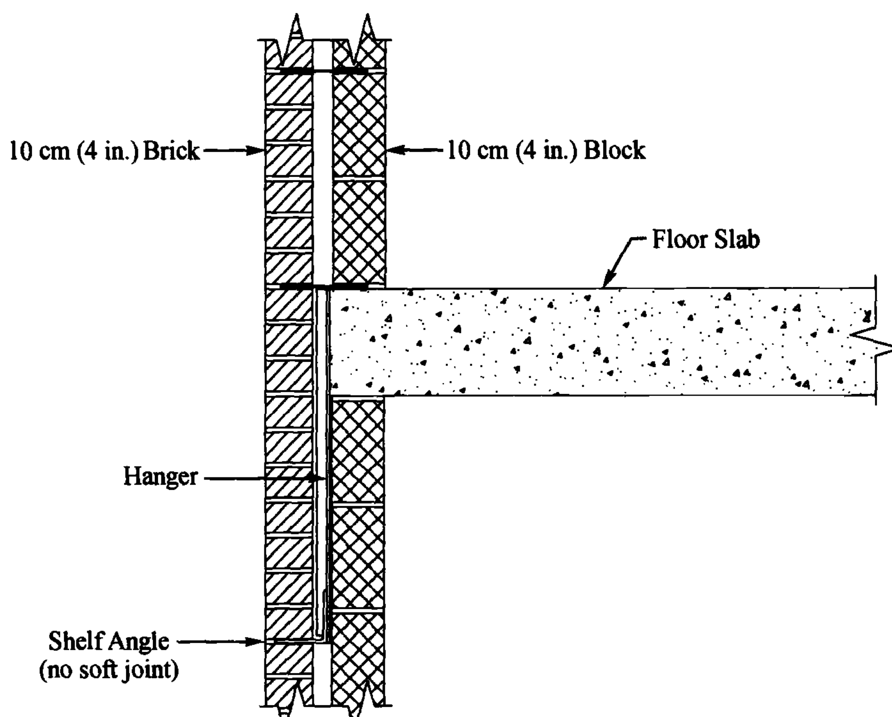

Figure 2 - Cross-Section Through Wall

Field Investigation of Existing Conditions

General Observations

From the ground we surveyed the building to gain an overall understanding the existing distress. We observed, in part, the following:

- The most obvious forms of distress are concentrated around the shelf angles. At shelf angles the faces of the brick veneer are often spalled, and the walls are bowed (in a scallop shape) near shelf angles. The distress is most severe at the lower floors and reduces at the upper floors, although there is similar distress throughout the height of the building.
- Previous attempts were made to repair the brick spalls adjacent to the shelf angles using a colored "mastic" type material.
- Several of the cast stone lintels that span across the continuous brick piers are spalled and have fallen.
- There are vertical cracks adjacent to inside and outside corners running the full height of the building.

Detailed Observations

After our ground-based survey, we made more detailed observations from swing stages (three drops in total) suspended from the roof deck. We made 16 exterior wall openings to document existing concealed conditions. We observed, in part, the following:

- There are no soft joints below the shelf angles. The angles typically are tight to the brick below; in some cases small gaps exist between the angle and the brick. There is a mortar plug at the toe of the shelf angle between the bricks above and below the angle (Figure 3).
- The mortar is soft and highly air entrained.
- The shelf angles are suspended from vertical steel angle hangers spaced at 76 cm

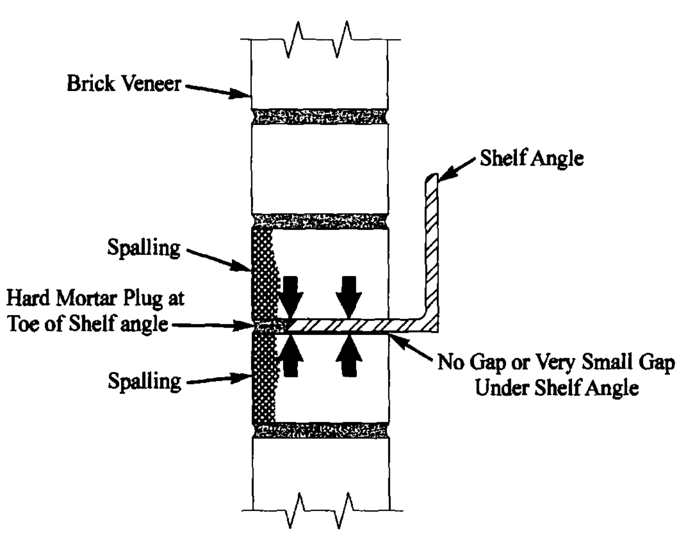

Figure 3 - Shelf Angle Bearing

(2 ft–6 in.) on center. The hangers are poorly anchored to the steel plates embedded into the edge of the slab.

- Nine-gauge unit Z ties, spaced 41 cm (16 in.) vertically and 61 cm (24 in.) horizontally, anchor the brick veneer to the block back-up. The ties generally do not show signs of corrosion or pull-out with respect to the lateral movement at the shelf angles. However, several are bent up into the cavity and do not engage the brick.
- The 10 cm (4 in.) block wythe is built tightly between the floor slabs at each story, although the space between the top block and floor slab above is not always completely filled.
- The shelf angles do not exhibit signs of corrosion. No leakage was reported in the apartments and no signs of water-related deterioration were observed.

Diagnosis of Wall Distress

After our preliminary investigation, we concluded that the masonry distress at the shelf angles was caused by a build-up of compressive stress in the brick wythe due to unaccommodated vertical differential movements between the brick veneer and concrete frame. These movements could not be accommodated because there were no horizontal control joints at shelf angle locations. This phenomenon is well described and documented in the literature, and is a problem we have encountered on several masonry buildings of this construction type, particularly of this vintage.

The lack of horizontal soft joints caused stress to concentrate at the outside face of the brick (through the mortar plug at the toe of the shelf angle) above and below the shelf angle. We suspect, but were not able to prove, that the stress concentration (and subsequent spalling) is worse where there were small gaps between the bottom of the shelf angle and the top of the brick below in the original construction, as opposed to other areas where there was no gap. The scallop-shaped bowing of the veneer at the floor levels is consistent with this load-transfer mechanism. The concentration of stress at the outer face of the brick causes flexural moments, which curl the wall outward at the shelf angles.

We did not observe problems resulting from overall compression in the exterior wythe or distress throughout the thickness of the brick. Even though the concrete frame shrinkage and creep is now minimal, we concluded that some long-term, irreversible growth in the brick wall would likely continue. Without remedial action, brick and cast stone spalls would continue to fall and create a hazard for the occupants of the building.

We also concluded that the vertical cracks near the inside and outside corners were caused by lack of vertical control joints to accommodate horizontal movements. This phenomenon also is well described and documented in the literature. The lack of regularly spaced vertical control joints allowed the walls to make their own control joints (cracks) at areas of stress concentration.

It is the former mechanism of vertical load transfer and spalling at the horizontal joints that was the subject of most of our investigation and is described in the balance of this paper.

Structural Assessment of the Walls

Normally one would prescribe cutting horizontal soft joints into the wall below each shelf angle to relieve the problematic vertical compressive stress. However, in this case, we suspected (and later proved) that, while the brick wythe was subjected to a concentration of compressive stress at the outer faces of the brick, which caused detrimental spalling above and below the shelf angles, the compression throughout the balance of the brick's cross section had a beneficial effect on the walls' overall lateral resistance. Thus, cutting new horizontal soft joint below the shelf angle would solve one problem but could create another by relieving the uniform compressive stress in the exterior wythe of brick.

Under out-of-plane wind loading, the walls span flexurally between floors. In flexure, the brick and block wythes behave as independent plate elements laterally linked by the masonry ties. The fractions of the total wind load carried by the brick and the block wythes depends on each wythe's relative bending stiffness.

Using both simple beam theory and the finite element method, we analyzed the stresses in the wall set up by out-of-plane wind loads. While detailed description of this analysis is beyond the scope of this paper, a general summary follows:

- The design wind loads prescribed by the code under which the building was built vary from 0.71 to 0.96 kPa (15 to 20 psf). However, more current codes indicate that realistically occurring wind loads with 50- to 100-year mean return intervals could be 1.3 to 1.4 kPa (27 to 30 psf) in the general wall areas and higher at the building corners.
- Under a 0.96 kPa (20 psf) wind load, flexural stresses in the brick wythe are 0.28 to 0.40 mPa (40 to 60 psi); 0.21 to 0.34 mPa (30 to 50 psi) in the block. The stresses are proportionately higher under a 1.44 kPa (30 psf) wind load.

Our analysis indicated that the walls' out-of-plane resistance could not be justified by classical rational structural analysis. Not only were the flexural stresses well beyond code allowables, they were well above the bond strength of brick masonry, which we determined with in-situ bond-wrench testing.

Our conclusion was not surprising given our experience with masonry walls of this vintage. During the 1950s and 1960s it was common practice to design exterior non-loadbearing walls using empirical h/t ratios rather than rational engineering methods. However, the good performance in out-of-plane resistance of the walls throughout the life of the building was not supported by our analysis. The answer to the discrepancy between the theoretical and "real" worlds seemed to lie with the compressive stress in the exterior wythe of brick. Even though the compressive stress was causing brick spalling at shelf angle locations, we surmised that this stress had a beneficial effect of offsetting the high flexural tensile stresses (caused by wind loads) in the brick wythes.

If this hypothesis held true, then a solution to the problem appeared to be the removal of the mortar plug at the toe of the shelf angle only (not cutting soft joints fully through the brick wythe and thus allowing the beneficial overall compression in the rest of the exterior wythe to remain).

According to the ASTM method the average compressive stress in the masonry is calculated by the following equation:

$$f_m = K_j K_a p$$

where f_m = average compressive stress in the masonry
K_j = flatjack calibration constant (<1.0)
K_a = slot-to-flatjack area constant (<1.0)
p = internal stress (hydraulic pressure) in the flatjack

For reasons not generally understood, the ASTM flatjack technique has not proven to be precise or readily repeatable. The precision and bias statement of the standard states that the coefficient of variation of the test method can be as great as 20% and recommends that a minimum of three tests be conducted in the same general area to verify results.

Other Flatjack Literature

A break-through in improving the accuracy of the flatjack method was reported by Ronca[1]. To explain the inaccuracy of classic flatjack testing, Ronca noted that ASTM assumes linear-elastic behavior but recognized that the deformations around the slot are, in part, plastic and non-linear. Therefore, Ronca hypothesized that the location of the gauge points is critical for accurate results.

Ronca tested this assumption through laboratory testing by installing sets of gauges at different points along the length of the slot in several prisms and compared the results of each test with the known stress induced in the prisms from a load frame.

In her paper Ronca concludes, in part, the following:

- Inelastic deformations are most severe around in the middle of the cut and result in increases in the total displacement.
- Placing the gauge points to the extremes of the cut reduces the total displacement due to inelastic deformation. The most accurate locations of the gauge points are 6 cm (2.4 in.) inboard and outboard of the cut, and at the edge of the cut (Figure 4).
- The initial state of stress on the wall is determined when the load-deflection curves of all three gauge points converge.
- The above-mentioned convergence point does not correspond to zero displacements across the length of the slot; some residual strain from inelastic behavior remains.

Ronca was not the first to recognize the importance of inelastic behavior in flatjack testing. In 1986, Landirani and Taliercio[2] reported results of finite element analyses they conducted on models simulating prisms subjected to flatjack tests. Their models accounted for the non-linear behavior of the masonry through an elasto-plastic constitutive relationship and a triaxial yield criterion. Qualitatively, Landirani and Taliercio demonstrated that under conditions of moderate stress in the wall, compressive yielding occurs near the end of the slot due to stress concentrations (Zone 1 in Figure 4) and that traction (shear) yielding occurs in the midregion of the wall over and under the slot (Zone 2 in Figure 4)

Because Ronca's research strongly suggested an improved method over the ASTM method, we conducted our own in-house research program to verify the accuracy of her method.

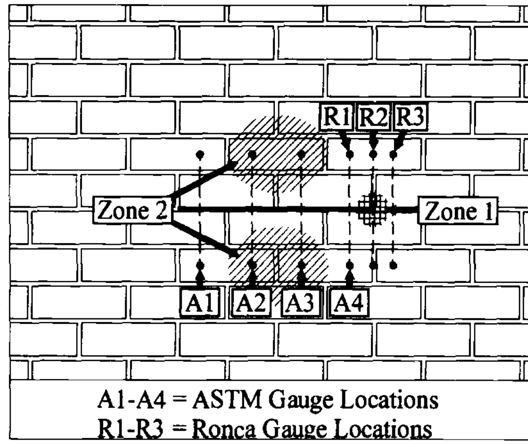

Figure 4 - Flat Jack Cut and Gauge Locations

SGH Laboratory Testing and Results

We built three prisms of varying strength and stiffnesses and placed the gauge points on each prism as defined by the ASTM test standard and recommended by Ronca. Because the prisms were two large to install in a compression testing machine, we built a load frame to conduct the tests (Figure 5). Rather than using a Whitimore Gauge to measure displacements, we fabricated aluminum brackets that were attached to the masonry above and below a 40 cm (16 in.) cut slot, using screws and nylon inserts drilled and set into the masonry. We inserted dial gauges with an accuracy of 1/10,000th in. into the upper bracket and attached them with nylon-tipped set screws. We then set invar bar receptors at the dial gauges and aluminum brackets (Figure 6). We read each gauge point twice and marked the bars to indicate a specific gauge location. During the testing, we

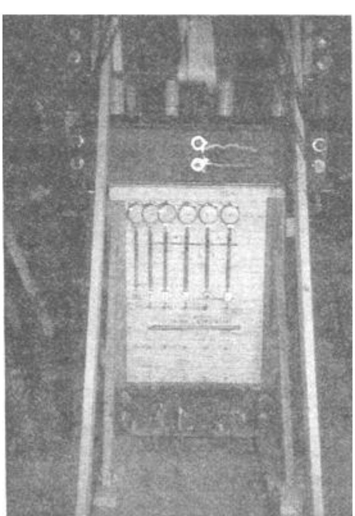

Figure 5 - Laboratory Prism Test Setup

Figure 6 - Gauge Setup on Prism

observed cracking in the head joint centered above the slot.

The external stresses induced into the individual prisms by our load frame were 0.61, 1.6, and 3.2 mPa (88, 230 and 466 psi). The results of our tests are found in Table 1.

Table 1 – Laboratory Test Results

Test No.	Compressive Strength of Prisms mPa (psi)	External Load mPa (psi)	Results of Ronca Gauge Points mPa (psi)	Ronca Accuracy (% of applied stress)	Results of ASTM Gauge Points mPa (psi)	ASTM Accuracy (% of applied stress)
1	7.09 (1028)	0.61 (88)	0.65 (95)	108	0.75 (109)	124
2	20.1 (2919)	1.6 (230)	1.62 (235)	102	1.88 (272)	118
3	32.3 (4689)	3.2 (466)	3.3 (480)	103	3.10 (450)	97

Load-deflection plots of the laboratory tests are given in Figures 7 and 8 for the Ronca gauge points and ASTM points respectively. Results show that the Ronca points yielded much better accuracy than the standard ASTM method, and the load-deflection behavior of the Ronca gauges was superior.

Figure 7 shows that, in general, the load-deflection plots of Ronca Points 1 and 3 (the outer points of the triplet) were better behaved and converged more reliably to the actual compression than did Ronca Point 2. The likely reason for this is discussed in the Conclusions below.

Field Application and Work

On the building, we measured the compressive stress in two parallel, continuous brick piers – before and after the mortar plugs were removed. The first series of tests were done along the height of one continuous brick pier, and the second series were done on the parallel pier after the mortar plug was removed. The second series of tests were carried out at the same elevation as the first tests. To determine the reduction of stress in the wall after the mortar plug was removed, we verified that there was a "balance" of stress in the brick piers at a given elevation before cutting. This verification testing took place at the third floor level.

Our tests were conducted along one drop of the north side of the building. Because our field experiments were carried out in the summer, we chose the north elevation to minimize the effects of the radiational heating due to direct exposure to the sun. The test locations are shown in Figure 9. Results are shown in Table 2. Typical load-deflection plots are given in Figure 10.

To justify this approach we needed to determine the following:

- The compressive stress in the brick was sufficient to result in adequate flexural capacity to resist reasonably anticipated wind loads.
- The existing compressive stress in the walls did not exceed an allowable axial compressive stress after the repairs were made.
- The removal of the mortar plug at the toe of the shelf angle did not result in loss of compressive stress in the wall that would yield insufficient flexural resistance.

To determine the compressive stress in the brick wythe, we turned to the flatjack method. We concluded an acceptable residual compression in the wall would be between 0.80 and 5.3 mPa (120 and 800 psi).

Background of Flatjack Procedure and Research

Since the early 1980s, flatjacks have been used to determine both the axial compression in and deformability of masonry. The flatjack concept is based on cutting a slot in a compressed masonry wall, inserting and inflating a flatjack diaphragm. The jacks are inflated until the wall deformations induced during cutting are fully removed.

In the United States, flatjack methods are defined in ASTM C1196, Standard Test Method for In-Situ Compressive Stress Within Solid Unit Masonry Estimated Using Flatjack Measurements, and ASTM C1197, Standard Test Method for In-Situ Measurement of Masonry Deformability Properties Using the Flatjack Method. Below the in-situ stress evaluation technique is discussed.

Methodology of In-situ Stress Determination

To determine the level of in-situ compressive stress in a masonry wall the following general procedures are used:

- Choose a bed joint in the wall and measure the distance between certain fixed points above and below the bed joint to be cut.
- Cut a slot in the bed joint and remeasure the distance between the fixed points.
- Subtract the first set of measurements from the second to determine deflection in the masonry after cutting.
- Install a flatjack in the slot.
- Pressurize the flatjack until the deflections in the masonry are removed.
- Use the hydraulic pressure in the flatjack to calculate the stress in the wall.

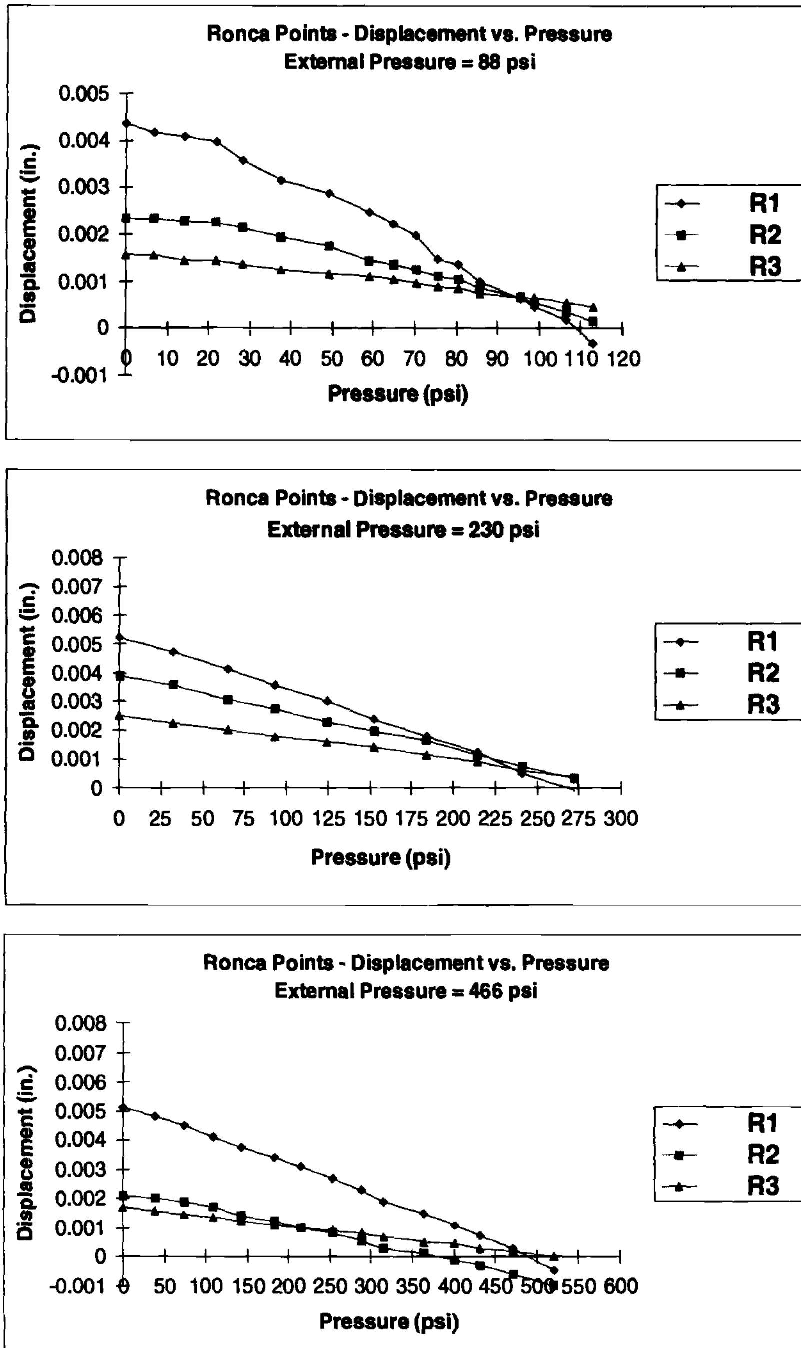
Ronca Points - Displacement vs. Pressure
External Pressure = 88 psi
Displacement (in.)
0.005
0.004
0.003
0.002
0.001
0
-0.001
0 10 20 30 40 50 60 70 80 90 100 110 120
Pressure (psi)
R1
R2
R3
Ronca Points - Displacement vs. Pressure
External Pressure = 230 psi
Displacement (in.)
0.008
0.007
0.006
0.005
0.004
0.003
0.002
0.001
0
0 25 50 75 100 125 150 175 200 225 250 275 300
Pressure (psi)
R1
R2
R3
Ronca Points - Displacement vs. Pressure
External Pressure = 466 psi
Displacement (in.)
0.008
0.007
0.006
0.005
0.004
0.003
0.002
0.001
0
-0.001
0 50 100 150 200 250 300 350 400 450 500 550 600
Pressure (psi)
R1
R2
R3

Figure 7

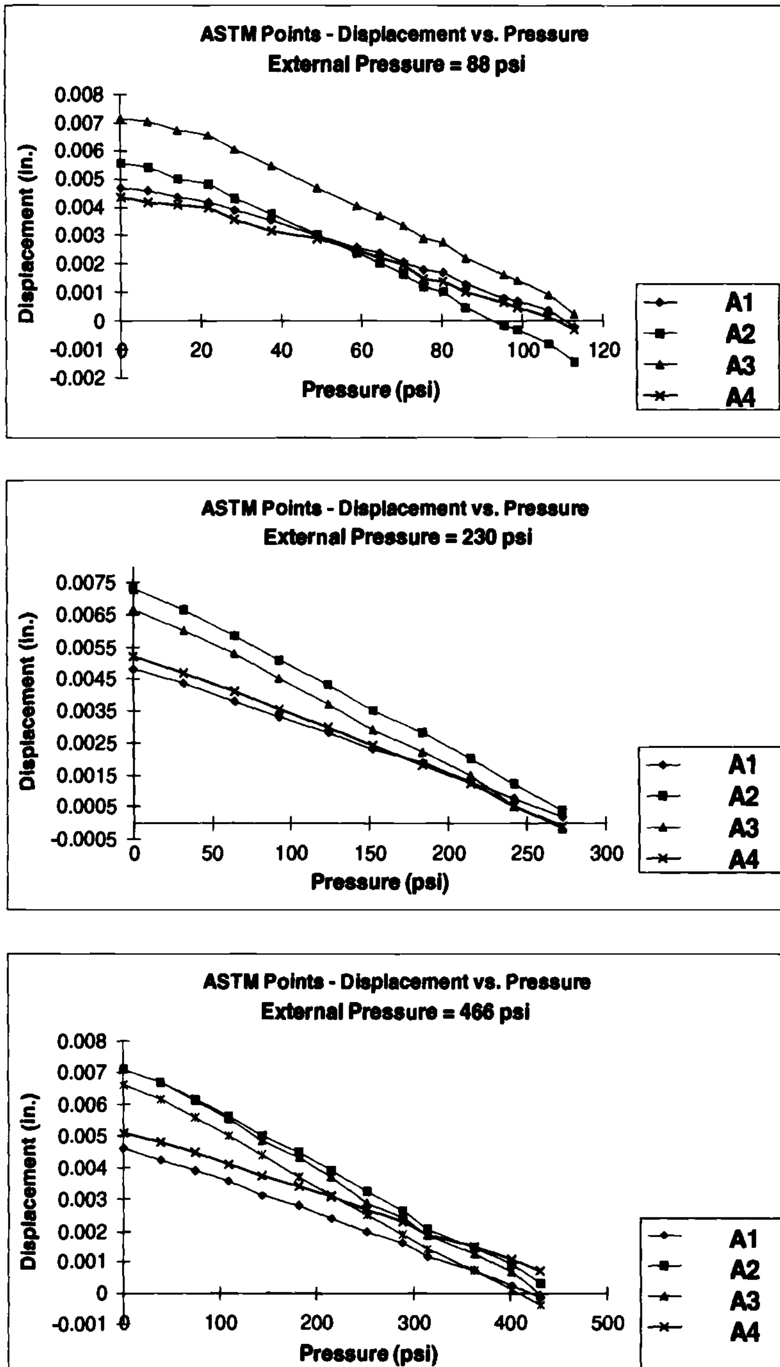
ASTM Points - Displacement vs. Pressure
External Pressure = 88 psi
Displacement (in.)
0.008
0.007
0.006
0.005
0.004
0.003
0.002
0.001
0
-0.001
-0.002
0
20
40
60
80
100
120
Pressure (psi)
A1
A2
A3
A4
ASTM Points - Displacement vs. Pressure
External Pressure = 230 psi
Displacement (in.)
0.0075
0.0065
0.0055
0.0045
0.0035
0.0025
0.0015
0.0005
-0.0005
0
50
100
150
200
250
300
Pressure (psi)
A1
A2
A3
A4
ASTM Points - Displacement vs. Pressure
External Pressure = 466 psi
Displacement (in.)
0.008
0.007
0.006
0.005
0.004
0.003
0.002
0.001
0
-0.001
0
100
200
300
400
500
Pressure (psi)
A1
A2
A3
A4

Figure 8

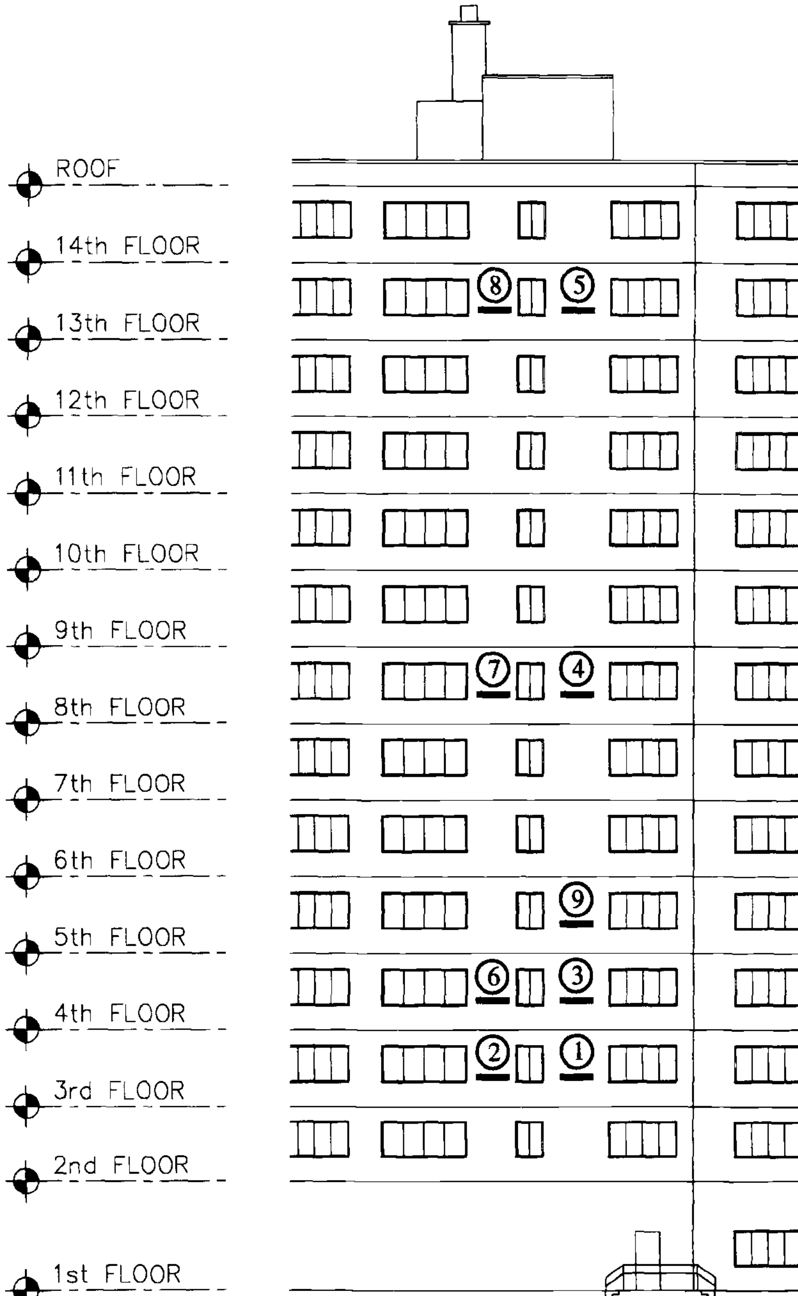

Figure 9 - Test Locations on Wall

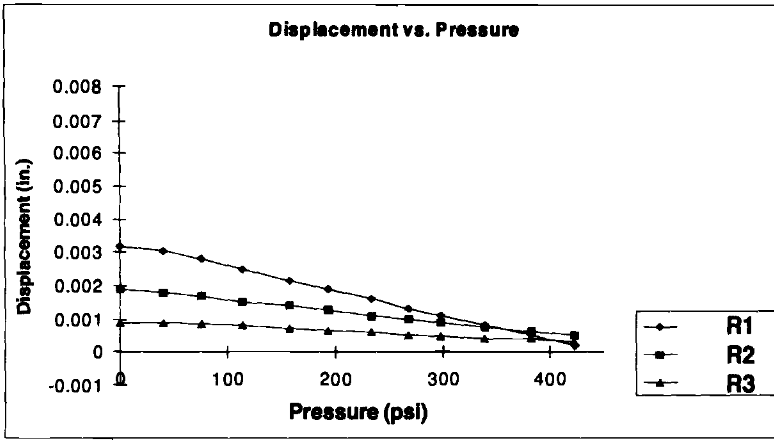
Displacement vs. Pressure
0.008
0.007
0.006
0.005
0.004
0.003
0.002
0.001
0
-0.001
Displacement (in.)
0
100
200
300
400
Pressure (psi)
R1
R2
R3

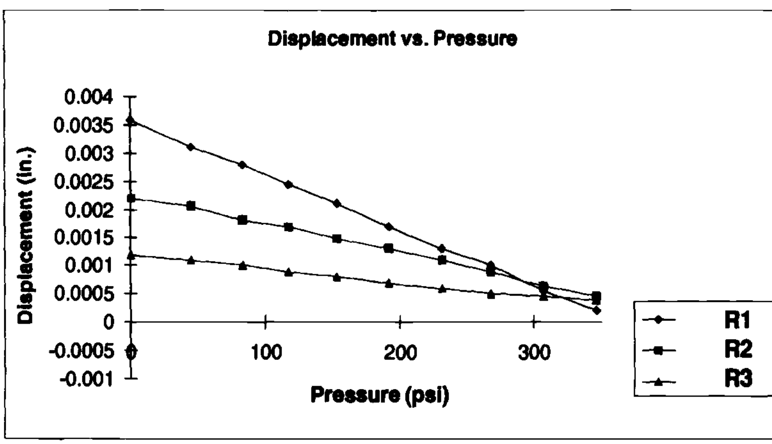
Displacement vs. Pressure
0.004
0.0035
0.003
0.0025
0.002
0.0015
0.001
0.0005
0
-0.0005
-0.001
Displacement (in.)
0
100
200
300
Pressure (psi)
R1
R2
R3

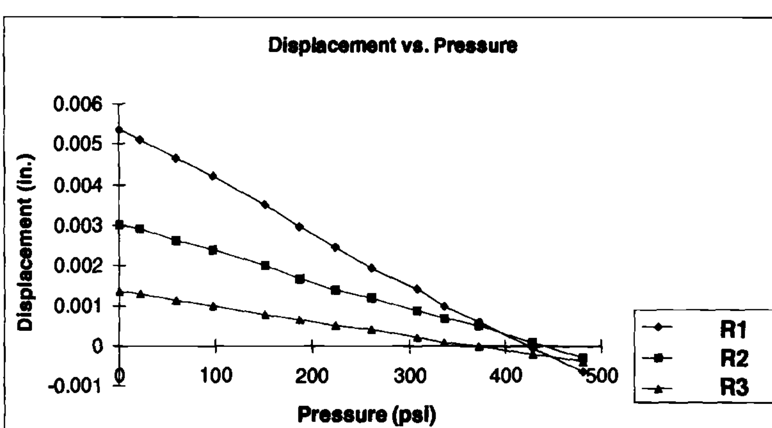
Displacement vs. Pressure
0.006
0.005
0.004
0.003
0.002
0.001
0
-0.001
Displacement (in.)
0
100
200
300
400
500
Pressure (psi)
R1
R2
R3

Figure 10

Table 2 – Results of Field Testing

Test Number	Floor Level	Before (B) or After (A) Mortar Removal	Measured Compressive Stress (mPa (psi))
1	3	B	2.69 (390)
2	3	B	2.83 (410)
3	4	B	3.17 (460)
4	8	B	1.72 (250)
5	13	B	1.90 (275)
6	4	A	2.21 (320)
7	8	A	3.07 (445)
8	13	A	1.21 (175)
9	5	A	1.90 (275)

As illustrated, there was a general reduction of stress when the mortar plug was removed, but the reduction was modest. The resulting stresses were within an acceptable ranges mentioned above.

Conclusions

Flatjack Procedures

- Our laboratory tests confirmed the improved accuracy (better than 10%) of flatjack testing when gauge points are moved near the end of the cut slots as suggested by Ronca.
- The apparent reason that the standard ASTM gauge points yield inaccurate results is that inelastic traction (shear) behavior in the masonry in the mid-region over and under the slot negates the principle of superposition that is essential for the flatjack method. This inelastic behavior produces difficult-to-predict displacements in the wall in the region of the "middle" ASTM gauge points. This is further supported by the cracking we observed in the head joint centered above the slot.
- By moving the gauge points to three points near the end of the slot, the inelastic behavior effecting these gauge readings, which is compression yielding near the end of the slot, affects all three points approximately the same.
- A caveat to the above-mentioned conclusion is Ronca Point 2 (the middle of the three end points), which behaved more erratically in our laboratory and field testing than the other two points. The explanation for the less predictable behavior of this middle point is that it is in the midst of the region of compression yielding at the end of the slot. As such, it is more likely to be affected by subtleties in the extent of the compression yielding zone than the other two Ronca points.

- The ASTM procedure should be improved with modified gauge points per Ronca's findings, as corroborated by our work.
- The flatjack must fit snugly into the slot before inflation. The main reason for this is that the jack behavior is highly nonlinear at large inflation displacements. Experimenting with different techniques, we found the best way to ensure a snug fit is to use a second jack as a "shim" in parallel with the "test" jack. After installation of the shim jack and the test jack, the shim jack is inflated until both jacks are snug in the slot. Then the shim jack is locked off and inflation of the test jack begins.

Field Test Results

- The flatjack field testing was successful in the field. However, the technique requires almost surgical care in preparation, installation, and gauge reading to be accurate and repeatable. We found that with each subsequent test, our technique and the apparent quality of the results improved.
- The measured in-situ compressive stress in the wall fell within the acceptable range, both before and after removal of the mortar plug, demonstrating the efficacy of the proposed repair method.

References

[1] Ronca, P., "The Significance of the Gauging System in the Flatjack In-Situ Stress Test for Masonry: Experimental Investigation," Masonry Society Journal, Vol. 14, No. 1, August 1996, pp. 79-86.

[2] Landriani, G. S. and Talierico, A., "Numerical Analysis of the Flatjack Test on Masonry Walls," Journal of Theoretical and Applied Mechanics, Vol. 5, No. 3, 1986, pp. 313-339.

Bruce S. Kaskel,[1] Edward A. Gerns,[2] and Kenneth DeMuth[3]

Renovation of Existing Masonry Buildings to Residential Lofts

---

REFERENCE: Kaskel, B. S., Gerns, E. A., and DeMuth, K., "**Renovation of Existing Masonry Buildings to Residential Lofts,**" *Masonry: Materials, Testing, and Applications, ASTM STP 1356,* J. H. Brisch, R. L. Nelson, and H. L. Francis, Eds., American Society for Testing and Materials, West Conshohocken, PA, 1999.

ABSTRACT: Major cities throughout North America are recently undergoing a residential revitalization of buildings in their urban centers. Many of these buildings are used as masonry "loft" structures, converted from buildings originally built for industrial or commercial occupancy. The renovations of these buildings typically address structural concerns, such as corrosion of embedded metals, and serviceability concerns, such as water–tightness. Masonry repairs can range from being relatively minor to relatively major, often depending on the condition of the building. Frequently, disputes arise between those who directed the renovation project and those who ultimately reside in these buildings. There are few guidelines in the current literature that identify the degree of masonry repairs that should be anticipated by all parties. Such guidelines would help resolve conflict in this type of work. This paper will present some of the authors' observations in this area and identify common concerns raised by these projects.

KEYWORDS: loft conversions, masonry walls, masonry distress, evaluation, repair

---

Background

Throughout the US and Canada it is commonplace in urban centers to see conversion of old commercial masonry buildings to loft residences. One city in the 1990s had 48 loft conversions, resulting in over 5 000 living units [1]. The trend to loft conversions results in part from two influences; first, many urban centers have a ready stock of under-utilized industrial and warehouse structures, and second, there is a renewed demand for city living.

---

[1] Consultant, Wiss, Janney, Elstner Associates, Inc. (WJE), 120 N. LaSalle Street, Suite 2000, Chicago, IL, 60602.

[2] Senior Engineer, WJE.

[3] Principal Architect, Pappageorge/Haymes Ltd, 814 N. Franklin, Suite 400, Chicago, IL. 60610

Most loft buildings were built in an era which required multi-story densities, ready access to rail and transportation systems and a nearby population of workers. Modern assembly line practices, the expressway network, higher urban business costs, the general conversion of urban areas from manufacturing centers to financial and service centers, have greatly diminished the desirability of these buildings for commercial business. These older buildings however are often not suited for today's industries, as pointed out in one building journal, "While these buildings vary in age, they typically have mechanical systems, infrastructures and floor plates that make them ill-suited for the needs of today's corporate user" [2].

Until recently, only a few "urban pioneers" lived at the fringes of city centers. However, sprawl and traffic congestion have placed the suburbs beyond reasonable travel times for some urban workers. In addition, "empty-nesters" are finding it more desirable and convenient to live in an urban environment closer to work, theaters and restaurants. The proximity of lofts to downtown business districts, their durability and the charm of materials and architecture make them a natural choice for residential use. High urban land costs lead to loft developments that are almost universally multi-family.

Government regulations have also influenced loft redevelopment. In the early 1980's tax credits were available for renovation projects. While these credits are no longer in vogue, the early loft conversions exposed developers to the viability of loft conversions. Soon zoning ordinances and building codes were modified to address the unique qualities and problems associated with conversion of loft structures.

Loft Characteristics

Loft buildings have several distinguishing features that set them apart from new construction. Heavy structural timber members, massive brick walls, high ceilings, large windows and deep floor plates are among the differences. Other elements, such as freight elevators, boiler plants, sprinkler piping and water towers occur in multi-story lofts. These features are often exploited for their aesthetic qualities in addition to the functional roles they play.

Although the variety of building types and materials are part of the allure of the market, the following are some common features in most residential loft conversions:

1. Masonry buildings were built with multiple-wythe bearing walls 8 to 16 in. thick with windows set in masonry openings. Stone, terra cotta, and face brick might face the street elevations of the building, while elevations with less prominent views would often be faced with common brick. Backup wythes were common brick or structural clay tile tied with masonry headers and the collar joints in the walls were filled with mortar. The facade typically does not have any control or expansion joints. Window openings would usually be framed with loose laid steel lintels, seldom with any flashing and weeps installed.

2. The buildings are often unoccupied for several years prior to the renovation. The condition of the building may have been allowed to deteriorate. Water entry through open joints in the exterior walls, may have caused deteriorated mortar joints, masonry units, and metals embedded in the wall. Water leakage may be occurring, although there may not be anyone familiar with where leaks occur.

3. Loft conversions are often sold as condominiums. The prospective owners often have input into the interior layouts. Open floor plans with unimpeded views are desired. Often only kitchens and bathrooms are partitioned. The original building walls and floors are left "as-is". Exposed masonry, whether common brick or structural clay tile, is considered aesthetically appealing and in some projects is sold as a premium.

Existing Guidelines for Loft Conversions

Preservation Guidelines

A literature review found few sources that offer guidelines on the conversion of older loft buildings to residential use. The following guides for historic buildings may be used for loft conversions.

1. "If the various materials, features and spaces that give a building its visual character are not recognized and preserved, then essential aspects of its character may be damaged in the process of change"[3].

2. "Where the severity of deterioration requires repair or limited replacement of a distinctive feature, the new material will match the old in composition, design, color and texture" [4].

However many loft conversions would not satisfy these guidelines, since changes are often made to improve the marketability of the project. New windows and balconies hung from the exterior facades, for example, are not in keeping with this preservation intent.

Masonry Industry Guidelines

The masonry industry provides some guidelines useful to the conversion of loft buildings. The Brick Institute of America, in their Technical Notes on Brick Construction 7F, entitled "Moisture Resistance of Brick Masonry Maintenance" [5], describes general inspection and specific maintenance measures which consist in part of remedial cleaning, sealant replacement, grouting of mortar joints, tuckpointing of mortar joints and replacement of brick units.

Application of surface sealers, in an attempt to limit water infiltration, is another practice employed in some conversions. The application of such sealers can, however, have detrimental effects, depending on the product and substrate condition to which they are applied. Even if the sealers are properly selected and applied, reapplication is required to remain effective.

To revitalize the aesthetics of the exterior, the façade may also be cleaned. Aggressive cleaning techniques, such as high-pressure water washing, sand blasting or acid-cleaning can damage the brickwork and mortar. This may impact the durability of the masonry and its need for on-going maintenance.

Other repairs such as replacement of corroded steel lintels and shelf angles and installation of expansion joints are also performed when necessary. Flashings and weeps are not often installed unless the masonry above a lintel or shelf angle is deteriorated and needs replacement. Without flashing and weeps, it is assumed that the wall acts as a barrier to water leakage, since there is no effective drainage system incorporated in the wall design.

Deterioration or replacement of other materials, such as sealants, window and doors, will effect the performance of the facade. Numerous sources are available regarding evaluation and repair of these materials [6].

Masonry Repair Issues

Brick is one of the most enduring building materials known. This is well understood both by the building professional and the loft buying public. Unfortunately, this reputation is often misunderstood or misrepresented to mean things such as "maintenance free," "airtight" or "waterproof", which in fact are not true.

The onset of a typical development will include an analysis of the zoning regulations and building codes together with a Property Report that documents the existing conditions and repair needed. Government regulations may also require assessments and estimates to be prepared for annual operating expenses, expected maintenance and energy usage.

At the time of conversion, some masonry loft buildings may not require significant repairs due to their relatively newer age; the quality of their original construction; or the level of their maintenance and upkeep. Conversely, for some buildings, significant repair of the masonry façade may be required. Most projects fall within the extremes. In the majority of projects, decisions need to be made about the level and quantity of masonry repairs. Decisions need to be made on issues such as how many joints should be tuckpointed or grouted, what level of corrosion requires steel replacement and whether cracked masonry should be sealed or replaced.

A review of recent conversions reveals that the percentage of the total budget spent on masonry repairs was relatively low. On one project, masonry repairs were 2 percent of construction cost [7]. Another project spent almost twice as much on masonry repairs, which was still only 3 ½ percent of the total cost [8].

Although some loft conversions have thorough drawings and specifications that describe the necessary masonry repairs, many projects have scant documentation on repairs. It often is left to the mason on the job to decide on the scope and intent of repairs. We have seen that after the fact, these repair decisions are often called in question by the owners, tenants or condominium boards. Their issues frequently revolve around the following concerns:

- Water leakage into habitable space
- Deterioration and/or efflorescence of interior exposed masonry
- Quality and quantity of repairs performed
- Level of continued masonry maintenance

Water Leakage

The most endemic problem in loft conversion projects is water leakage through exterior walls. When water leaks occur in an occupied unit, everyone scrambles to determine its source and how to stop it. They also critique why sufficient repairs were not performed in the first place to stop water leakage. There is much literature on the identification of water leakage sources in contemporary masonry construction and its remediation [9]. The differences between contemporary masonry buildings and lofts however are:

1. Contemporary masonry drainage walls are designed to collect water that gets into the masonry wall and direct it out at flashing and weep locations. Loft buildings are usually barrier walls that rely on the mass of masonry to hold moisture and allow it to evaporate after a rain.

2. As previously stated, the building may not have previously been leak-free. Most residential occupants want a more watertight wall than may have been needed for the previous industrial occupant.

When water leakage occurs there is an immediate need to search for the source of the leakage. The leaks may not be directly related to the masonry. Often, building sealants, windows and doors may contribute to leakage if they are improperly installed or not properly maintained.

Subsequently, repairs need to be implemented to stop the leakage. Common masonry repairs consist of sealers, tuckpointing or the installation of flashings and weeps. Materials and installation techniques of tuckpointing and flashings vary greatly. The performance and durability of the repairs, regardless of the scope, is often directly related to the quality of the materials selected and the care taken in installation.

Deterioration and/or Efflorescence of Interior Exposed Masonry

Second only to water leaks is the problem of deterioration of the interior wall surfaces. The lack of interior wall finishes allows greater scrutiny of the exterior wall than contemporary construction which typically has finished walls. Discoloration and deterioration of the common masonry backups will occur as moisture moves through the wall. Chalking, efflorescence, and loose masonry debris, which would not be noticed in a finished space, may be objectionable to some occupants in loft buildings. Sandblasted interiors tend to shed gritty dust, requiring frequent clean-up. No foolproof solution exists for complete removal and cleaning of interior masonry surfaces. Toxicity and residual collection of cleaning materials are significant issues for interior applications.

Quality and Quantity of Repairs Performed

Condominium boards will often retain engineering professionals to offer an independent review of the developer's work, after the work is completed. It is not uncommon during these reviews to find that the developer did not perform all possible masonry repairs at all locations. For instance, the developer may have endeavored to "spot" tuckpoint walls, where the independent engineer may recommend that all walls be tuckpointed 100%. The engineer may also determine that tuckpointing was not performed to masonry industry standards (noted above). This is commonplace in most conversion projects. Repair judgements on replacement of deteriorated and cracked masonry are also called into question.

Level of continued masonry maintenance

Along with the concern for the quality and quantity of repairs performed, is a concern for the level of continued masonry maintenance. Older masonry buildings by their nature will require more frequent maintenance than new construction. This is often not conveyed to the owners, who have a mistaken understanding of the obligations to maintain the property. Disputes which center on issues of quantity and quality of repairs are often as much about whether or not the developer was obliged to provide construction commensurate with the lowest level of ongoing maintenance.

Proposed Performance Levels for Loft Conversions

In order to resolve the disputes that arise from loft conversions, it would be helpful to establish performance levels that would inform both developers and owners as to the impact of different types of masonry repairs. The following table presents the authors' proposed performance levels for the most common types of repairs. Two levels of performance are identified; one which would provide a relatively low level of continued maintenance; and one which would require routine maintenance on an on-going basis. By promoting the use of these types of performance levels, the developers and owners will both be aware of their obligations in the process:

Table 1--*Performance Levels of Common Repairs for Masonry Loft Conversions*

	Performance Level	
Repair Type	Level A: Limited On-going Maintenance	Level B: Frequent On-going Maintenance
Cracked Brickwork		
Replacement of cracked brickwork Filling cracks with mortar or sealant	X	X
Embedded Steel Repairs		
Replacement of corroded steel Painting of corroded steel	X	X
Flashing and Weeps		
Installed at lintels and shelf angles	X	
Flashing and weeps not installed		X
Tuckpointing		
100% tuckpointing	X	
Spot tuckpointing		X
Surface grouting alternative to tuckpointing		X
Cleaning		X

Conclusions

Masonry loft conversions to residential occupancy is a relatively recent trend that is becoming commonplace in North American cities. Although the masonry buildings have well withstood the test of time, their new usage often leads to problems. Water leakage, deterioration of interior exposed masonry, the quality and quantity of repairs already performed, and the level of continued maintenance required are often the source of contention between those who develop the loft conversion and those who reside in them. These problems which perhaps were tolerated when the buildings were used as manufacturing facilities are tolerated less by the new residential owners. Consequently, the need to establish performance levels that are clearly understood to both developers and owners are desirable. This paper suggests two possible performance levels; one that would require limited on-going maintenance and the other that would require frequent on-going maintenance. Each level has advantages and disadvantages, the former would minimize the owner's on-going maintenance obligations and increase the cost of the converted building, while the later would minimize the up-front costs of the conversion and require more maintenance. The important aspect is that both buyer and seller have the same understanding of what they are getting when they decide to own an old masonry loft converted to residential living.

References

[1] "Chicago Loft Boom," B.K. Hower, Focus Architecture Chicago, June 1998, p. 25.

[2] "Second Career for Obsolete Office Buildings," Hugh Cook, Building Design and Construction, Mid-May 1997, p. 46.

[3] Preservation Briefs No. 17: "Architectural Character: Identifying the Visual Aspects of Historic Buildings as an Aid to Preserving Their Character," Lee H. Nelson U.S. Department of the Interior National Park Service Preservation Assistance Division.

[4] The Secretary of the Interior's Standards for Treatment of Historic Properties with Guidelines for Preserving, Rehabilitating Restoring and Reconstructing Historic Buildings, Kay Weeks and Anne Grimmer, U. S. Department of the Interior National Park Service Cultural Resource Stewardship and Partnerships, Heritage Preservation Services, Washington, D.C., 1995.

[5] Technical Notes on Brick Construction 7F, "Moisture Resistance of Brick Masonry Maintenance," The Brick Institute of America, Reston, Virginia, 1987.

[6] Masonry: Design and Construction, Problems and Repairs, J. Melander and L. Lauersdorf, Eds., American Society for Testing and Materials, STP 1180, Philadelphia, PA, 1983.

[7] "Century Plaza Apartments" Gordon Wright, Building Design and Construction, October 1995, p. 46.

[8] "Former Factory Meets Loft Goals," Building Design and Construction, August 1996, p. 46.

[9] Water Leakage Through Building Facades, R.J. Kudder and J.L. Erdly, Eds., American Society for Testing and Materials, STP 1314, West Conshohocken, PA, 1998.

A. Michel Alexander[1] and Richard W. Haskins[2]

New NDE Technologies for Evaluating Reinforced Concrete Masonry

REFERENCE: Alexander, A. M. and Haskins, R. W., "**New NDE Technologies for Evaluating Reinforced Concrete Masonry,**" *Masonry: Materials, Testing, and Applications, ASTM STP 1356,* J. H. Brisch, R. L. Nelson, and H. L. Francis, Eds., American Society for Testing and Materials, 1999.

ABSTRACT: Researchers at the Waterways Experiment Station (WES) have demonstrated that two new nondestructive evaluation technologies show promise in making a more accurate diagnosis of the structural condition of concrete masonry walls than prior technologies. Traditionally, sounding with a hammer has been used to determine the presence and quality of the grout fill around the reinforcing bars in concrete masonry units (CMU's). First, WES has developed a new grout detection system, which senses the reverberating energy in the CMU's with a microphone. This energy is introduced into the CMU by using a pistol to fire a metal BB against the face of the block. A microphone and spectrum analyzer replaces the function of the human ear to distinguish different pitches of sound through sounding. Since a technician is more likely to get consistent results with the new system, it is not as subjective as sounding. Next, WES has evaluated the new digital steel detectors. A reinforced concrete masonry structure can contain many combinations of steel: vertical bars, horizontal bars, size of bar, number of bars, splices, etc. Digital steel detectors with microprocessors have the potential to provide much more information than traditional analog types.

KEYWORDS: reinforced concrete masonry, nondestructive testing, steel detection, grout detection

Introduction

Background of Ft. Bragg Investigation

The U. S. Army's 82nd Airborne Division at Ft. Bragg military base in North Carolina was building some new barracks. The barracks were suspected to be deficient in presence, location, and quantity of steel and in presence and quality of grout fill, which was placed around the steel in the concrete masonry units (CMU) [1]. The Waterways

[1] Research Physicist, Structures Laboratory, Waterways Experiment Station, Vicksburg, MS 39180.

[2] Electrical Engineer, Information Technology Laboratory, Waterways Experiment Station, Vicksburg, MS 39180.

Experiment Station (WES) was requested by the Savannah Corps of Engineer District Office to provide to the Army an independent 10% inspection of the work of the testing agency that was performing the nondestructive evaluation (NDE) on the barracks [2].

Construction Practice

Structures built with CMU's require that reinforcing steel have a definite spacing, size, and amount of steel in the walls of higher floors and even a closer spacing and more steel in the walls of lower floors. Design specifications require many combinations of bar diameter and number in various types of masonry walls [3]. Also, grouting is required in those cells that contain reinforcing bars. Where reinforcing bars and grout are deficient or missing, it can present structural problems, as the embedded steel reinforcement is intended to satisfy tensile and/or flexural strength requirements. NDE can help determine whether the grout and steel are in compliance with the design specifications.

Principle of Sounding

Grout detection in reinforced concrete masonry is typically conducted by tapping the masonry with a small hammer and detecting the characteristic sound by ear (sounding). No measurement standards exist for this diagnostic task. Sounding is simple, inexpensive, and rapid, however, it can be subjective under certain conditions. The content of the sound as the energy reverberates between the walls of the room can be confusing and can vary considerably when the type of room varies: solid walls, closets, doors, windows, etc. A considerable amount of practice is required to train an operator to detect the characteristic sounds from grouted cells of known quality in the midst of extraneous reflections in the room. The equipment consists only of a small hammer constructed with two components: a steel sphere of about ½ in. (12 mm) diameter and a stiff wire handle of about 1/8 in. (3 mm) diameter and about 18 in. (450 mm) in length. At a minimum, the operator's hearing ability must be capable of discerning the difference between a hollow sound that indicates an empty cell and a ringing sound that indicates a cell filled with consolidated grout. Partially filled cells emit a sound that is more difficult to describe and detect.

Principle of Steel Detection

The general principle of operation of most steel detection devices is the transmission and detection of magnetic flux lines into the concrete through a probe mechanism. Upon encountering steel in the concrete, the magnetic flux lines traversing the steel increase in number relative to concrete that does not contain steel. A sensing circuit in the device detects the increase in the field strength, which is due to a lower resistance path for the magnetic flux lines. (This is analogous to how an electric current increases in magnitude in an electrical circuit when a piece of metal causes a short in the circuit.) A stronger signal will be transmitted through the steel under these conditions: a larger diameter for the reinforcing bar, a greater number of bars, and a thinner concrete cover. The transmitted signal is then received, processed, and displayed or recorded by a digital readout, audible beep, meter pointer, or a change in pen movement on a chart recorder.

WES's Experience

WES has been instrumental for a number of decades in the development of new NDE tools and techniques for concrete. WES designed an ultrasonic pulse echo system to replace sounding for locating delaminations in bridge decks in the mid 90's [4]. Currently the chain drag and hammer are two sounding techniques that are used by 95 percent of the states in the U. S. for detecting delaminations in bridge decks. Based on WES's experience with this and other NDE systems, they felt they could provide improved NDE equipment and techniques to replace sounding for measuring the integrity of the grout fill and for determining the type and amount of the steel present in the cells for masonry structures. Very few NDE measurement standards exist in the field of concrete structures and even fewer in the field of masonry. For that reason, researchers at WES needed to design and test some new diagnostic tools and test some other existing high-technology tools that would permit a more accurate diagnosis of the structural condition of the masonry walls.

Problem

The problem when determining the quality of grout fill in a CMU is that destructive testing (DT) is usually not desirable and sounding can be too subjective. Also, the mapping out of the many combinations of steel arrangements in reinforced concrete masonry structures is difficult without performing an extensive calibration on known combinations of steel using the new digital steel detectors.

Remedy

The proposed remedy in this investigation was to develop better and more objective NDE systems and procedures for diagnosing masonry structures.

Purpose

This report will explain the testing, development, calibration, etc of two NDE technologies that was used to diagnose the type and amount of steel and the integrity of the grout fill around the steel for walls constructed of CMU's.

Thesis Statement

This article will show that the two new NDE technologies, BB gun/microphone system and a pachometer having extensive calibration, show promise in improving the evaluation of reinforced masonry.

Laboratory and Field Testing

Initial Assessment

WES made a preliminary assessment of the situation at Ft. Bragg. Sounding, ultrasonic pulse velocity (UPV), and steel detection measurements were made on adjacent CMU's just above and below where DT had been performed by the testing agency. UPV measurements could not be conducted on CMU's that had DT performed on them. The major part of the DT was conducted in solid walls away from openings. In this case the reinforcing bars and grout existed in vertical columns of cells. For those limited walls tested containing doors and windows the reinforcing bar is positioned horizontally for lintels and sills and so the adjacent cells that were tested in this case were on either side of the cell damaged by DT.

Construction Details

A study by WES of the construction drawings of the barracks revealed that there were many reinforcing bar configurations in the masonry walls. Different types of walls; interior walls, exterior walls, shear walls, walls on different floors, etc; require different amounts of steel. Specifications vary on the size of the reinforcing bar and the number of reinforcing bars for a given part of a wall such as a door, window, interior wall, exterior wall, etc. Specifications also varied based on whether the wall was load bearing or non-load bearing. Also, there were variations in the amount and configuration of steel around the doors and windows, etc. Jambs, lintels, and sills had their own requirements on the design specifications of the steel.

The following represents some of the possible deficiencies suspected in the walls: (1) absence of vertical and horizontal reinforcing bars, (2) incorrect spacing of reinforcing bars, (3) incorrect number of reinforcing bars in a cell, (4) incorrect size of reinforcing bars, (5) absence of horizontal joint reinforcement (block lock), (6) absence of grout in cells containing reinforcing bars, and (7) improper consolidation of grout in the cells.

V-meter Measurements at Field Site

The V-meter, an ultrasonic pulse velocity device, was used onsite on cells, that were adjacent to the ones that had undergone DT, to measure the time of arrival (TOA) of compression waves through the CMU's [5]. Figure. 1 shows the V-meter. It was used in hopes that it could analyze the adequacy of the grout fill in the cells of the CMU's. WES personnel wanted to verify the condition of the cells to see if the actual condition of the grout corresponded with the interpretation given to the sounding tests. Unfortunately, in those cases where the grout was poorly consolidated, the grout still provided a continuous path for the stress wave energy to pass through the CMU. Therefore, in this situation, the V-meter did not prove to be useful as a method of control, since it gave a TOA indicative of a high quality cell rather than a poor quality cell. It was discarded as a control test.

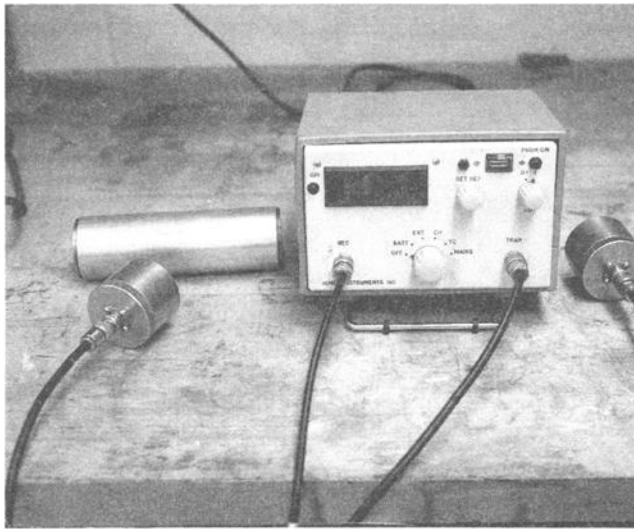

FIG. 1--*V-meter with transmitting and receiving transducers.*

FIG. 2--*A typical sounding hammer.*

Sounding Measurements

The sounding technique relies totally on the ability of the technician to detect and identify frequency components by ear that relate to a filled, unfilled, or partially filled cell. Figure 2 shows a typical sounding hammer. The ear is a remarkable spectrum analyzer, but it requires a considerable degree of practice for a person to listen to the sound made from an impact on a CMU and correlate that sound to the cell's condition. It is entirely possible that there are some people who have an ear for pitch who might be able to discern all the nuances of pitch that are required to determine the integrity of a cell. However, all technicians do not have that ability. Training begins with knowing the condition of the grout or performing DT to determine the condition of each cell. Empty cells and full cells bracket each end of the total range of quality and are easier to detect than partially filled cells. For example, it would be more difficult for the average technician to rank partially grouted cells in the correct order of quality than it would be to simply detect full and empty cells.

Sounding at Field Site

Since WES was notified of the project after the DT had already been performed on the barracks, it was not possible for WES to make NDE tests on the CMU's before they were damaged by the DT. This would have provided an opportunity for WES personnel to attempt to "calibrate theirs ears" on cells of known condition. However, the testing agency was able to make sounding tests prior to the DT and test the performance of their personnel to interpret the meaning of the sound from the hammer impacts. The testing firm classified all cells under three types of condition: empty (E), full (F), and partially filled (PF). The face of each CMU had been labeled by the testing firm with the letters 'E',' F', or 'PF' for each of the two cells of a CMU. WES was able to perform sounding tests on cells adjacent to the DT and compare their readings with the testing firm's results on the target cells. WES was not able to get the same results on many measurements as the testing firm got and for that reason decided that a better technique was needed than sounding.

Objective Technique Needed

WES investigators wanted to replace the use of the human ear with a sensor and spectrum analyzer that could detect the frequency components emitted from the CMU's when impacted. An instrument to record the response of the grout in the cells would permit objective results to be obtained by all test equipment operators. By the measurement of definite signal features displayed on a spectrum analyzer, all operators could get similar results.

Testing the total cell

When the grout is placed into the cells but not properly consolidated, the grout may not flow around both sides of the reinforcing bar(s) and completely fill the space in the cell. Assume the reinforcing bar is near the center of the cell. If the grout fills the cell space between one face of the CMU and the reinforcing bar, but not between the reinforcing bar and the opposite face, one can get totally different readings when using the sounding technique on either side of the wall. Where the grout is in solid contact with the face of the cell, the sounding will give a high frequency ringing sound indicating high quality grouting in the cell. The ringing sound is the reverberation of the longitudinal energy between the face of the cell and the back of the grout near the reinforcing bar.

Where the grout is not in contact with the face of the cell the sounding technique will give a low frequency hollow sound indicating a poorly grouted cell. The hollow sound is the flexural vibration of the approximate 8 in. (200 mm) x 6 in. (150) x 1 in. (25 mm) section between the cell space and one of the faces of the 8 in. (200 mm) x 8 in. (200 mm) x 16 in. (400 mm) CMU.

Laboratory Models for Testing Grout Detector

Numerous physical models were fabricated in the laboratory at WES for calibration purposes on experimental grout detectors. Cells of CMU's were filled with simulated consolidated and unconsolidated grout. Some of the grout had various amounts of Styrofoam beads embedded in the grout to simulate various percentages of air voids.

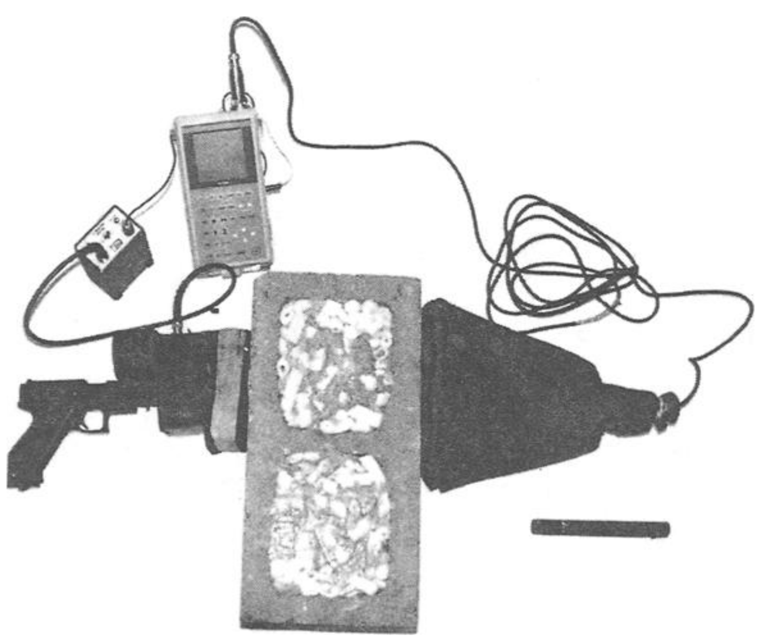

FIG. 3--*BB gun/Microphone grout-fill detector.*

Figure 3 shows one of the CMU's whose cells contain Styrofoam beads. Tests were made on the flawed and unflawed CMU's to show the potential of the various grout detection systems that WES experimented with to detect the quality of the grout in the cells. The grout detectors were calibrated on cells that were filled, unfilled, and partially filled. It was not possible at Ft. Bragg to precisely calibrate a grout detector by making detection measurements on cells adjacent to the target ones, which were damaged by DT. However, the laboratory models provided CMU's of known integrity and permitted an accurate calibration.

Development of BB Gun/Microphone System

WES experimented with a number of ultrasonic through-transmission techniques (transmitter on one side of the wall and receiver on opposite side of the wall). The introducing of energy by impacts from metallic BB's and picking up the spectrum of the sound on the opposite side of the cell with a high-fidelity microphone was shown to have the most potential for detecting grout fill in the CMU cells. Figure 3 shows the BB-gun/microphone grout-fill detector system. Figure 4 shows the typical spectra seen of cells by the grout-fill detector: fully compacted grout, partially honeycombed grout, no grout, and highly honeycombed grout.

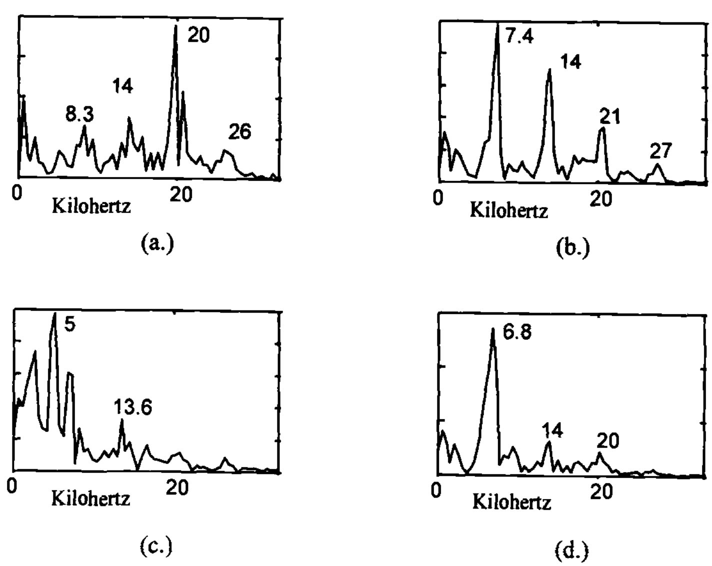

FIG. 4--*Typical spectra seen of cells by the grout-fill detector (a.) fully compacted grout, (b.) partially honeycombed grout, (c.) no grout, and (d.) highly honeycombed grout.*

Merits of Through-Transmission System

For the problem of a partially-filled cell as mentioned above, WES researchers developed the BB gun/microphone system to check the integrity of the total cell, since a fault on either side of the reinforcing bar in the cell is, in actuality, a fault for the total cell. This was done successfully with the through-transmission measurements using the BB gun to introduce acoustic energy into the CMU and using the microphone to detect the response on the opposite wall. A foam-rubber baffle covered the microphone and isolated the extraneous energy, such as reflections and external noise in the room, from the desired energy propagating through the CMU. Through-transmission measurements (two-sided) have another advantage. Boundary effects (wave reflections from corners of rooms, windows, floors, etc.) are not a problem with through-transmission measurements. They measure the frequency of echoes in the CMU before unwanted reflections from the room arrive at the microphone.

Merits of Low Frequency Energy

Standard frequency (54 kHz or greater) ultrasonic transducers for concrete require the use of a coupling medium, such as water or grease, between the transducers and the concrete in order to eliminate the air film. In short, air coupling is not possible with the V-meter. This air film blocks both the transmission of sound into the concrete from the transmitter and the reception of sound from the concrete by the receiver. By contrast, sonic or low frequency sound (less than 20 kHz) generated by the impacts of the BB's and picked up by a microphone will travel through the air film. The microphone sensor is desirable because air coupling between the sensor and the masonry surface will permit a more rapid testing rate than standard ultrasonic transducers requiring an application of coupling grease between the sensor and the masonry surface.

Improved Steel Detectors

Recently, microprocessors have been incorporated into steel detectors resulting in devices much improved over past systems [6]. These steel detectors are known as "cover meters" or pachometers. The technology of reinforcing steel detection devices has evolved in sophistication over the years to currently include state-of-the-art electronic integrated circuits, recorders, digital readouts, microprocessors, battery operation, etc. Previous state-of-the art analog equipment generally used a coil movement with a needle pointer and scale for reading purposes. The new digital detector devices now offer improved features of speed, weight, power, resolution, penetration, and interpretation, which have removed some of the impediments that may have hindered routine usage of the devices in the past.

Calibration of Pachometer at Field Site

A microprocessor-based pachometer, the Profometer 3 distributed by SDS Inc., was used at Ft. Bragg [7]. The Profometer Model 3 is shown in Figure 5. The profometer was calibrated at the field site on the adjacent cells just above and below the cells where DT had been performed. The missing concrete influences the reading to a certain extent and precludes the use of NDE measurements directly on the face of the CMU where DT has taken place. Figure 6 shows a typical CMU and a #4 and #7 steel reinforcing bar.

Steel Detection

The WES crew also performed steel-detection measurements at the field site using the profometer. From the preliminary examination on the masonry walls that had DT performed on them, the investigators gained confidence in the accuracy of detection of the steel using the profometer. Although readings had to be taken on adjacent cells to the target cells, it was assumed that the adjacent cells could be depended upon to have the same steel in them as the target cells for the most part. The cell space is typically 5-½ in. (140 mm) x 6 (150 mm) in. and 8 in. (200 mm) in height. The reinforcing bar(s) can be anywhere in that space.

The lowest reading from the profometer is 0 for no steel and 2000 for probe contact with the steel. The strength of the field is given in relative numbers and not fundamental units. The onsite calibrations yielded the following correlation's for a #5 reinforcing bar: a reading of 460 or more represented two or more reinforcing bars, a reading between 259 and 460 represented two reinforcing bars, a reading between 241 and 259 represented one or two reinforcing bars, a reading between 180 and 259 was one reinforcing bar, and a reading between 140 and 180 is possibly a reinforcing bar. No reinforcing bars exist below a reading of 140. Calibrations were performed for those cases where the number of steel reinforcing bars could be seen from DT.

Extensive Calibration Needed

The new steel detectors that contain microprocessors have the potential to provide much more information when an extensive calibration is performed under a variety of conditions. Because there are so many combinations of steel (horizontal reinforcing bar, vertical reinforcing bar, horizontal block lock, splices for two reinforcing bars, various diameters of steel, number of bars, etc.) within a wall, a calibration will permit a variety of readings to be correlated with many combinations. Some of the considerations include: the reading at the intersection when a vertical reinforcing bar crosses a horizontal reinforcing bar, two horizontal reinforcing bars crossing one vertical reinforcing bar, the influence of horizontal block lock on one vertical reinforcing bar, on two vertical reinforcing bars, influence of a splice on a reading, influence of metal door jamb near vertical steel, etc.

Averaging is Critical

The readings from one side of the wall were not sufficient to indicate the amount of steel in the walls. Averaging the two readings on either side of the wall yielded better results than a reading from only one side. Because the space within the cell is large, the reinforcing bar can be in front of, in the center, in back of the cell, or anywhere in between the front and back of the cell. The reading is highly dependent on how close the steel is to the probe.

FIG. 5--*Profometer Model 3 and concrete specimen with steel.*

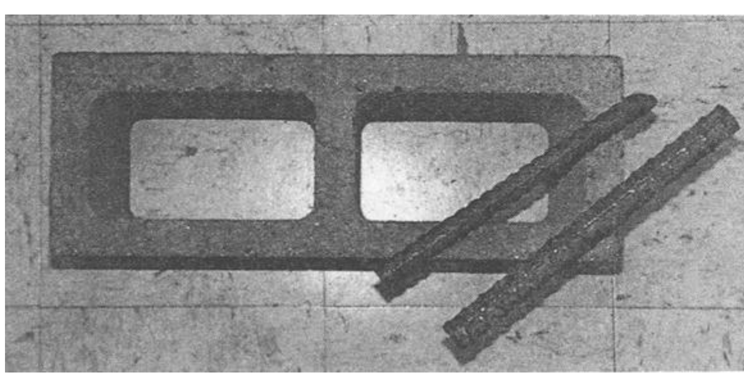

FIG. 6--*Typical CMU and a #4 and #7 reinforcing bar.*

Example Plot

An example of the results shown in Figure 7 shows the location of the reinforcing bars in one of the masonry walls of the barracks. As this wall is without any sills and lintels (windows and doors) most of the reinforcing bar is located vertically in the cells. The darkest shaded cells represent where the most reinforcing bar exists in the wall and the lightest shade represents cells that do not contain steel. Six full columns of reinforcing bar can be seen in this wall with 3 or 4 shorter columns of steel. It is not clear why steel is in the shorter columns. The horizontal bond beam containing steel reinforcement at the top of the wall is visible in the plot.

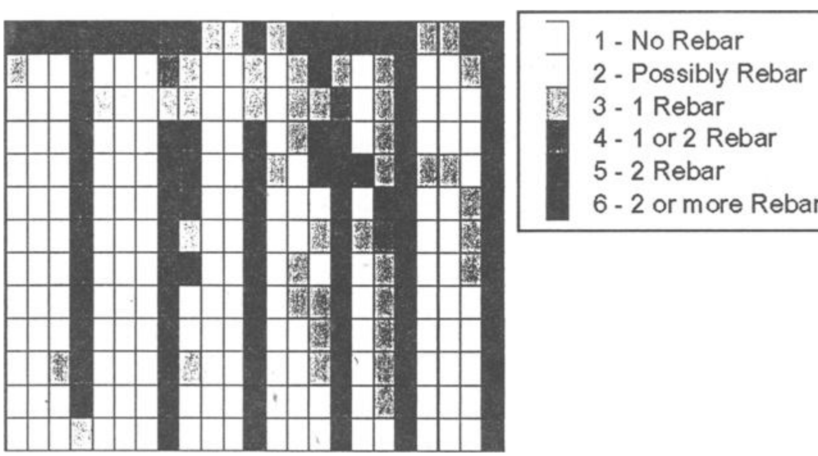

FIG. 7--*Results of using Profometer on cells of a typical wall.*

Results

The results of the new grout detection system closely agreed with sounding tests performed by the testing agency.

The Profometer 3 indicated that the amount of the vertical and horizontal steel in the cells was generally sufficient, except for about three rooms. Some rooms contained more steel than was required. However, steel was missing in some key locations. WES has about *70 % confidence* in these results. Building and calibrating some models in the laboratory containing various configurations of steel could improve the steel detection calibration.

The profometer indicated that the steel in the bond beams was missing in three rooms.

The profometer indicated that about 30 % of the horizontal joint reinforcement were missing. We have about *95 % confidence* in these results.

About 70 % of the grout were deficient as indicated by the BB gun/microphone system. This serious grout deficiency may nullify the purpose of the steel. WES has about *85 % confidence* in these results.

It is the opinion of WES personnel that the quality of grout in the barracks was adequate only in a few places, based on the area we checked with the new system. The grout was generally honeycombed, incomplete, or missing altogether. Lack of grout consolidation by vibration and cleaning of the cells by the contractor is also obvious.

Many cells that the testing firm classified as full based on their sounding tests, WES classified as partially filled, and some that the agency found partially filled, WES classified as empty using the BB gun/microphone system.

Conclusions

The grout detection system developed by the Waterways Experiment Station (WES) and the pachometer used by WES showed promise for improving the evaluation of the condition of reinforced concrete masonry walls. The new grout detector may perform better than sounding, as the technique of sounding can be subjective and heavily influenced by external factors.

More objective nondestructive evaluation (NDE) techniques and equipment are needed for evaluating construction materials and this investigation should help improve the state of the art of tools and techniques available for masonry.

Increasingly, unskilled labor is being replaced by skilled labor, as the construction industry is demanding a concrete product with tighter specifications. This practice will require a greater use of NDE in the future.

Currently, neither the steel- nor grout-detection methods used at Fort Bragg exist as measurement standards. Until measurement standards are developed, nationwide NDE quality assurance tests will not be common practice on masonry structures. The quality of masonry walls will, in general, continue to be verified by destructive testing (DT). However, the new testing methods do serve to provide assistance in locating anomalies (grout or steel).

It is not possible to claim a high degree of certainty in the results of NDE interpretation in the field of concrete and masonry. Sometimes the answers obtained from concrete/masonry flaw-detection equipment as to whether flaws exist are not a crisp "yes" or "no," but a "maybe." That does not mean that the testing and evaluation are unimportant. It simply means that, for now, a degree of uncertainty must be taken into account when concrete/masonry structures are being tested.

Recommendations

Although the two new technologies show promise in improving the evaluation of reinforced concrete masonry structures the grout detection system should be further refined and both the grout and steel detection systems demonstrated in field tests. Also, the results of the new grout-fill detector should be compared against the known quality of the grout determined by fabrication or DT to verify the performance of the new tool. Also, those trained in performing sounding to determine which test method is better overall should conduct sounding tests.

By incorporating a microprocessor into the grout detector system a digital signal processing algorithm could be developed that would classify the signals from the grout detector and hence the grout condition in a number of categories, for example: excellent, good, questionable, poor, and very poor. This would reduce the amount of training required for operators to learn how to interpret the signals from the grout detector.

References

[1] Engineering News-Record, "Barracks Project won't be one worth bragging about," Vol. 236, No. 3, Jan. 22, 1996.

[2] Waterways Experiment Station. Letter report to Savannah Corps of Engineer District in Jan. 1996 on results of grout and reinforcing bar detection on military barracks at Ft. Bragg. Report not published.

[3] American Concrete Institute. Building Code Requirements for Masonry Structures (ACI 530-95/ASCE 5-95/TMS 402-95). Reported by the Masonry Standards Joint Committee. American Concrete Institute, American Society of Civil Engineers, and The Masonry Society. TH1199 B85, 1996. IBSN 0-7844-0115-2.

[4] Alexander, A. M. and Haskins, R. W., Cook, R., Baishya, M. and Kelly, M. "Technologies for Improving the Evaluation and Repair of Concrete Bridge Decks: Ultrasonic Pulse Echo and Polymer Injection," WES CPAR Technical Report SL-98-1, In press.

[5] James Instruments Inc., "Ultrasonic Testing of Concrete using the V-Meter," Technical Paper F-6063, 4048 North Rockwell Street, Chicago, Illinois 60618, 1978.

[6] Alexander, A. M. and McDonald, W. E., "Performance of Microprocessor-Based Reinforcing Steel Detector for Concrete Structures", *The REMR Bulletin*, Vol. 8, No. 4, Dec. 1991.

[7] SDS Company, Brochure No. 880745E, P.O. Box 844, Paso Robles, CA, 93447, Feb. 1988.

ISBN 0-8031-2600-X